Development and Evaluation of Situationally Specific Inlet Systems for Gas Chromatography and Multi-Dimensional Gas Chromatography

by

Peter Thomas Stevens

A dissertation submitted in partial fulfillment
of the requirements for the degree of
Doctor of Philosophy
(Chemistry)
in The University of Michigan
2008

Doctoral Committee:

Professor Michael D. Morris, Co-Chair
Professor Richard D. Sacks, Co-Chair (Deceased)
Assistant Professor Kristina I. Hakansson
Assistant Professor Kevin Joel Kubarych
Jack H. Waite Jr., Southwest Research Institute

ACKNOWLEDGEMENTS

I would like to take this opportunity to thank my Research Advisor, Dr. Richard Sacks. His passion for science and the joy he found in it set an example that I will always strive to attain. He was not only my advisor, but a cherished friend. He may be gone, but he will live on through the many students, scientists, and people whose lives are better for the time they spent with him.

I would also like to thank Dr. Michael Morris and Dr. J. Hunter Waite. Dr. Morris, thank you for agreeing to take me under your wing and help me complete my degree after Dr. Sacks' passing. Dr. Waite, thank you for always being there for me, both scientifically and personally as I made this journey. I would like to thank those past and present who have served on my committee; Dr. Kristina Hakansson, Dr. Kevin Kubarych, Dr. Zhan Chen and Dr. Charlie Hasselbrink.

I would like to take this opportunity to thank Aiko Nakatani, the Manager of Academic Services for the Department of Chemistry. Aiko, I don't know if I would have made it without you. Whenever something was amiss, I knew I could count on you to help get me back on track.

To the members of Dr. Sacks' Research Group; Tincutta Veriotti, Joshua Whiting, Megan McGuigan, Jeff Driscol, Mark Libardoni, Randy Lambertus, Cory Fix, Shaelah Reidy, Amy Payeur and Visiting Scholars Dr. Juan Sanchez and Dr. Shai Kendler, what can I say. You were my co-workers and are my friends. I can't imagine what graduate school would have been like without you.

Finally, thank you to my family for being there for me and allowing me to pursue my dreams. It has been a bumpy road and many times the outcome was in doubt. Frank, Karen Jon, Jay, Sarah, and your families, I couldn't have done this without you.

TABLE OF CONTENTS

ACKNOWLEDGEMENTS..... ii
LIST OF FIGURES.....vi
LIST OF TABLES.....ix

CHAPTER
1. INTRODUCTION AND BACKGROUND.....1
Introduction 1
Background 4
References 17

2. VACUUM-OUTLET GC OF LARGE-VOLUME AIR SAMPLES USING AN IN-LINE MULTIBED SORPTION TRAP, AT-COLUMN HEATING, AMBIENT AIR AS CARRIER GAS AND PHOTOIONIZATION DETECTION.....18
Introduction 18
Experimental Section 21
Results and Discussion 22
Conclusions 33
References 46

3. LARGE-VOLUME VAPORSAMPLING FOR GC IN THE C_5 TO C_{24} VOLATILITY RANGE 48
Introduction 48
Experimental Section 51
Results and Discussion 53
Conclusions 56
References 64

4. ANALYSIS OF HUMAN BREATH UTILIZING A MULTI-BED SORPTION TRAP AND COMPREHENSIVE TWO-DIMENSIONAL GAS CHROMATOGRAPHY.....65
Introduction 65
Experimental Section 69
Results and Discussion 73
Conclusions 80
References 92

5. ANALYSIS OF HUMAN BREATH UTILIZING A POLYDIMETHYL SILOXANE FOAM TRAP, A CRYOGENICALLY COOLED - THERMAL DESORPTION INLET AND COMPREHENSIVE TWO-DIMENSIONAL GAS CHROMATOGRAPHY……..……...……..93
Introduction ……93
Experimental Section ……..94
Results and Discussion ……97
Conclusions ……98
References ……...109

6. CONCLUSIONS…….……110

LIST OF FIGURES

Figure

1.1 A schematic of the multi-bed sorption-based preconcentrator (SPC)…….13

1.2 Chromatograms showing the analysis of a 42 component synthetic mixture.
(a) initial chromatogram for normal trap configuration
(b) memory effect chromatogram for normal trap configuration
(c) initial chromatogram for reverse trap configuration
(d) memory effect chromatogram for reverse trap configuration…14

1.3 A schematic of the probe/interface of the CDS PyroProbe 2000……....16

2.1 Diagram of the complete GC system and detail of the cross-section of the low thermal mass RVM column. F, flow controller; HC, hydrocarbon trap; R, capillary restrictor; V_1, metering valve; VP, vacuum pump; T, multi-bed sorption trap; V_2, metering valve; P, pressure gauge; PID, photo ionization detector. ……..……..36

2.2 The effects of make up gas and outlet pressure on the qualitative features of the chromatograms from the separation of a 5-component mixture. For chromatogram (a) p_o was 0.7 atm and no makeup gas was used. For chromatogram (b), p_o was maintained at 0.7 atm, and detector makeup gas (ambient air) was added at a flow rate of about 5 cm^3/min at ambient pressure. For chromatogram (c), p_o was 0.25 atm, and no makeup gas was used. ……...…….….37

2.3 Quantitative data on system efficiency for the isothermal separation of 3-octanone at 36 ^oC. Plot (a) (Golay plot), shows the height equivalent to a theoretical plate *H* versus average carrier gas velocity, and plot (b) shows the height equivalent to a theoretical plate versus column outlet pressure…….38

2.4 Chromatogram of a 16-component mixture obtained with a p_o value of 0.25 atm. …….39

2.5 Analytical curves of log (peak relative area) versus log (sample collection time) for the wet samples. ……...40

2.6 Results of a study of the decomposition of α-pinene (A) and β-pinene (B) using hydrogen carrier gas (solid lines) and air carrier gas (broken lines). ……..42

2.7 Plots illustrating the effects of analyte structure and molecular weight on the extent of sample loss by thermal decomposition with air as carrier gas. ……...43

2.8 Plots showing the decomposition of some common biogenic compounds. Isoprene (Plot 2) is the building block (monomer) for the terpenes. The data from Figure 6 for α-pinene and β-pinene in air are repeated for comparison with the other compounds. ……...44

3.1 A schematic of the pyrolysis-preconcentration interface developed and evaluated in this paper. ……58

3.2 A schematic of gas flow. The direction of carrier gas flow during sample collection is shown in (a). The direction of carrier gas flow during desorption is shown in (b). ……..……59

3.3 Flowcharts showing the gas flow path during each mode (arrows) and closed valves that must be allowed to back-pressurize before desorption (**X**). ……...60

3.4 Individual traces for the C_{10} through C_{13} straight chain alkanes with the phase trap held at 25 °C during sample collection. The phase trap was desorbed at the 200 sec mark and the multi-bed sorption trap was desorbed at the 260 sec mark. …….61

3.5 A chromatogram of a sample containing the even numbered straight chain alkanes from hexane through tetracosane. ……62

3.6 A plot of peak widths at half height versus carbon number for the component peaks shown in Figure 3.5. ..……...63

4.1 Schematic of the GC × GC instrument used for human breath anaysis. A multi-bed sorption trap is used for sample collection and introduction into the GC × GC-FID. ……82

4.2 Two-dimensional (contour) chromatogram of a 40-component test mixture containing compounds found in human breath. The insets show expanded views of portions of the chromatogram containing overlapping peaks. …84

4.3 Three-dimensional view of GC × GC chromatograms of human breath sample collected from two individuals. A sample collection time from the 1-L gas sampling bags of 300 s at a flow rate of 50 cm^3/min was used. …86

4.4 Two-dimensional (contour) chromatogram of human breath sample collected from the same individual as in Fig. 3(a), but using a sample collection time from the gas sampling bag of 960 s at a flow rate of 50 cm^3/min. ……89

4.5 Three-dimensional views of GC × GC chromatograms collected from human breath sample of an individual just prior to smoking a cigarette (a) and 5 min after smoking a cigarette (b). A sampling time of 300 s at a flow rate of 50 cm^3/min was used. Identified compounds and selected quantitative results are listed in Table 3, column 5. Peak (15) represents 2,5-dimethyl furan, a bio-marker for cigarette smoke. Prior to smoking, the concentration of 2,5-dimethyl furan was 19 ppb, 5 min after smoking a cigarette, the concentration of 2,5-dimethyl furan was 81 ppb. …….90

4.6 Three-dimensional views of GC × GC chromatograms from human breath sample obtained from an individual 5 min (a), 30 min (b), and 60 min (c) after chewing a piece of fruit-flavored gum. Major breath components are displayed on the chromatograms and show a decrease over time. …….91

5.1 A schematic of the TDU/CIS 4 GCxGC-TOFMS system. ……..100

5.2 A representation of the PDMS foam inside of the TDU tube. ……101

5.3 A figure showing the TDU/CIS 4 inlet system as mounted on the GCxGC-TOFMS. ……102

5.4 A schematic of the sampling apparatus used to transfer the breath sample from the sampling bag to the PDMS foam. ……..103

5.5 A GCxGC chromatogram of a 1 L sample of human breath taken prior to the consumption of orange juice. The 3D surface plot is shown in the inset……...104

5.6 A GCxGC chromatogram of a 1L sample of human breath taken 15 minutes after the consumption of 10 oz. of orange juice. The 3D surface plot is shown in the inset. ……....105

5.7 A GCxGC chromatogram of a 2 L sample of human breath taken prior to the consumption of a sugar-free energy drink. The 3D surface plot is shown in the inset. ……...106

5.8 A GCxGC chromatogram of a 2 L sample of human breath taken after the consumption of 16 oz. of a sugar-free energy drink. The 3D surface plot is shown in the inset. ……...107

LIST OF TABLES

Tables

1.1 Adsorbents used in the multi-bed trap and their characteristics……...15

2.1 List of test compounds and boiling points. ……..36

2.2 Statistical data from plots of log (peak area) versus log (sampling time) for dry and wet samples. ….…….41

2.3 Recoveries (peak areas) of some of the compounds in Table 1 at a desorption temperature of 385 ^{o}C with no stop flow and at 200 ^{o}C with a 5-s stop flow relative to the peak areas obtained for a desorption temperature of 200 ^{o}C with no interruption of the carrier gas flow. …...45

4.1 A 40-component mixture based on compounds found in human breath samples. ..…….83

4.2 Statistical data from calibration plots of 13 compounds found in the test mixture. ……..……...85

4.3 Compounds identified in human breath samples. ……..87

5.1 A table showing the change in area and percentage change for six selected components from prior to the consumption of the sugar-free energy drink to after the consumption of the energy drink……..…….108

CHAPTER 1

INTRODUCTION AND BACKGROUND

INTRODUCTION

The gas chromatograph is the most commonly used instrumentation for the analysis of volatile and semi-volatile organic compounds (VOCs) worldwide. Recent estimates place the number of GCs currently in use at over 300,000 instruments. Analysis of ambient atmospheric vapor samples for VOCs is relevant in industrial safety compliance monitoring, environmental quality monitoring and the diagnostic analysis of human breath. Most current methods rely on on-site sample collection with the samples then being transported to an off-site analytical laboratory for analysis. These methods have drawbacks in that there is a storage and transport time between collection and analysis. Current sample collection techniques require collection of samples on sorbents or in sample bags or canisters. During this time, volatile samples can be lost from sorbent traps. Electro-polished canisters require considerable expense and involve intensive cleaning procedures.[1,2,3] Reactions between sampled compounds can also occur during storage.[4,5,6] One way to minimize the sample loss due to these effects is to analyze the samples on-site, thereby minimizing the time between sample collection and sample analysis. On-site analysis of volatile and semi-volatile organic vapors by gas chromatography is an area of research seeing considerable recent activity.[7,8,9,10,11,12,13]

Direct injection of an atmospheric sample presents the problem of there being enough analyte in the sample aliquot to be detected. Many components in atmospheric samples occur at trace levels. For analysis of compounds occurring at trace levels, it is necessary to preconcentrate samples in order to improve detection limits. By passing a large volume of sample through a sorption-based preconcentrator (SPC) and then thermally desorbing the analyte into the analytical column, the concentration of analyte in the injection can be elevated above the limit of detection while minimizing the necessary injection volume, thereby improving chromatographic performance.

Pyrolysis, which is defined as "decomposition or transformation of a compound caused by heat",[14] is often used to fragment large molecules, often from solid samples, which are normally not volatile enough to be analyzed by gas chromatography, into more volatile fragments for analysis. Normally, pyrolysis is done in an inert atmosphere, such as helium or nitrogen, to minimize possible reactions between the pyrolyzed fragments and the atmosphere. One of the most common applications for the pyrolysis-gas chromatograph (Pyr-GC) combination is the analysis of kerogens by the petroleum industry. Kerogens are "A solid, waxy, organic substance produced by the partial decay of organic matter that when heated can produce coal macerals as well as oil and gas."[15] Pyr-GC has limitations though. Flash pyrolysis, in which the sample is heated to the pyrolysis temperature very rapidly (<< 1 sec), produces a narrow plug of pyrolysate, but is only applicable for smaller sample sizes (~ 10 mg maximum). Slow pyrolysis allows for larger samples, but pyrolysis occurs over a much longer time frame (minutes). This makes its use as an injector for GC much less attractive. Trace samples would require the use of slow pyrolysis in order to obtain a detectable level of analyte because the required

sample size necessary for detection of trace components would be too large for flash pyrolysis. By combining the SPC with Pyr-GC, the pyrolysate can be passed through the trap, where it is collected. From there, it can be desorbed as a relatively narrow injection plug into the analytical GC column for analysis. In this way, the very wide slow-pyrolysis plug can be narrowed to an acceptable width as well as preconcentrating trace analytes to detectable levels.

Comprehensive two-dimensional gas chromatography (GCxGC) is a technique that utilizes two columns of different selectivities, connected in series, to increase resolution and peak capacity. The columns are joined by a modulator. The purpose of the modulator is to collect several seconds of effluent from the first column or first dimension, focus it into a narrow plug, and rapidly inject it onto the second column, or second dimension, where a rapid separation is performed every cycle, or modulation period. In the most commonly used configuration, a longer column, often 10 to 30 m in length, with a non-polar stationary phase, such as polydimethylsiloxane, is used in the first dimension. A shorter, generally 0.5 to 2 m, narrower bore column with a polar stationary phase, often a wax, is used in the second dimension. The conditions used are such that the elution bands at the end of the first dimension are significantly wider than would be observed under conditions optimized for a single column separation. As these elution bands exit the first dimension column, they enter the modulator, where they are focused into a narrow plug and injected onto the short second dimension, where a second rapid separation is performed. The second dimension column is usually of a narrower bore than the first dimension column in order to increase velocity on the second column. This is necessary because each second dimension separation must be completed before

the next desorption of the modulator. The modulator functions in such a fashion that all effluent from the first dimension column is transferred onto the second dimension column. The signal, as seen from the detector, is that of a series of short second dimension chromatograms, one for every modulation period. There are two primary classes of modulators in use today, thermal modulators and flow modulators. The thermal modulator uses temperature variations to focus and re-inject analytes in the modulator. Flow modulators uses pressure variations to control flow in the modulator. Examples of thermal modulators are a slotted, rotating heater that would sweep over the modulator to desorb analytes trapped in the modulator[16], a movable cryogenically cooled zone[17], a set of hot and cold gas jets[18] and a modulator utilizing a stream of cold gas and a resistively heated capillary.[19] A modulator using differential flow has been described by Seeley, et. al.[20,21]

BACKGROUND

Sorption-based Preconcentrator - Sorption-based devices have been used as sample collection devices.[22,23,24,25] They have advantages over bags and canister sampling methods because of their small size and lower cost. In many cases, these devices consist of a single type of sorbent housed in a device through which the target atmosphere can be passed, and the desired analytes can be collected on the sorbent. Sorption-based sample collection methods still suffer problems resulting from loss of sample due to reactions of analytes with each other and with the adsorbent during transport and storage. By sampling on an adsorbent and then immediately desorbing the analytes into the analytical

column of a GC, these undesirable effects can be minimized. In this way, the sample collection device also serves as the inlet for the GC.

The design of the SPC involves several elements. The basic design is that of discrete beds of carbon-based adsorbents housed in a tube that can be resistively heated for thermal desorption. A first-generation SPC is housed in an 80 mm piece of Inconel 600 tubing, a nickel-chromium alloy, with an internal diameter of 1.30 mm. The adsorbent beds are packed between small plugs of glass wool with plugs of stainless steel mesh at the ends to hold the beds in place inside the tube (Figure 1).

A single-bed trap can be optimized for a single analyte or a simple mixture of similar analytes. A complex mixture of many different analytes requires a different approach. While a relatively strong adsorbent is needed to trap very volatile components, that same adsorbent retains less volatile components so strongly that they may be difficult if not impossible to completely desorb from the sorbent bed. Less volatile components would be easier to desorb from a weaker adsorbent bed, but components that are more volatile would pass through the bed without being trapped. To address this, sorption-based preconcentrators utilizing multiple discrete beds of carbon-based adsorbents have been developed.[8,9,12,13] The order in which the sorbent beds are placed in the tube is critical to the proper functioning of the SPC. If the strongest sorbent bed were to be exposed to the less volatile components, trap function would be impaired due to desorption issues. The beds are arranged in the tube in a sequential fashion such that during sample collection, the first sorbent bed encountered is of the weakest sorbent. This bed traps the least volatile components. The beds increase in sorbent strength until the last bed. In this way, after passing through each bed, the least volatile components

remaining in the mixture are trapped in the next bed until the last bed, which is only exposed to the most volatile components.

To prevent memory effects and improve desorption efficiency, a reverse flow method is used. If the SPC were to be desorbed with the flow in the sampling direction, the least volatile components would be swept by the carrier gas onto the more strongly retaining sorbent beds. The memory effects resulting from reversing the order of the sorbent beds during sampling and desorption can be seen in Figure 2. Traces (a) and (b) were run using the specified bed order, as designed, with a flow reversal between sample collection and injection. Chromatogram (a) is the primary chromatogram, and (b) is a subsequent chromatogram obtained without additional sampling. This nearly featureless trace shows the absence of memory effects. Traces (c) and (d) were run with the SPC reversed so that the Carboxen 1000 bed was the first bed encountered. Here, very pronounced memory effects are observed. With the direction of flow through the SPC reversed during desorption, (a) and (b), the least volatile components pass directly into the analytical column. The most volatile components in the most strongly retaining sorbent bed then pass through the beds through which they passed at the lower sampling temperature and then onto the column. In this way, the most strongly retained compounds are never exposed to the strongest sorbent beds.

The adsorbents chosen for the SPC are all carbon-based materials. For the current version of the SPC, the sorbents used, from weakest to strongest, are Carbopack Y, Carbopack B, Carbopack X, and Carboxen 1000. The Carbopacks are made from graphitized carbon and the Carboxen 1000 is a molecular sieve. Information on these adsorbents can be found in Table 1. Determining the correct amount of adsorbent for

each bed is also critical to the correct functioning of the SPC. If the mass of the sorbent bed is too small, breakthrough can occur. This can lead to incomplete recoveries and memory effects. If the mass of the sorbent in the bed is too large, it will be more difficult to desorb the analytes as a narrow plug. This can be attributed to the increased time needed for heat transfer to the center of the sorbent bed and increased volume of the trap. Studies by Lu and Zellers determined the masses needed for a trap of similar design to be approximately 2.2 mg per sorbent bed for a trap diameter of 1.15 mm assuming analyte concentrations in the ppm or lower range for 1-L sample bags.[8,9] For the multi-bed trap it is desirable to have a total sorbent mass of less than 10 mg to minimize the pressure drop along the SPC.

Injection Plug Width and Systems Performance - The multi-bed, sorption-based preconcentrator serves as the injector for the GC. One important requirement for a GC injector is that the analyte plug that is injected onto the analytical column be as narrow as possible. The efficiency of the analytical column is defined by *H*, the height equivalent to a theoretical plate. The efficiency of the column is maximized as *H* is minimized. The height equivalent to a theoretical plate in capillary gas chromatography is calculated by using equation 1, the Golay Equation.

$$H = \frac{2D_g}{\bar{u}} + \frac{1+6k+11k^2}{24(k+1)^2}\frac{r^2}{D_g}\bar{u} + \frac{2}{3}\frac{k}{(k+1)^2}\frac{d_f^2}{D_s}\bar{u} \qquad (1)$$

The binary gas diffusion coefficient in the specified carrier gas, D_g, is expressed in cm^2/sec. The average carrier gas velocity $\bar{u}$ is expressed in cm/sec. The retention factor *k*, is defined as the quantity of the analyte in the stationary phase divided by the quantity of the analyte in the gas phase, and is unit-less. The radius of the analytical column *r*, is

expressed in cm. The film thickness of the stationary phase d_f, is also expressed in cm. Equation 1 is often written in the shortened form shown in equation 2.

$$H = \frac{B}{u} + \left(C_g + C_s\right)\bar{u} \qquad (2)$$

In equation 1, the first term, $\frac{2D_g}{\bar{u}}$, is the B term and accounts for band broadening due to longitudinal diffusion. The second term, $\frac{1+6k+11k^2}{24(k+1)^2}\frac{r^2}{D_g}$, is the C_g term and accounts for band broadening due to the resistance to mass transport in the gas phase. The third term, $\frac{2}{3}\frac{k}{(k+1)^2}\frac{d_f^2}{D_s}$, is the C_s term and accounts for band broadening due to the resistance to mass transport in the stationary phase. The Golay-Guiochon equation takes into account extra-column sources of band broadening through the addition of the term D_{ec}, as shown in equation 3.[26]

$$H = \frac{B}{u} + \left(C_g + C_s\right)\bar{u} + D_{ec}\bar{u}^2 \qquad (3)$$

The D_{ec} term is expanded in equation 4.

$$D_{ec} = \frac{\Delta t^2}{L(k+1)^2} \qquad (4)$$

The sum of the extra-column variances in the system Δt^2, where L is the column length, contains dead time contributions from the inlet, t_{inlet}, the outlet, t_{outlet}, and electronic contributions as shown in equation 5.

$$\Delta t = \sum\left(t_{inlet} + t_{outlet} + t_{electronic}\right) \qquad (5)$$

For the inlet and the outlet, the dead time is a function of their respective dead volumes and carrier gas volumetric flows. The electronic dead time is a function of the

electrometer and detector time constants. Detector dead time is not a major contributor to overall dead time in the case where a flame ionization detector (FID) is used. This is because the FID is an open cell detector and only an increase in the distance between the flame tip and the collector electrode would increase the detector dead time. In the case of a closed cell detector, such as a photo ionization detector (PID), which has a finite dead volume, the effect of dead volume may be much larger. In either case, assuming that electronic dead time is not a major contributor to overall dead time, the major contributor for system dead time is inlet flow and inlet dead volume. In the case of an in-line system, such as the SPC, the linear flow of the carrier gas in the analytical column is optimized to minimize H in the absence of the injector. This leaves inlet dead volume as the parameter that must be minimized in order to minimize the height equivalent to a theoretical plate for the overall system, thereby maximizing system efficiency.

For conditions where the linear velocity of the carrier gas in the SPC is low, thermal decomposition of some analytes is an area of concern. This is particularly true for thermally labile compounds, such as aldehydes and terpenes. When the carrier gas velocity is low, a compound's residence time in the heated portion of the SPC is increased. This increased exposure to the higher temperatures used to desorb the analytes from the sorbent beds increases the likelihood for them to experience thermal decomposition. For these thermally labile compounds, it is desirable to minimize their bed residence times during desorption. Since the volumetric flow rate is determined by the necessary carrier gas velocity on the analytical column, the approach needed to minimized bed residence time is to decrease the volume of the tube housing the SPC, thereby increasing the carrier gas velocity over the sorbent beds.

Pyrolysis - Pyrolysis is used to desorb compounds from a solid or liquid matrix as well as to fragment large molecules into smaller, more volatile pieces. Pyrolysis is defined as "the application of thermal energy to a sample in the absence of oxygen."[27] Analytical Pyr-GC is commonly used for the analysis of polymers and humic organic matter.

In analytical pyrolysis, there are two common techniques, slow pyrolysis and flash pyrolysis. In slow pyrolysis, the sample is heated slowly to the desired pyrolysis temperature. Slow pyrolysis is generally used when larger samples are required. This is because the larger volume samples require longer for heat to transfer from the outer surface to the center of the sample. By using slow pyrolysis where the temperature is raised in steps, the pyrolysis products generated at different temperatures can also be investigated. In cases where a pyrolysis oven is used, slow pyrolysis is the only option. A representative low pyrolysis temperature ramp rate is generally in the 0.3 °C/sec range and a sample can weigh several grams. In flash pyrolysis, the sample is heated to the pyrolysis temperature as rapidly as possible. A commercial pyrolysis instrument, the CDS PyroProbe 2000, is available in our laboratory. The maximum programmable temperature ramp is 20,000 °C/sec (nominal) with a maximum temperature of 1400°C. This equates to a total ramp time of approximately 69 milliseconds for a ramp from 25 °C to the maximum temperature of 1400 °C. It is unlikely that heating is this fast. The need for rapid heat transfer necessitates very small sample sizes. For the PyroProbe 2000, it is recommended that the maximum sample mass be no larger than approximately 100 μg. For Pyr-GC, flash pyrolysis is more desirable because the very short pyrolysis time helps to minimize the width of the injection plug introduced into the analytical column as well as reducing post-pyrolysis sample alterations.

The CDS PyroProbe 2000 is the most commonly used pyrolysis inlet for Pyr-GC. A schematic of the probe/interface is seen in Figure 3. It consists of a heated interface, which is fixed in place on the standard split/splitless injector of an Agilent 6890 GC, and a probe, which is inserted into the interface for pyrolysis. The 6890 is part of a Leco Pegasus III GC-TOFMS system. The sample is placed into a 1.9 mm i.d. quartz tube approximately 25 mm in length. The end of the probe is hollow and contains a coiled platinum wire, which is resistively heated. The sample is placed between two plugs of quartz wool in the center of the quartz tube. The tube is inserted into the center of the wire coil in the end of the probe. The probe is then inserted into the heated interface. The chamber in the interface is purged with helium, or whichever pyrolysis gas is desired. At this time the purge gas is vented and the carrier gas bypasses the interface directly to the column. If the sample contains water, and the interface is heated above 100 °C, the sample can be dried by leaving the system in the purge position until the water vapor is vented. The interface valve is then switched so that the carrier gas passes through the interface and pyrolysis can be initiated. As the sample is pyrolyzed, the pyrolysate is swept from the sample tube onto the analytical column. From this point the analysis progresses as a normal GC analysis.

For the analysis of sediment and solid samples for organic matter, this system has two weaknesses. If the target analytes occur at trace levels in the sample, the sample size necessary to obtain detectable levels can rapidly exceed the sample capacity of the inlet. Second, any analytes that are not volatile at ambient temperature, but are volatile at the drying temperature, can be lost from the purge vent during the drying process.

Comprehensive Two-Dimensional Gas Chromatography – The initial pioneering work in two-dimensional gas chromatography was done by John Phillips, et al. in the early 1990's.[28] It has become a valuable technique for the analysis of complex samples, such as in the petroleum industry[29], the fragrance industry[30], the food industry[31], environmental analysis[32], and metabolomics[33], where co-elutions in single dimension separations are commonplace in samples that often contain hundreds or thousands of components. Each component in a two-dimensional chromatogram has two distinct retention times, one on the first column and one on the second column. Since these two separations are ideally performed on columns with separation mechanisms that are independent from each other, the two retention times are features of each component and reduce the possibility of coelutions. A two-dimensional chromatogram is often presented as a "contour plot", where retention time on the first column is plotted on the *x*-axis, retention time on the second column is plotted on the *y*-axis and intensity is plotted on the *z*-axis. This results in the peaks being distributed along a plane instead of along a single axis. The peak capacity is the product of the peak capacities of each individual axis on the retention plane.

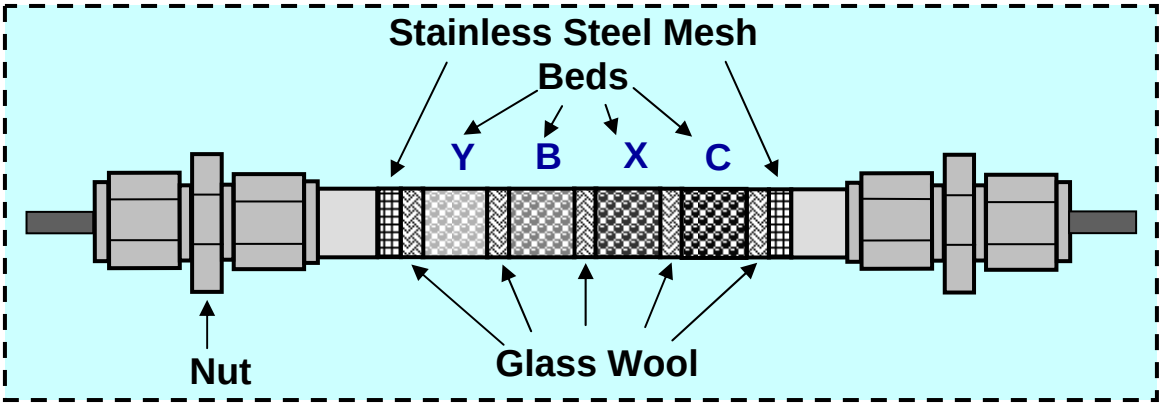

Figure 1.1 – A schematic of the multi-bed sorption-based preconcentrator (SPC)

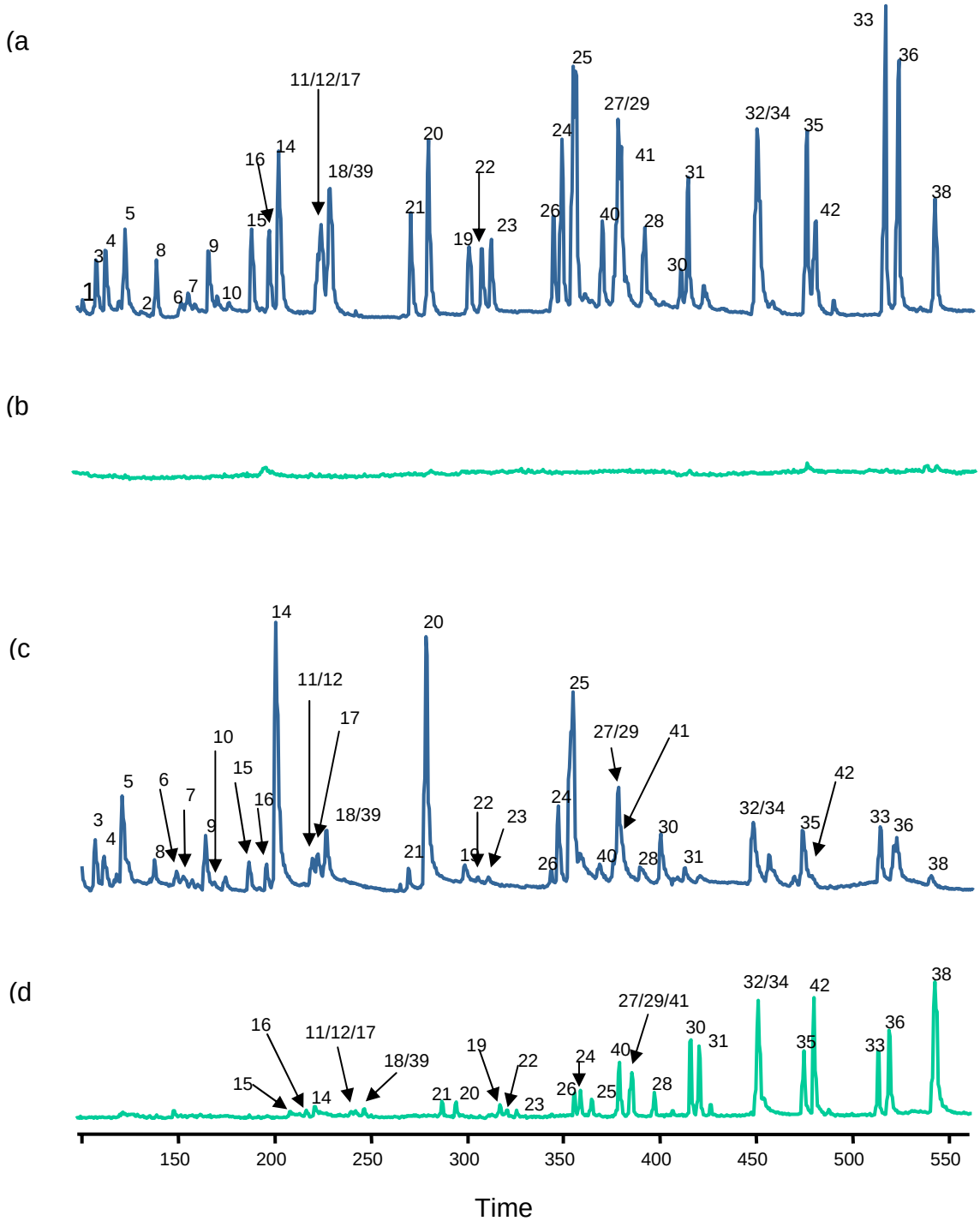

Figure 1.2 - Chromatograms showing the analysis of a 42 component synthetic mixture.
(a) initial chromatogram for normal trap configuration
(b) memory effect chromatogram for normal trap configuration
(c) initial chromatogram for reverse trap configuration
(d) memory effect chromatogram for reverse trap configuration

Symbol	Adsorbent	Mesh	Surface (m^2)	Density ((g/mL)	Application
Carbon Molecular Sieve					
C	Carboxen 1000	60/80	1200	.44	C2 to C5
Graphitized Carbon					
Y	Carbopack Y	40/60	25	.42	C12 to C20
B	Carbopack B	60/80	100	.36	C5 to C12
X	Carbopack X	40/60	250	.41	C3 to C5

Table 1.1 - Adsorbents used in the multi-bed trap and their characteristics

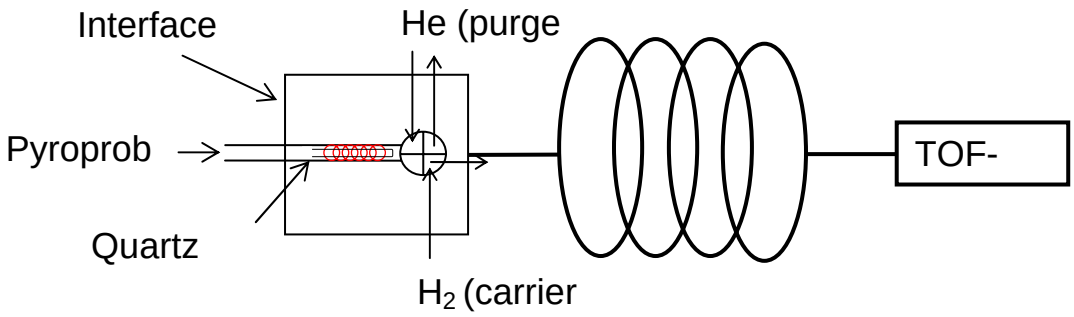

Column: 7.0 m Rtx-5 (0.18 mm id, 0.20μm

Sample: 10-100 μg sample between plugs of glass wool in a quartz tube

Interface: set at any temperature up to 350°C with a heating rate up to 60°C/minute

Pyroprobe: set at any temperature up to 1400°C with a heating rate up to 20,000°C/s

Figure 1.3 – A schematic of the probe/interface of the CDS PyroProbe 2000

REFERENCES

[1] Dewulf, J.; VanLangenhove, H. *Atmos. Environ.* **1997**, *31*, 3291.
[2] Woolfenden, E. *J. Air Waste Manage. Assoc.* **1997**, *47*, 20.
[3] Dewulf, J.; VanLangenhove, H. *J. Chromatogr. A*, **1999**, *843*, 163.
[4] Cao, X.; Hewitt, C. *J. Chromatogr. A*, **1994**, *688*, 368.
[5] Helming, D. *J. Chromatogr. A*, **1996**, *732*, 414.
[6] Dettmer, K.; Knobloch, T.; Engewald, W. *Fresenius J. Anal. Chem.* **2000**, *366*, 70.
[7] Whiting, J.; Sacks, R. *Anal. Chem*. **2003**, *75*, 2215.
[8] Lu, C.; Zellers, E. *Anal. Chem*. **2001**, *73*, 3449.
[9] Lu, C.; Zellers, E. *Analyst* **2002**, *127*, 1061.
[10] Feng, C.; Mitra, S. *J. Chromatogr. A*, **1998**, *805*, 169.
[11] Grote, C.; Pawliszyn, J. *Anal. Chem*. **1997**, *69*, 587.
[12] Sanchez, J.M.; Sacks, R.D. *Anal. Chem*. **2003**, *75*, 978.
[13] Sanchez, J.M.; Sacks, R.D. *Anal. Chem*. **2003**, *75*, 2231.
[14] *http://www.dictionary.com*
[15] *http://nasc.uwyo.edu/coal/library/glossary.asp*
[16] Phillips, J.; Gaines, R.; Blomberg, J.; van der Wielen, F.; Dimandja, J.; Green, V.; Grainger, J.; Patterson, D.; Racovalis, L.; de Geus, H.; de Boer, J.; Haglund, P.; Lipsky, J.; Sinha, V.; Ledford, E. *J. High Res. Chromatography*, **1999**, *22*, 3.
[17] Marriot, P.; Kinghorn, R. *Anal. Chem.*, **1997**, *69*, 2582.
[18] Ledford, E.; Billesbach, C. *J. High Res. Chromatography*, **2000**, *23*, 202.
[19] Libardoni, M.; Waite, J.; Sacks, R. *Anal. Chem.*, **2005**, *77*, 2786.
[20] Seeley, J.; Kramp, F.; Hicks, C. *Anal. Chem.*, **2000**, *72*, 4326.
[21] Seeley, J.; Bueno, P. *J. Chromatogr. A.*, **2004**, *1027*, 3.
[22] Mitra, S.; Xu, Y.; Chen, W.; Lai, A. *J. Chromatogr. A*, **1996**, *727,* 111.
[23] Groves, W.; Zellers, E.; Frye, G. *Anal. Chim. Acta*, **2001**, *73*, 3449.
[24] Peng, C.; Batterman, S. *J. Environ. Monit.*, **2000**, *2*, 313.
[25] Helmig, D.; Vierling, L. *Anal. Chem.*, **1995**, *67*, 4380.
[26] Gaspar, G.; Annino, R.; Vidal-Madjar, C.; Guiochon, G. *Anal. Chem*. **1978**, *50*, 1512.
[27] Settle, F. *Handbook of Instrumental Techniques for Analytical* Chemistry, Prentice Hall, 1997, pg. 895.
[28] Liu, Z.; Sirimanne, S.; Patterson, D.; Needham, L.; Phillips, J. *Anal. Chem.*, **1994**, *66*, 3068.
[29] Blomberg, J.; Schoenmakers, P.; Beens, J.; Tijssen, R. *J. High Res. Chromatography*, **1997**, *20*, 539.
[30] Shellie, R.; Marriott, P.; Cornwell, C. *J. High Res. Chromatography*, **2000**, 23, 554.
[31] Hoogenboom, L.; Traag, W.; Bovee, T.; Goeyens, L.; Carbonnelle, S.; van Loco, J.; Beernaert, H.; Jacobs, G.; Schoeters, G.; Baeyens, W. *Trends in Anal. Chem.*, **2006**, *25*, 410.
[32] Phillips, J.; Xu, J. *Organohalogen Compd.*, **1997**, *31*, 199.
[33] Libardoni, M.; Stevens, P.; Waite, J.; Sacks, R. *J. Chromatogr. B.*, **2006**, *842*, 13.

CHAPTER 2

VACUUM-OUTLET GC OF LARGE-VOLUME AIR SAMPLES USING AN IN-LINE MULTIBED SORPTION TRAP, AT-COLUMN HEATING, AMBIENT AIR AS CARRIER GAS AND PHOTOIONIZATION DETECTION

Introduction

Instrumentation for on-site GC is evolving rapidly. Emphasis in recent developments is on new column heating techniques that require no convection oven [1,2,3,4], micro-scale in-line preconcentrators and inlet devices [5,6,7,8,9,10], solid-state sensor detectors [11,12,13] and techniques for the enhancement of column selectivity.[13,14,15] These devices and techniques are being developed to incorporate in micro-fabricated vapor analysis systems. [15,16,17]

While most GC instruments designed for on-site analysis require the use of compressed gases, both for carrier gas and detector gas, some recent efforts have addressed the use of vacuum-outlet GC with ambient air as the carrier gas and detection devices that require no on-board gas supplies [14,18,19]. This reduces the need for consumables to only electrical power and thus provides a high level of instrument autonomy. However, the use of air as the carrier gas poses several problems including relatively poor column efficiency at high carrier gas flows and, in some cases, rapid stationary phase decomposition at elevated temperatures. Both polar and non-polar fused-silica open-tubular columns using dimethyl polysiloxane and trifluoropropylmethyl

polysiloxane stationary phases, respectively have been shown to be sufficiently robust for extended use in air for both dry and wet samples at temperatures up to about 200 °C.

Micro-fabricated sensors, including surface acoustic wave devices [11,12] and chemiresistor devices [13] have been developed for GC detection with miniaturized and micro-fabricated instruments. While these devices hold great promise, robustness and sensitivity remain significant challenges. Photoionization detectors (PID), which require no support gases, are available, robust and satisfactory for use with vacuum-outlet GC and air as the carrier gas. In addition, PID's are very sensitive for aromatic compounds as well as other compound classes of interest in atmospheric monitoring.

Many organic compounds found in the atmosphere are present at very low concentrations, and numerous sorption-based preconcentration devices, which remove organic compounds from large-volume air samples, have been described. [5,6,7,8,9,10] Thermal desorption is usually used to liberate the organic compounds from the preconcentrator, but usually, an additional focusing step, often involving the use of a cryo-trap, is needed to obtain a sufficiently narrow injection plug width for GC analysis [20]. Sample loss, contamination and decomposition are often associated with these preconcentration techniques, particularly when they are used off-line. [9,15,21,22]

Recently, an in-line preconcentrator (trap) has been described that effectively reduces many of these problems. [9,10] The device uses a four-bed sorption trap consisting of three beds of different grades of graphitized carbon and one bed of carbon molecular

sieves. The beds are arranged with the weakest adsorbent located at the upstream end of the trap and the strongest adsorbent at the downstream end during sample collection. The device quantitatively removes most organic compounds from both dry and wet samples. The graded strength of the beds coupled with a reversal in the direction of the gas flow through the device between sample collection and desorption results in relatively small vapor plug width, which allow for direct injection into the column without an additional focusing step. Previous studies have shown that complete desorption of 46 compounds more volatile than *n*-C_{12} occurs at a desorption temperature of 300 °C with no memory effects. The compounds studied included hydrocarbons, organic chlorides, alcohols and carbonyl compounds.

Previous studies with this preconcentrator involved a conventional GC using flame ionization detection and hydrogen carrier gas. [9,10] The work described here combines the preconcentrator with at-column heating of a fused-silica capillary column and a PID operated at reduced pressure with ambient air carrier gas to obtain a GC system compatible with the needs of on-site monitoring of large-volume atmospheric samples. Instrument design and performance are considered. The effects of extra-column band broadening are described. The issue of sample decomposition during desorption is considered for a range of compound functionalities. These studies provide guidelines for the establishment of performance limits for ambient-air driven GC instruments for environmental applications.

Experimental Section

Apparatus - The complete system is shown in Figure 1. Gas flow control through the trap, T, is provided by miniature valves V_1 and V_2 (Model LFVA1230113H, The Lee Co., Westbrook, CT). To collect a sample, both valves are opened and vacuum pump VP_2 (Model UN86KNI, KNF Neuberger Inc., Trenton, NJ) pulls the air sample through the trap at a flow rate of 80 cm^3/min. Bold lines with arrows indicate the gas flow directions during sampling and analysis. After sample collection is complete, both valves are closed and vacuum pump VP_1 pulls carrier gas (ambient air) through hydrocarbon trap HC, capillary restrictor R, the trap, the column and the PID. The restrictor (50 cm x 0.25 mm I.D. deactivated fused-silica capillary tubing) is needed to limit the carrier gas flow to VP_2 during sample collection.

The 10.0 m x 0.25 mm I.D. fused-silica wall coated capillary column was wrapped with heater wire and sensor wire for at-column heating. The assembly is wound into a toroid about 7 cm in diameter and then wrapped in metal foil. The column assembly and the computer board used for column temperature control were manufactured by RVM Scientific, Santa Barbara, CA. Connecting lines with independent heating are also provided by the manufacturer. The column used a 0.25 μm thick film of 5% phentl, 95% dimethyl polysiloxane (DB-5, J & W Scientific, Folsum, CA).

The PID used in this study (Model PI-52-02A, HNU, Newton, MA) has a cell volume of less than 100 μL as stated by the manufacturer and used a 10.2 eV lamp. In

order to increase flow rate through the PID, make-up gas (ambient air) is introduced to the gas flow from the column. A needle valve (model SS-SS2, Nupro, Willoughby, OH) is used to control the make-up gas flow. Flow rates are measured with a soap bubble flow meter (Alltech, Deerfield, IL). All component connections in the flow path from the sorption trap to the detector are low-dead-volume all glass splitters (Alltech, Deerfield, IL).

Material and Procedures - The compounds listed in Table 1 were used to challenge the preconcentrator. These compounds were chosen to include a variety of functionalities with consideration of the response characteristics of the PID. Saturated aliphatic hydrocarbons show low response relative to the compounds in Table 1, and were not included in the test mixture. Individual components or mixtures were injected as liquids into 12 L gas sample bags (SKC Inc., Eighty Four, PA) and diluted with either dry air or air that was saturated with water vapor. Concentrations in the diluted samples were in the range from 8 ppm to 35 ppm (v/v). The amount of sample challenging the sorption trap was controlled by adjustment of the sampling time.

Results and Discussion

Operating Conditions and Extra-Column Band Broadening - The use of vacuum-outlet GC with ambient air as carrier gas provides for more autonomous instrument operation since electrical power is the only consumable. However, the constraint of a one atmosphere pressure drop through the system limits both average carrier gas velocity and volumetric flow rate of carrier gas at the inlet. These limitations

can effect the dead time of both the detector and the sorption trap inlet, as well as column efficiency.

For the case where the inlet pressure, p_i, to outlet pressure, p_o, is greater than about 5, which is readily achievable with vacuum outlet GC, the average carrier gas velocity, u, the volumetric flow rate at the column inlet, F_i, and the volumetric flow rate at the column outlet, F_o, are given by equations 1-3 respectively [14,18,19],

$$u = \frac{3r^2 p_i}{32\eta L} \qquad (1)$$

$$F_i = \frac{\pi r^4 p_i}{16\eta L} \qquad (2)$$

$$F_o = \frac{\pi r^4 p_i^{\,2}}{16\eta L p_o} \qquad (3)$$

where η is the carrier gas viscosity at the column temperature, r, is the column radius and L, is the column length.

Note that neither u or F_i is dependent on the outlet pressure for the case where the inlet-to-outlet pressure ratio is relatively large. In conventional GC, variation of the inlet pressure is a convenient means for adjusting u. However, in the work reported here, the inlet pressure is fixed at ambient pressure, and thus the average carrier gas velocity and the inlet flow rate reach upper limits as the outlet pressure is reduced. For the conditions used in this study, the maximum carrier gas velocity is about 86 cm/s at the starting

column temperature of about 30 °C and the maximum inlet flow rate is about 1.8 cm^3/min, or about 3 μL/s. Note that both of these values decrease slightly with increasing temperature because of the increase in carrier gas viscosity.

Unlike F_i and u, which become independent of p_o for sufficiently small values of p_o, F_o scales inversely with p_o. Thus, at a sufficiently low outlet pressure, F_o should be sufficiently large to minimize extra-column band broadening from the PID. However, a large value for F_o does result in smaller peak areas due to the dilution of the sample vapor. Note that for air as a carrier gas, optimal carrier gas velocity (the value giving the minimum height equivalent to a theoretical plate) is substantially lower than with hydrogen or helium as the carrier gas, and loss of efficiency with increasing velocity above the optimal value is much greater with air [19].

Figure 2 shows the effects of make-up gas and outlet pressure on the qualitative features of the chromatograms from the separation of a five component mixture. For all chromatograms, the column temperature was 30 °C for 60 s, followed by a linear ramp of 10 °C/min to 150 °C. Peak numbers correspond to compound numbers in Table 1. For chromatogram (a), p_o was 0.7 atm and no makeup gas was used. For chromatogram (b), p_o was maintained at 0.7 atm, and detector make-up gas (ambient air) was added at a flow rate of about 5 cm^3/min at ambient pressure. For chromatogram (c),), p_o was 0.25 atm, and no make-up gas was used.

Chromatogram (a) shows broad peaks with obvious tailing. Inadequate resolution is obtained for peaks 3 and 4. The chromatogram is complete in about 380 s. For chromatogram (b), the peaks are much narrower and have smaller areas. Baseline resolution, is obtained for components 3 and 4. For chromatogram (c), retention times are smaller by a factor of two and both peak shapes and areas are comparable to those in chromatogram (b). The resolution of peaks 3 and 4 in chromatogram (c) is poorer than in chromatogram (b), but still adequate.

The use of larger volumetric flow in the detector in order to achieve reduced detector dead time is demonstrated in both chromatograms (b) and (c), but the additional flow is obtained by added gas in (b) and by carrier gas decompression in (c). Note, that in both cases, dilution from the increased flow results in large reductions in peak area. At the lower pressure used for chromatogram (c), the average carrier gas (ambient air) velocity is about twice that obtained at the higher outlet pressure. The result is a faster separation but with somewhat poorer column efficiency.

Quantitative data on system efficiency is shown in Figure 3 for the isothermal separation of 3-octanone at 36 °C. The retention factor for *n*-octanone at this temperature is 9.5. Make-up gas was used to minimize extra-column band broadening in the detector. Plot (a) (Golay Plot), shows the height equivalent to a theoretical plate, *H*, versus average carrier gas velocity, and plot (b) shows the height equivalent to a theoretical plate versus column outlet pressure. Each point represents the average of five injections at the indicated outlet pressure, and error bars show standard deviations. Because of substantial

extra-column band broadening from the sorption trap inlet, these plots show the efficiency of the complete system.

The optimal average carrier gas velocity, u_{opt}, for the column used here was computed by the use of equation 4. [19]

$$u_{opt} = \frac{C(k) D_{go} f_2}{r} \qquad (4)$$

Where *C(k)* is a function of retention factor only, f_2 is the Martin-James gas compression correction[23] and D_{go} is the binary diffusion coefficient of the solute in air at the column temperature and outlet pressure. Equation 4 neglects solute band broadening from extra-column sources and broadening in the stationary phase, which is a reasonable approximation for the 0.25 mm I.D. x 0.25 μm film column used here. A value of 0.08 cm^2/s for D_{go} at 1.0 atm outlet pressure was used. This value is typical for VOCs in air. The value for D_{go} used in equation 4 is given by D_{go} (1atm)/p_o. For the conditions used here, the value for u_{opt} occurs at a P_o of 0.87 atm and has a linear velocity of 15.4 cm/s and a volumetric flow of 0.453 mL/min. Thus all data presented in Figure 3 represent average carrier gas velocity values that are substantially greater than the optimal value.

In a previous study, injection plug widths, for a sorption trap inlet of similar design and dimensions, were measured for polar and non-polar compounds with boiling points in the *n*-C_5 to *n*-C_{12} range. Most values (full width at half height) were in the range of 0.7 s to 1.3 s for a column inlet flow rate of 1.7 cm^3/min (28 μL/s). Since the

dead volume connecting the sorption trap to the column is about 14 μL, the corresponding dead time is about 0.5 s and this may set a lower limit on the injection plug width. For the vacuum-outlet system used here, the carrier gas flow rate (column inlet flow) ranges from 1.75 cm^3/min for an outlet pressure of 0.25 atm to 1.0 cm^3/min at an outlet pressure of 0.7 atm. Thus, over the entire range of outlet pressures in Figure 3, injection plug widths are expected to be at least 0.7 to 1.3 s and substantially larger values may occur at the higher p_o values where volumetric flow rate at the inlet is low.

The plots in Figure 3(a) reflect reduced extra-column band broadening from the sorption trap and increased band broadening from poorer column efficiency with increasing u (decreasing p_o). The minimum plate height occurs with a u value of about 65 cm/s corresponding to an outlet pressure of 0.5 atm. At this pressure, about 7500 plates are obtained from the system. At higher u values, H decreases more rapidly due to reduced column efficiency. Note that the range of plate height values in Figure 3 is relatively small and all further work was performed with a p_o value of 0.25 atm. This results in substantial reductions in analysis time with a relatively small loss in component-pair resolution relative to a p_o value of 0.5 atm.

Figure 4 shows the chromatogram of a 16 component mixture obtained with a p_o value of 0.25 atm. The initial column temperature was 30 °C and a 10 °C/min ramp to 60 °C was initiated 1.0 min after the injection. No make-up gas was used. Peak numbers correspond to component numbers in Table 1. Some peak tailing is observed, especially for the early eluting peaks. This tailing may be the result of detector dead volume.

Peak Area Linearity with Sample Mass - The mass of analyte challenging the sorption trap was varied by adjustment of the sample collection time. Sample concentrations in the gas sampling bag were in the range from 8 ppm to 35 ppm. Analytical curves of log (peak relative area) versus log (sample collection time) were generated for a number of compounds in Table 1 using samples prepared with dry air and with water saturated air. Sample collection times varied from 2.5 s to 20 s. Examples for the wet samples are shown in Figure 5. Slopes of the log-log plots and correlation coefficients for both the dry and wet samples are presented in Table 2.

Very good linearity is observed. All r^2 values are greater than 0.991, and 18 of the 25 values in Tablle 2 are greater than 0.997. Slope values are all near the 1.00 value expected for complete peak area linearity with sample collection time. The greatest deviation from linearity is for acetone (Plot 1 in Figure 5). Previous studies have suggested that some sample loss from the trap occurs for very volatile polar compounds, including acetone, in wet samples because of retention and breakthrough of water from the carbon molecular sieve bed in the multi-bed trap . The other (graphitized carbon) beds do not retain significant water.

Sample Decomposition - Sample decomposition of airborne VOCs during collection, transport and injection to the GC are important issues. Collection of air samples in electropolished canisters, followed by cryogenic or sorbent preconcentration and GC analysis is an established EPA method.[24,25] Canister sampling techniques,

however, are more complicated than sorbent-trap techniques. They also require sophisticated equipment for cleaning and cannot be used for real-time measurements.[26,27,28] Batterman et al. evaluated the stability of some aldehydes and terpenes in electropolished canisters and found that recoveries, for all terpenes and most aldehydes evaluated, dropped substantially within the first hour, followed by a more gradual decrease [29].

In-line sorption traps allow for immediate analyte injection to the GC column after sample collection is complete. This eliminates the risk of sample loss and decomposition during transport and storage. An important problem in the use of sorbent-trap technique is the relatively high temperature required for the complete and rapid desorption of the trapped compounds, which can lead to extensive thermal decomposition of some analytes.[30]

Biogenic volatile organic compounds are of great interest in the analysis of outdoor and indoor air. Large quantities of reactive compounds, including terpenes and oxygen-containing terpene structures, are emitted into the atmosphere by vegitation.[31,32,33] Some terpenes are readily oxidized and both the emitted compounds and their oxidation products are found in air and aerosol samples.,[34] Terpene concentrations in the atmosphere are increasing, due in part to the increased use of natural products including wood, terpene-based cleaning solvents and fragrances. The low-boiling-point monoterpenes are the most ubiquitous, and α- and β-pinene and carene have attracted significant attention.[25]

Stability of terpenes has been widely evaluated because of their reactivity and atmospheric relevance.[35,36,37,38 39,40,41,42,43,44,45,46] Thermal degradation of terpenes often yield different terpenes and aromatic compounds.[35,37,38,41] The chemistry of terpenes adsorbed on carbon-based materials is complex, and the higher temperatures required for the complete and rapid desorption from these materials may lead to extensive decomposition of the trapped compounds.[47,48,49] If any of these degradation products are also targeted analytes, false positives and quantification errors will occur. Previous studies showed different and contradictory results. Some reported degradation of terpenes at desorption temperatures as low as around 200^{o}C.[37,38,39] Others did not report degradation after heating the sorption-trap to 220-250^{o}C, whereas others found decomposition of α- and β-pinene at temperatures between 90^{o}C and 130^{o}C.

The work reported here is unique in that ambient air is used as carrier gas and thus is present in the trap during sample desorption. The presence of air and possibly traces of more reactive gases including NO_x and O_3 may increase thermal decomposition of sensitive compounds. Figure 6 shows results of a study of the decomposition of α-pinene (A) and β-pinene (B) using hydrogen carrier gas (solid lines) and air carrier gas (broken lines). Peak areas for the different desorption temperatures are individually normalized for the four plots to a value of 100 for the lowest desorption temperature (200 ^{o}C). The plots for hydrogen used the same multi-bed sorption trap but with a previously described instrument with pressurized hydrogen as carrier gas and flame ionization detection at ambient outlet pressure. Dry air samples were used in all cases.

With hydrogen carrier gas, normalized peak areas are nearly the same for desorption temperatures of 200 and 250 ^{o}C suggesting complete analyte recovery. Some loss in peak area is seen for both compounds in hydrogen at 300 ^{o}C with α-pinene showing the greater loss. The rate of loss of peak area with increasing desorption temperature is greater for both compounds for temperatures above 300 ^{o}C. Sample recoveries of only about 10% are observed for a desorption temperature of 385 ^{o}C. With air as carrier gas, sample decomposition is more extensive than with hydrogen as carrier gas. A significant decrease in peak area is observed for desorption at 250 ^{o}C relative to desorption at 200 ^{o}C, and the data suggest that some sample decomposition may occur for a desorption temperature of 200 ^{o}C. Lower temperatures were not investigated because of the large increase in injection plug width.

Figure 7 shows similar plots illustrating the effects of analyte structure and molecular weight on the extent of sample loss by thermal decomposition with air as carrier gas. Plot numbers correspond to compound numbers in Table 1. No saturated hydrocarbons were evaluated because of the poor sensitivity of the PID for these compounds. The plots for benzene (5), 1,2-dichlorobenzene (22) and tetrachloroethylene (10) illustrate that common chlorinated solvents and aromatic compounds show little decomposition even with desorption temperatures as high as 385 ^{o}C.

The situation for aldehydes (plots 17 and 26) is much different with significant decomposition indicated for desorption temperatures of 250 ^{o}C or less. For temperatures

above 300 °C, heptaldehyde (17) shows less decomposition than butyralehyde(26). Plots 3, 4 and 8 are for a homologous series of ketones. Decomposition at higher desorption temperatures is less than for the aldehydes, and in most cases, decomposition is lower for the higher molecular weight compounds.

Figure 8 shows decomposition of some common biogenic compounds. Isoprene (Plot 2) is the building block (monomer) for the terpenes. The data from Figure 6 for α-pinene and β-pinene in air are repeated for comparison with the other compounds.

Previous studies for a very similar multi-bed sorption trap with hydrogen carrier gas used a desorption temperature of 300 °C, which showed relatively little decomposition for all the compounds used in this study. Clearly, that is not the case for air as carrier gas. At 300 °C in air recoveries of 2-carene, α-pinene and β-pinene are no greater than 60-80%, and the recovery of aldehydes may be less than 80%.

While the use of lower desorption temperatures may be attractive for increased recoveries of biogenic compounds, increased injection plug width is a problem (9). Narrower injection plugs may be obtained by stopping the carrier gas flow for several seconds during desorption, and restoring flow immediately after desorption is complete. However, this increases the contact time of the analytes with the hot sorption beds. Table 3 lists recoveries (peak areas) of some of the compounds in Table 1 at a desorption temperature of 385 °C with no stop flow and at 200 °C with a 5-s stop flow relative to the

peak areas obtained for a desorption temperature of 200 ^{o}C with no interruption of the carrier gas flow.

For benzene, 100% recovery is obtained for both the high-temperature desorption with no stop flow and the low-temperature desorption with the 5-s stop flow. Note that both isoprene and limonene show relatively good recoveries for desorption temperatures as high as 385 ^{o}C if carrier gas flow rapidly removes the analyte vapor from the hot sorption beds. However, recoveries of only 54% and 68%, respectively, are obtained at 200 ^{o}C with a 5-s stop flow relative to the 200 ^{o}C case with no stop flow. In several other cases in Table 3, greater recoveries are obtained for the lower desorption temperature with the 5-s stop flow.

Thus, the decomposition of thermally sensitive compounds is governed by both the desorption temperature and the contact time of the vaporized analytes with the hot sorption beds. When the contact time of analytes with the hot surface increases, sample recovery is reduced. A high rate of sample transport during desorption appears to be as important as desorption temperature when reactive compounds are analyzed using air as the GC carrier gas and the transport gas during sample desorption. This may explain the contradictory data in the literature regarding the effects of desorption temperature on analyte recovery.

Conclusions

The system described in this report should be suitable for the relatively rapid on-site analysis of volatile organic compounds in large volume air samples. A high degree of instrument autonomy is achieved by the use of ambient air as carrier gas for vacuum-outlet GC with PID detection. Only electrical power is required. At-column heating is used to reduce column-heating power requirements to a small fraction of the power required to heat a typical convection oven.

The use of an in-line, multi-bed sorption trap with a flow direction reversal between sample collection and desorption provides relatively narrow solute injection plugs for direct injection into the separation column at the normal column flow rate. However, with air as carrier gas, optimal average carrier gas velocity, even under vacuum-outlet conditions is low, and the outlet pressure giving the greatest number of theoretical plates represents a compromise between the need for relatively high outlet pressure (closer to one atmosphere) to achieve high column efficiency and the need for lower outlet pressure to achieve narrower injection plugs during trap desorption. Lower outlet pressure also achieves substantially faster analyses.

A significant limitation for the combination of the in-line multi-bed sorption trap and air as carrier gas is greater decomposition of some sensitive compounds including some environmentally significant terpenes as well as aldehydes and ketones. Decomposition is reduced with lower desorption temperatures and reduced contact time between the desorbed analytes and the hot sorption beds.

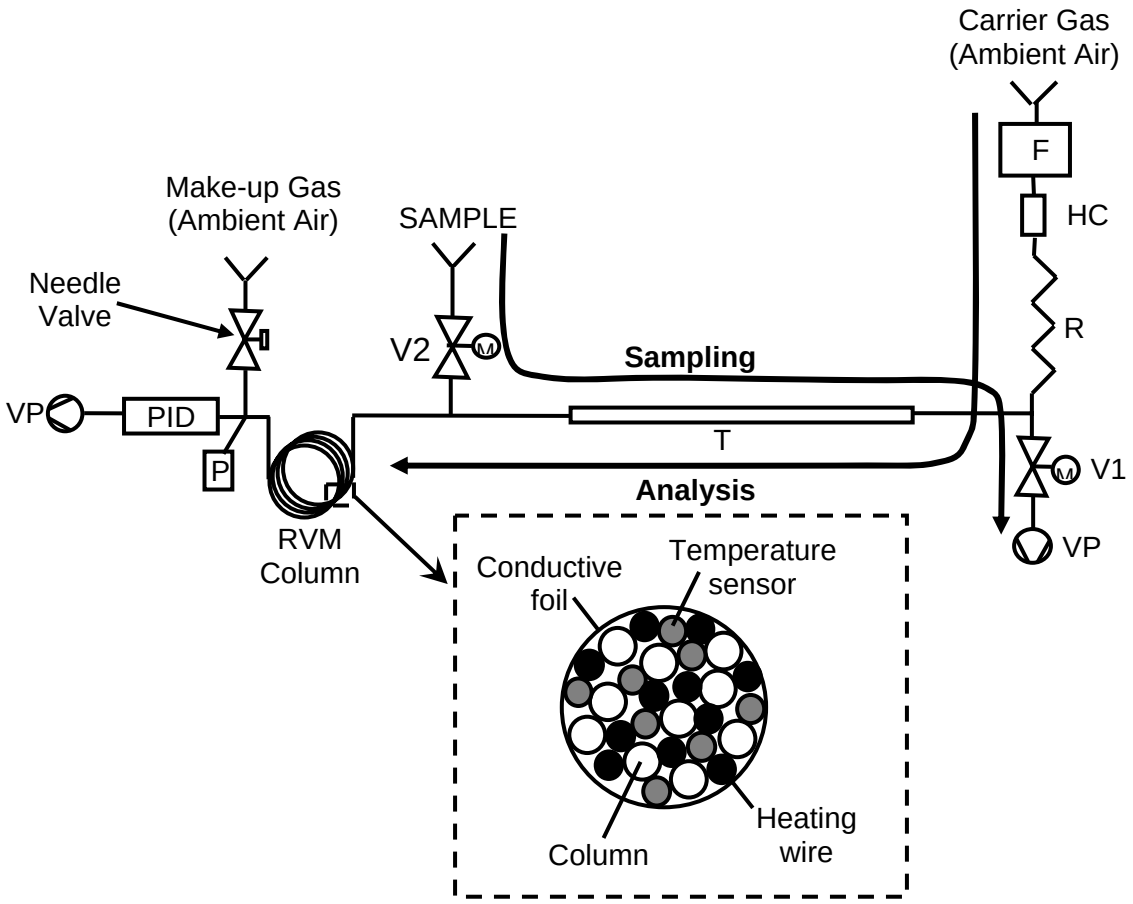

Figure 2.1 – Diagram of the complete GC system and detail of the cross-section of the low thermal mass RVM column. F, flow controller; HC, hydrocarbon trap; R, capillary restrictor; V_1, metering valve; VP, vacuum pump; T, multi-bed sorption trap; V_2, metering valve; P, pressure gauge; PID, photo ionization detector.

Peak number	Compound	Boiling point (^{o}C)
1	Acetone	56.2
2	Isoprene	34
3	2-Butanone	80
4	2-Pentanone	100-101
5	Benzene	80.1
6	Trichloroethylene	86.7
7	Toluene	110.6
8	2-Hexanone	127
9	Hexanal	131
10	Tetrachloroethylene	121
11	Chlorobenzene	132
12	m-, p-Xylene	138-139
13	Styrene	145-146
14	o-Xylene	143-145
15	2-Heptanone	149-150
16	α-pinene	155
17	Heptaldehyde	153
18	Cumene	152-154
19	Benzaldehyde	178-179
20	β-pinene	167
21	Limonene	175.5
22	1,2-Dichlorobenzene	180
23	1,2,3-Trimethylbenzene	175-176
24	1,2,4-Trimethylbenzene	168
25	3-Octanone	167-168
26	Butyraldehyde	75
27	2-Carene	167-168
28	3-Carene	
29	γ-terpinene	

Table 2.1 – List of test compounds and boiling points.

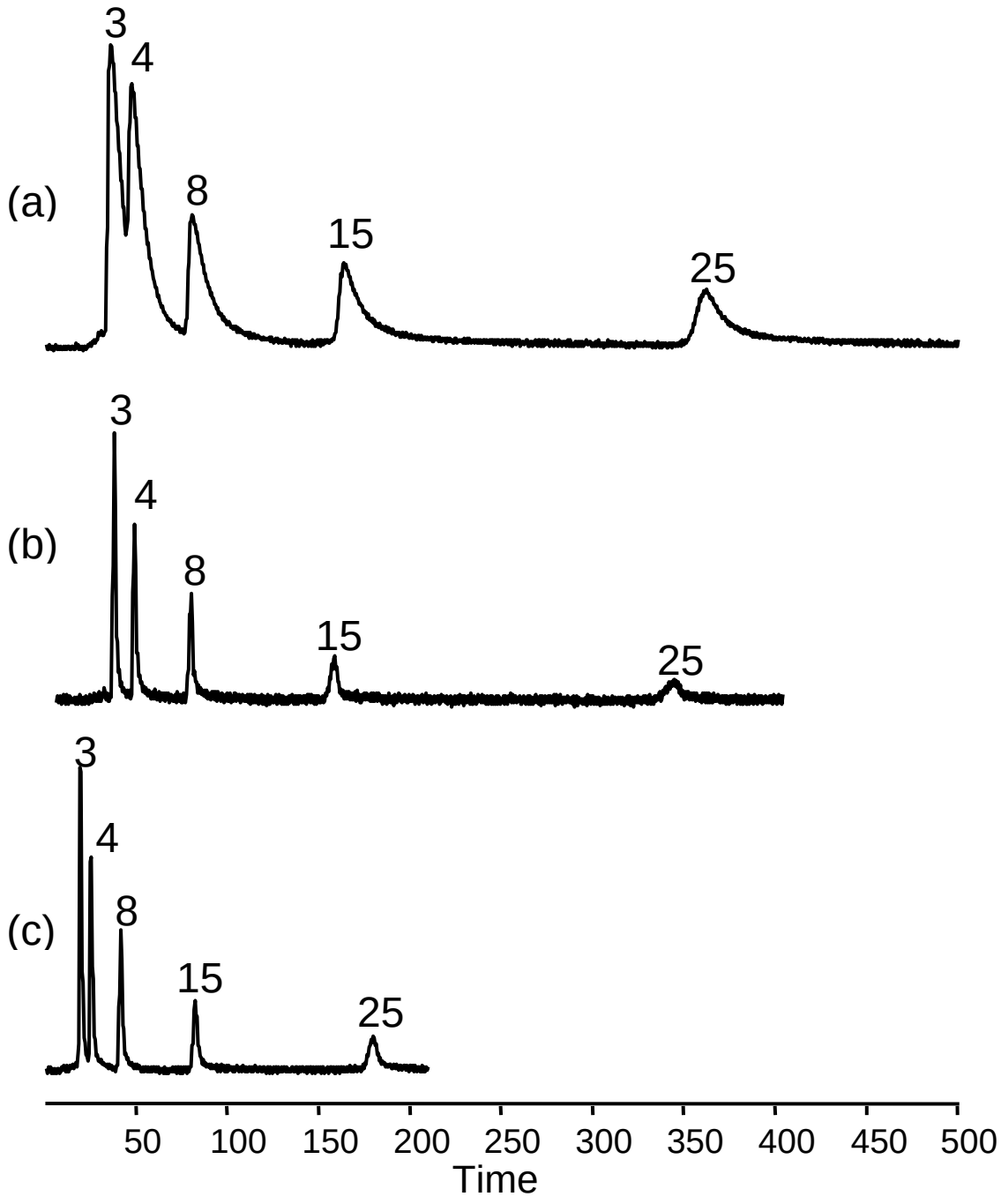

Figure 2.2 - The effects of make up gas and outlet pressure on the qualitative features of the chromatograms from the separation of a 5-component mixture. For chromatogram (a) p_o was 0.7 atm and no makeup gas was used. For chromatogram (b), p_o was maintained at 0.7 atm, and detector makeup gas (ambient air) was added at a flow rate of about 5 cm^3/min at ambient pressure. For chromatogram (c), p_o was 0.25 atm, and no makeup gas was used.

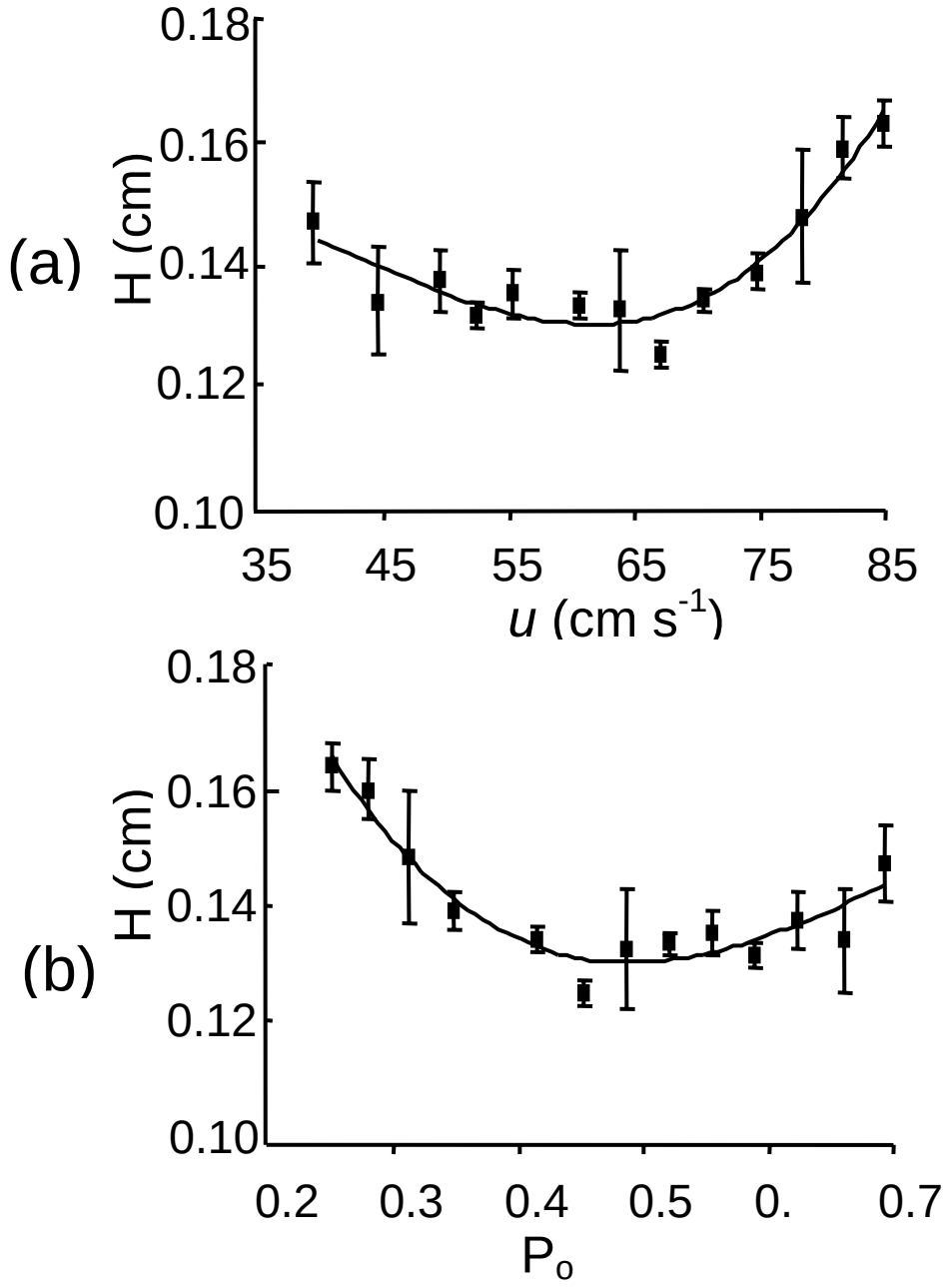

Figure 2.3 - Quantitative data on system efficiency for the isothermal separation of 3-octanone at 36 ^{o}C. Plot (a) (Golay plot), shows the height equivalent to a theoretical plate *H* versus average carrier gas velocity, and plot (b) shows the height equivalent to a theoretical plate versus column outlet pressure.

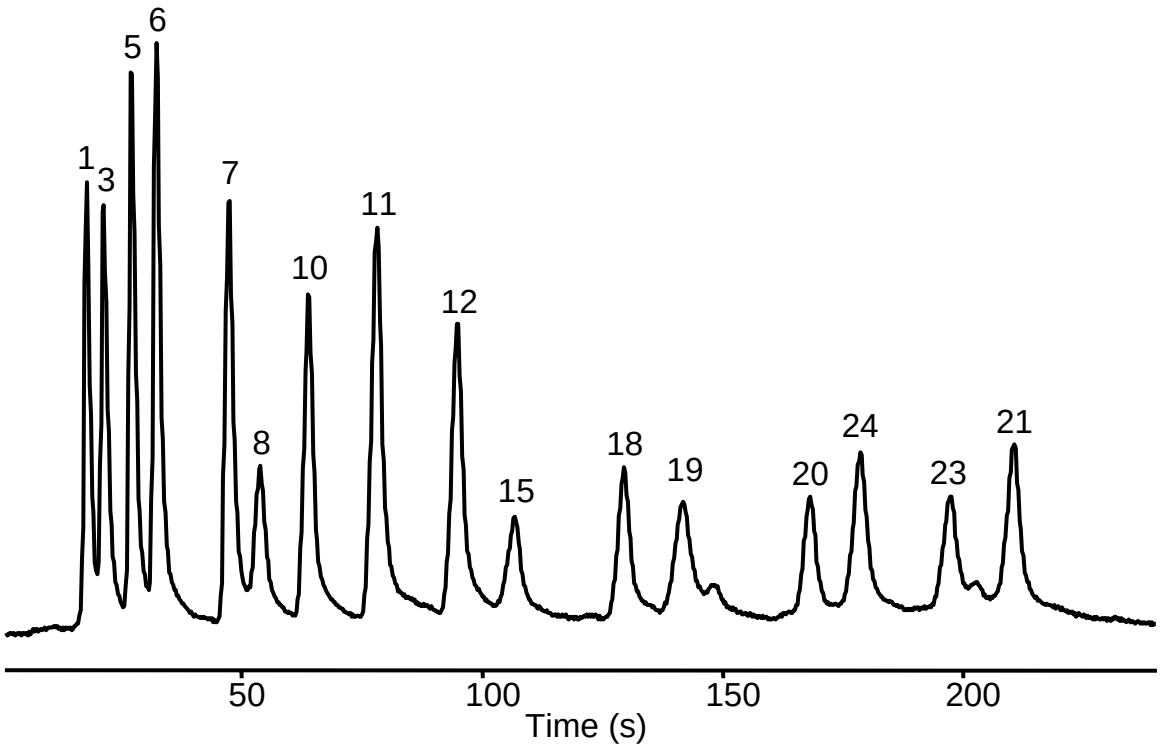

Figure 2.4 – Peak numbers correspond to component numbers in Table 1.

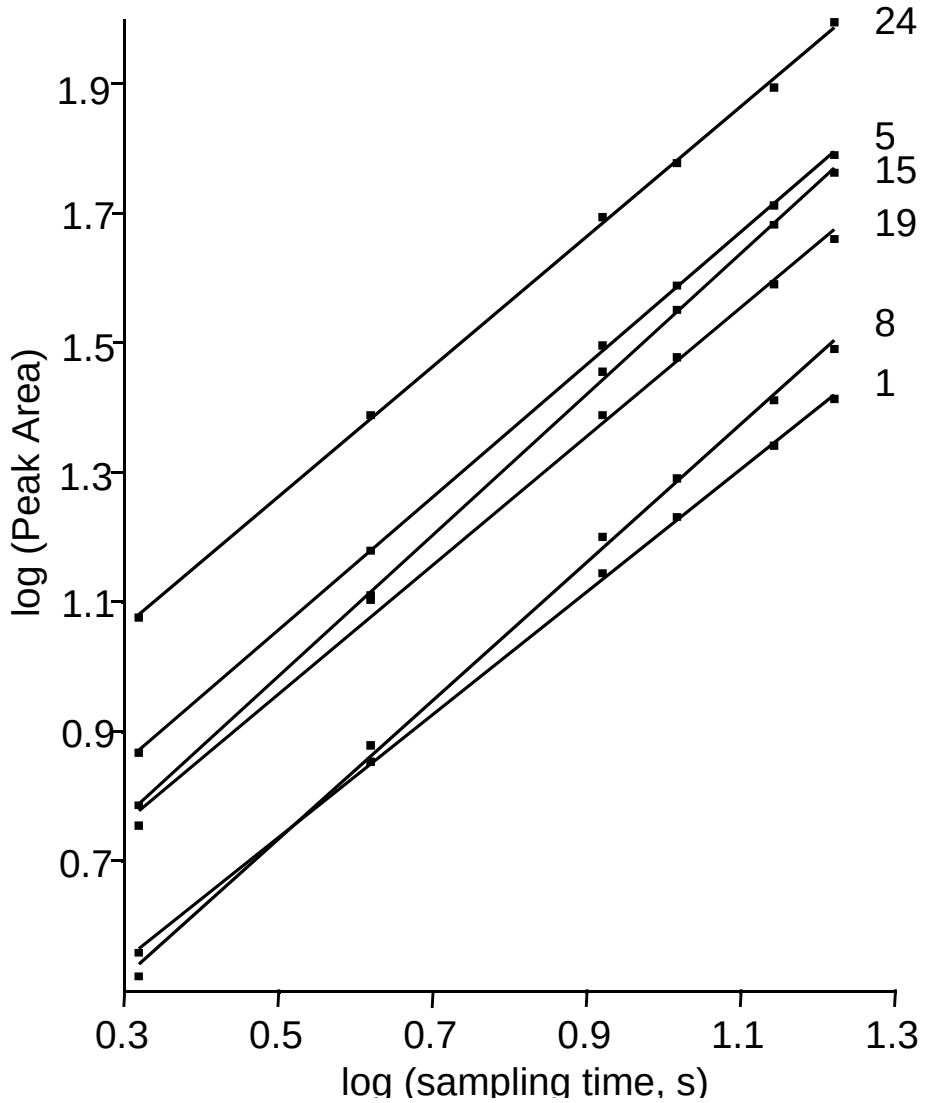

Figure 2.5 - Analytical curves of log (peak relative area) versus log (sample collection time) for the wet samples.

	Dry Samples		Wet Samples	
Compound	**Slope**	**r^2**	**Slope**	**r^2**
Acetone	0.9642	0.9998	0.9466	0.9998
2-Butanone	0.9608	0.9978	--	--
2-Pentanone	1.0318	0.9959	--	--
2-Hexanone	1.0356	0.9994	1.0664	0.9991
2-Heptanone	0.9829	0.9954	1.0864	0.9998
3-Octanone	1.0348	0.9958	--	--
Hexanal	1.0348	0.9958	--	--
Heptaldehyde	1.0228	0.9992	--	--
Benzaldehyde	0.9816	0.9912	0.9936	0.9986
Benzene	1.0306	0.9999	1.0229	0.9999
Toluene	1.0440	0.9999	--	--
Xylene	1.0104	0.9979	--	--
Cumene	1.0341	0.9988	--	--
1,2,4-Trimethylbenzene	1.0922	0.9998	1.0027	0.9996
Tetrachloroethylene	1.0000	1.0000	--	--
Chlorobenzene	0.9840	0.9977	--	--
Styrene	1.0011	0.9953	--	--
1,2-Dichlorobenzene	1.0766	0.9943	--	--
2-Carene	1.0408	0.9998	--	--

Table 2.2 - Statistical data from plots of log (peak area) versus log (sampling time) for dry and wet samples.

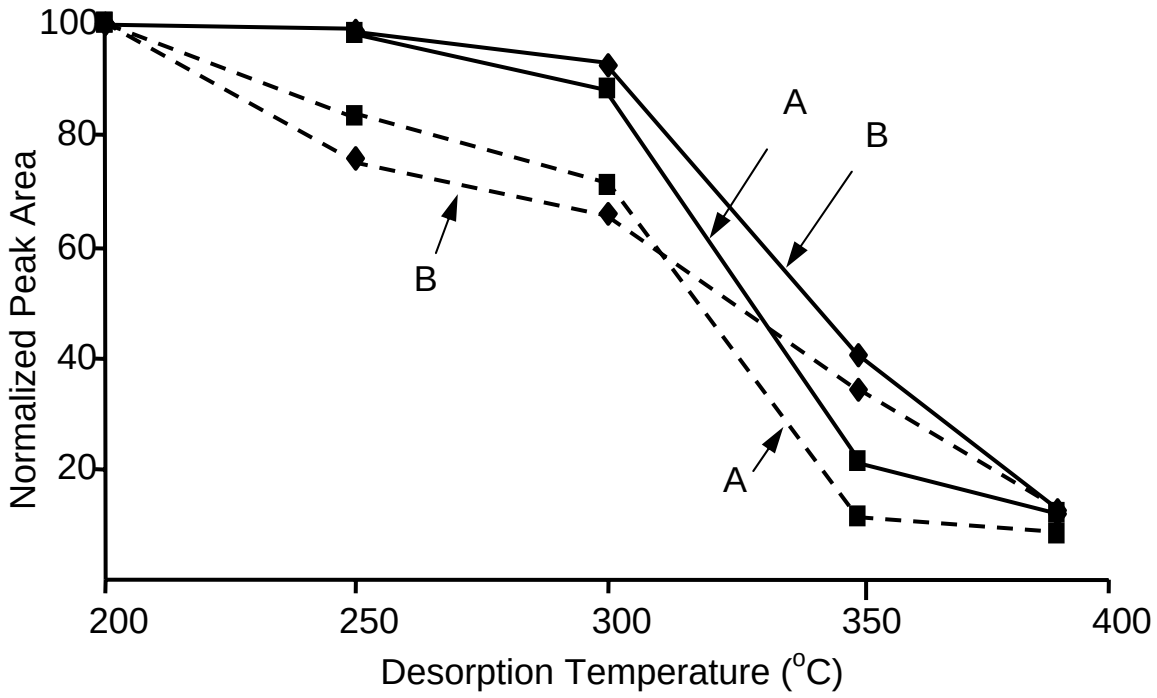

Figure 2.6 - Results of a study of the decomposition of α-pinene (A) and β-pinene (B) using hydrogen carrier gas (solid lines) and air carrier gas (broken lines).

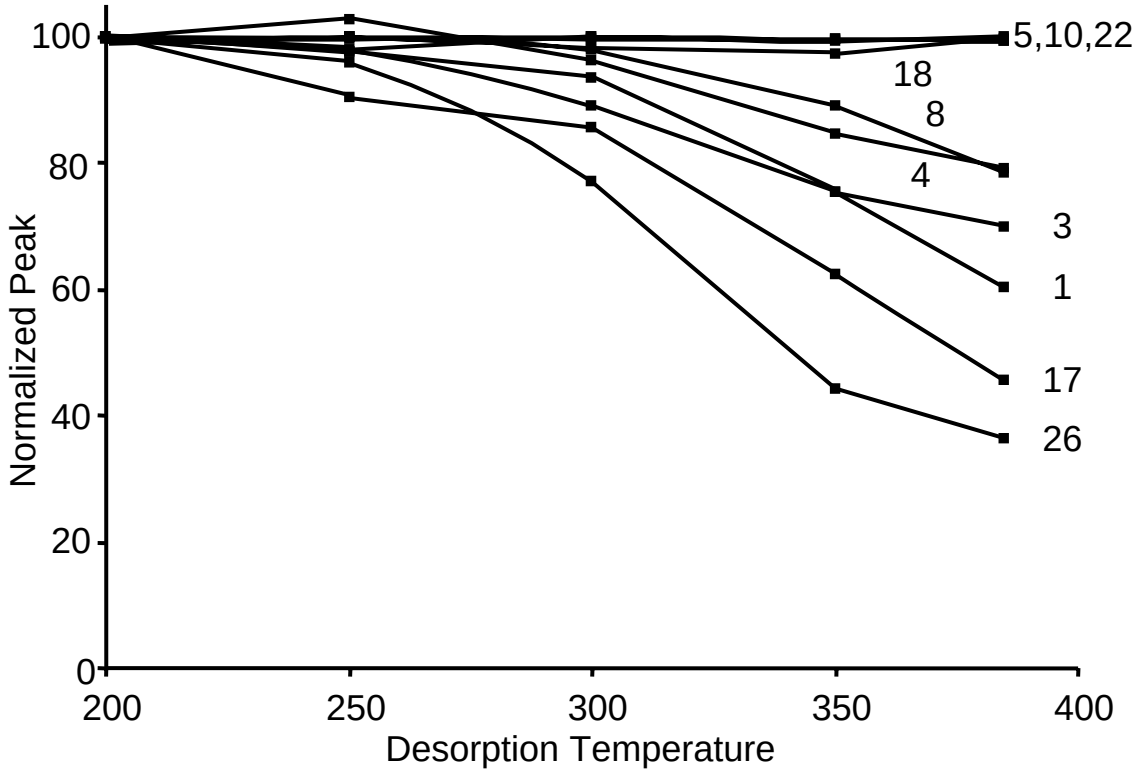

Figure 2.7 - Plots illustrating the effects of analyte structure and molecular weight on the extent of sample loss by thermal decomposition with air as carrier gas. Plot numbers correspond to compound numbers in Table 1.

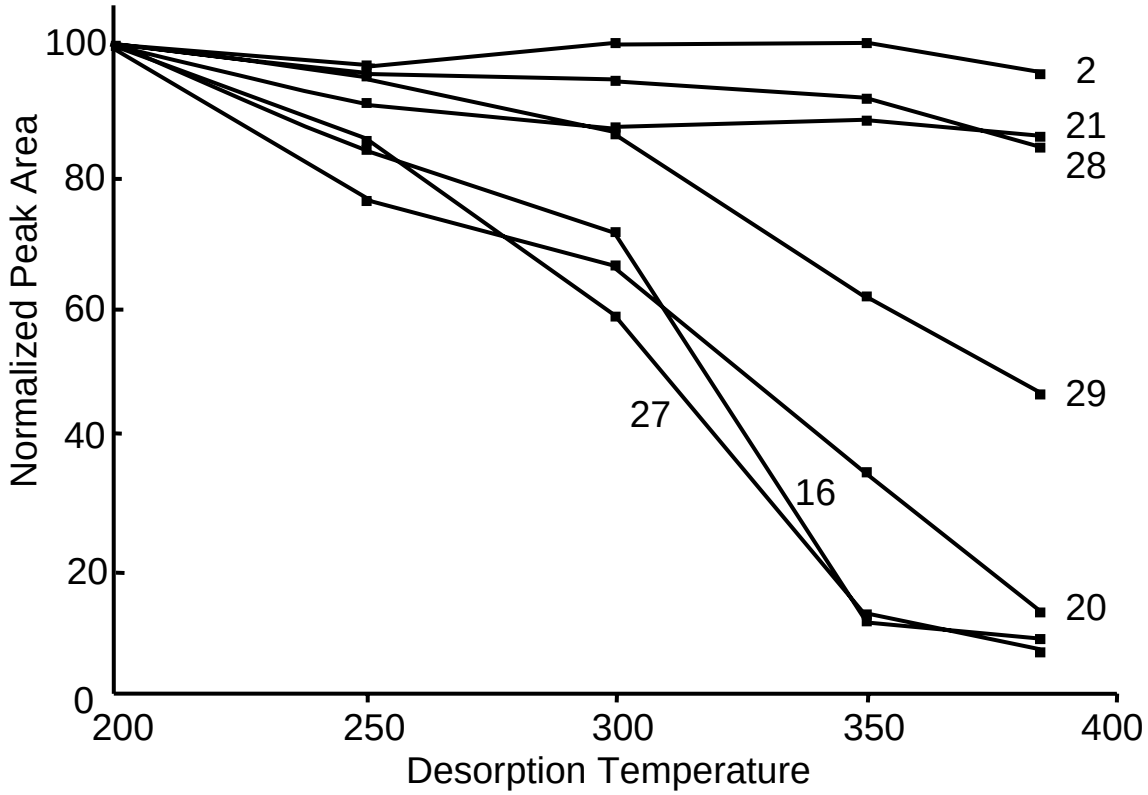

Figure 2.8 – Plots showing the decomposition of some common biogenic compounds. Isoprene (Plot 2) is the building block (monomer) for the terpenes. The data from Figure 6 for α-pinene and β-pinene in air are repeated for comparison with the other compounds. Plot numbers correspond to compound numbers in Table 1.

Compound	Desorption Conditions Temperature (^{o}C) / Stop flow time (s)	
	385 / 0	**200 / 5**
Acetone	60	87
Isoprene	97	54
Benzene	100	100
α-pinene	8	3
β-pinene	15	3
2-Carene	7	35
3-Carene	84	78
Limonene	93	68
γ-terpinene	46	67

Table 2.3 - Recoveries (peak areas) of some of the compounds in Table 1 at a desorption temperature of 385 ^{o}C with no stop flow and at 200 ^{o}C with a 5-s stop flow relative to the peak areas obtained for a desorption temperature of 200 ^{o}C with no interruption of the carrier gas flow.

REFERENCES

[1] Overton, B.; Carney, K.; Dahrmasena, H.; Ashton, B.; Roques, N. *Abstr. Pap. Am. Chem. Soc.* **1998**, *216*, 1.
[2] Hail, M.E.; Yost, R.A. *Anal. Chem.* **1989**, *61*, 2410
[3] Sloan, K.; Mustachich, R.; Eckenrode, B.; *Field Anal. Chem. Technol.* **2001**, *5*, 288.
[4] Whiting, J.; Sacks, R. *Anal. Chem.* **2003**, *75*, X
[5] Lu, C.; Zellers, E. *Anal. Chem.* **2001**, *73*, 3449.
[6] Lu, C.; Zellers, E. *Analyst*, **2002**, *127*, 1061.
[7] Feng, C.; Mitra, S. *J. Chromatogr. A*, **1998**, *805*, 169.
[8] Grote, C.; Pawliszyn, J. *Anal. Chem.*, **1997**, *69*, 587.
[9] Sanchez, J.; Sacks, R. *Anal. Chem.*, **2003**, *75*, 978.
[10] Sanchez, J.; Sacks, R. *Anal. Chem.*, **2003**, *75*, X.
[11] Frye-Mason, G.; Kottenstette, R.; Lewis, P.; Heller, E.; Manginell, L.; Adkins, D.; Dulleck, G.; Martinez, D.; Sasaki, D.; Mowry, C.; Matzke, C.; Anderson, L. *Proc. Micro Total Analysis Systems 2000*; Kluwer Academic Publishers; Boston, MA, 2000; 229.
[12] Whiting, J.; Lu, C.; Zellers, E.; Sacks, R. *Anal. Chem.*, **2001**, *73*, 4668.
[13] Cai, Q.; Zellers, E. *Anal. Chem.*, **2002**, *74*, 3533.
[14] Veriotti, T.; Sacks, R. *Anal. Chem.*, **2001**, *73*, 813.
[15] Whiting, J.; Sacks, R. *Anal. Chem.*, **2002**, *74*, 246.
[16] Libardoni, M.; McGuigan, M.; Sacks, R. *Anal. Chem.* **2003**, X.
[17] Center for Wireless Integrated Microsystems, Ann Arbor, MI 48109
[18] Microsystems: Science, Technology and Components, Sandia National Laboratories, Albuquerque, NM 87185
[19] Kolesar, E.; Reston, R. *IEEE Trans. Compon. Pack. Man. B,* **1998**, *21*, 324.
[20] Smith, H.; Zellers, E.; Sacks, R. *Anal. Chem.*, **1999**, *71*, 1610.
[21] Grall, A.; Zellers, E.; Sacks, R. *Environ. Sci. Technol.*, **2001**, *35*, 163.
[22] Klemp, M.; Peters, A.; Sacks, R. *J. Eviron. Sci. Technol.* **1994**, *28*, 369A.
[23] James, A.T.; Martin, A.J.P. *Biochem. J. (Londen)*, **1952**, *50*, 679.
[24] U.S. EPA Method TO-14A www.epa.gov/ttn/amtic/files/ambient/airtox/to-14ar.pdf
[25] U.S. EPA Method TO-15 www.epa.gov/ttn/amtic/files/ambient/airtox/to-15r.pdf
[26] Dewulf, J.; Van Langenhove, H. *Atmos. Environ.*, **1997**, *31*, 3291.
[27] Woolfenden, E. *J. Air Waste Manage. Assoc.*, **1997**, *47*, 20.
[28] Dewulf, J.; Van Langenhove, H. *J. Chromatog. A.*, **1999**, *843*, 163.
[29] Batterman, S.A.; Zhang, G.Z.; Baumann, M. *Atmos. Environ.* **1998**, *32*, 1647.
[30] Lockwood, G.B. *J. Chromatog. A.*, **2001**, 936, 21.
[31] Edwards, R.; Jurvelin, J.; Koistinen, K.; Saarela, K.; Janutunen, M. *Atmos. Environ.*, **2001**, *35*, 4829.
[32] Pliel, J.; Lindstrom, A. *Clin. Chem.*, **1997**, *47*, 723.
[33] Thrall, K.; Wetz, K.; Woodstock, A. *Toxicol. Sci.*, **2002**, *68*, 280.
[34] Andreae, M.O.; Crutzen, P.J. *Science*, **1997**, *276*, 1052.
[35] Rothweiler, H.; Wager, P.A.; Schlatter, C. *Atmos. Environ.*, **1991**, *25B*, 231.
[36] Janson, R.W. *J. Geophys. Res.*, **1993**, *98*, 2893.
[37] Cao, X.L.; Hewit, N. *Chemosphere*, **1993**, *27*, 695.
[38] Calogirou, A.; Larsen, B.R.; Brussol , C.; Duane, M.; Kotzias, D. *Anal. Chem.*, **1996**, *68*, 1499.
[39] Couer, C.; Jacob, V.; Denis, I.; Foster, P. *J. Chromatog. A.*, **1997**, *786*, 185.
[40] Atkinson, R.; Arey, J. *Acc. Chem. Res.*, **1998**, *31*, 574.
[41] McGraw, G.W.; Hemingway, R.W.; Ingram, L.L.; Canady, C.S.; McGraw, W.B. *Environ. Sci. Technol.*, **1999**, *33*, 4029.
[42] Caligirou, A.; Larsen, B.R.; Kotzias, D. *Atmos. Environ.* **1999**, *33*, 1423.
[43] Dettmer, K.; Knobloch, T.; Engewald, W. *Fresenius J. Anal. Chem.*, **2000**, *366*, 70.
[44] Schrader, W.; Geiger, J.; Klockow, D.; Korte, E.H. *Environ. Sci. Technol.*, **2001**, *35*, 2717.
[45] Choung, B.; Davis, M.; Edwards, M.; Stevens, P.S. *Int. J. Chem. Kinet.*, **2002**, *34*, 300.
[46] Hollender, J.; Sander, F.; Möller, M., Dott, W. *J. Chromatog. A.*, **2002**, *962*, 175.
[47] Hail, M.E.; Yost, R.A.; *Anal Chem.*, **1989**, *61*, 2402
[48] Amirav, A.; Tzanani, N.; Wainhaus, S.B.; Dagan, S. *Eur. Mass Spectrom.* **1998**, *4*, 7.

[49] Cramers, C.A.; Janseen, H.G.;Van Duersen, M.; Leclercq, P.A. *J. Chromatogr. A* **1999**, *856*, 315-329.

CHAPTER 3

LARGE-VOLUME VAPORSAMPLING FOR GC IN THE C_5 TO C_{24} VOLATILITY RANGE

Introduction

Large-volume vapor sampling is used frequently where vapor preconcentration is needed prior to analysis by gas chromatography (GC). Examples include ambient air analysis, dynamic head-space methods, industrial hygiene and homeland security applications. A variety of large-volume sampling devices have been described for both off-line[1,2,3,4] and in-line applications.[5,6,7,8,9,10,11,12] In-line methods, where the collected sample is directly injected into the GC, are preferred since they result in shorter turnaround times and reduce the risk of sample loss and contamination during transport and storage.[13] Some compounds, including low-molecular weight aldehydes and terpenes, are particularly prone to decomposition during storage.[14,15,16]

The dimensions of large-volume sampling devices often are incompatible with the required injection volumes for capillary GC, and additional vapor focusing often with a cryogenic trap, is required prior to injection into the GC.[1,3,17,18] This is particularly true for volatile compounds, which do not benefit significantly by on-column focusing with temperature programmed GC. However, for on-site applications where the entire analysis is performed at the point of sampling, the use of cryogenic materials is

usually prohibitive. Micro-scale and micro-fabricated preconcentrators are under development for these on-site applications.[19,20,21,22]

Most large-volume vapor sampling devices use adsorbing materials to collect and focus the vapor with thermal desorption to re-vaporize the sample and inject it into the GC. A wide variety of sorption materials have been used for preconcentration of analytes.[5,6,7,8,9,10] No single sorption material can be used over a wide boiling range. Strong (large surface area) materials are effective for volatile compounds, but higher-boiling-point compounds are difficult to thermally desorb. For this reason, most large-volume sampling devices use multiple beds utilizing several sorption materials.

A four-bed, micro-scale in-line device has been described, which is useful for the volatility range from n-C_5 to n-C_{12}.[20,21,22] Four discreet sorption beds are used, three of graphitized carbon and one of carbon molecular sieves. The beds are ordered in terms of absorption strength (surface area) so that during sample collection the weakest bed is the first experienced by the incoming sample. After sample collection the gas flow direction through the device is reversed, the device heated to about 300^{o}C and the beds desorbed directly into the capillary GC column. In this way, the higher molecular weight compounds never come in contact with the stronger adsorbents from which they would be difficult to thermally desorb.

Desorption vapor plug widths in the range 0.5 to 2.0 s are achieved for the volatility range n-C_5 to n-C_{12}, which are sufficiently narrow for direct injection into a GC

without the need for further focusing. The multi-bed trap works well for high-humidity samples and has been used for the collection of human breath samples.[23]. Recently, a splitter has been added to the device reducing injection plug widths to the 0.1 s to 0.5 s range for the same solute volatility range.[24]

A significant limitation of the multi-bed trap is its limited volatility range. Compounds less volatile than about n-C_{12} generate injection plug widths that are too wide for direct injection into the capillary GC column. Large-volume vapor samples with compounds less volatile than n-C_{12} are of considerable interest in numerous areas including pyrolysis GC, diesel vapor and exhaust analysis and homeland security applications.

In the present study, the multi-bed trap is combined with a segment of fused silica-lined capillary stainless steel tubing with a wall coating of dimethyl polysiloxane (PDMS phase-coated trap) in order to extend the volatility range from n-C_5 to n-C_{24}. The two traps are connected in series so that the sample gas first passes through the phase-coated trap. The stainless steel phase-coated trap is resistively heated by current from a power supply. During sample collection, the temperature of the phase-coated trap is adjusted relative to the sample gas flow rate and the sampling duration so that the distribution of solute volatility in the two traps can be controlled. After sample collection, the two traps can be thermally desorbed either simultaneously or sequentially. In this report, design features and operating conditions for the two traps are presented.

Sample chromatograms are presented illustrating how the volatility distribution in the two traps can be controlled.

Experimental

Apparatus - Figure 1 shows the experimental interface developed in this study. For this study, a pyrolysis inlet was used to introduce sample into the interface. The sample inlet consisted of the pyrolysis chamber (part 10S4-5005, CDS Analytical, Oxford, PA) and the associated pair of rotary valves (part 2460-0295, CDS Analytical, Oxford, PA) from a CDS AS2500plus Pyrolysis Autosampler. A Pyroprobe 2000 (CDS Analytical, Oxford, PA) was used to control the pyrolysis parameters. The lower valve in the assembly was located in a heated aluminum block. The heated transfer line between the pyrolysis chamber valve and the interface consisted of a 20 cm section of 0.28 mm i.d. Silcosteel® capillary (Restek Corp., Bellefonte, PA) wrapped in heat tape. The interface was connected to a Shimadzu GC-14 gas chromatograph chassis (Shimadzu Scientific Instruments, Columbia, MD). The detector used was a Varian Flame Ionization Detector from a Varian 3600 (Varian Inc., Palo Alto, CA).

A series of valves is used to control gas flows in the interface. V_1, V_2, and V_4 are toggle shut off valves (model B-OGS2, Swagelok Co., Solon, OH). V_3 is a 3-way ball valve (model B-41SX2, Swagelok Co., Solon, OH). During sample collection, V_1 and V_2 are open and V_3 is set to the "vent" position. To switch the interface gas flows from sample collection to sample desorption, V1 and V_2 are closed and V_3 is set to the "carrier gas" position. V_4 allows use of a splitter which permits for various desorption flows without altering the carrier gas flow on the analytical column. Figure 2a shows the gas flow paths in the sample collection configuration. A flow of auxiliary carrier gas is

supplied through V_2 sufficient to ensure that the entire sample flows through the preconcentrator. Figure 2b shows the gas flow path in the sample desorption configuration. When switching from the sample collection configuration to the sample desorption configuration, the start of sample desorption is delayed for a period of 80 seconds in order to allow the closed off lines to back pressurize and for flow to stabilize along the desired flow path. Figure 3 shows flow charts for the configuration of the valves and gas flow directions during both modes. The flows of pyrolysis gas and the auxiliary flow of carrier gas were controlled with a high resolution metering valves (part A-03214-82, Cole Parmer, Vernon Hills, IL). The flow of carrier gas was controlled with a programmable flow controller (model 32907-76, Cole Parmer, Vernon Hills, IL). The interface is composed of a tar trap, the preconcentrator and their associated heated transfer lines. The tar trap is used to condense refractory compounds in order to prevent fouling of the preconcentrator. It consists of a 200 cm section of 0.28 mm i.d. Silcosteel® capillary (Restek Corp., Bellefonte, PA). The tees in the interface are Valco® Zero Dead Volume Silcosteel® Tees (part 20581, Restek Corp., Bellefonte, PA). The preconcentrator consists of two sections, the phase trap and the sorption trap. The phase trap is a 100 cm length of 0.25 mm x 1.0 µm df MXT-1 Silcosteel® capillary column. The multi-bed sorption-based trap used in this interface has been previously described by Sanchez and Sacks.

Preconcentrator Design - The preconcentrator is designed so that during the sampling period, the sample passes through the phase trap before entering the sorption trap. In this way, less volatile compounds, which would be difficult or impossible to quantitatively desorb off of the sorption trap, are retained in the phase trap. The volatile compounds

pass through the phase trap to be collected on the multi-bed sorption trap. Distribution of compounds between the two traps can be controlled by varying the temperature of the phase trap during the sampling phase. As the temperature of the phase trap during sampling is decreased, less volatile compounds are retained on the phase trap. A temperature range from 25°C to 45°C was evaluated for sample collection. Not all compounds are discretely distributed between the phase trap and the sorption trap. The temperature of the phase trap during sampling is set so that compounds that are distributed between the two traps or entirely on the phase trap have a sufficiently high boiling point to experience on-column focusing at the beginning of the analytical column. For desorption of the preconcentrator and injection of the collected sample onto the analytical column, a two-step desorption process is used. After the gas flow is reversed and allowed to equilibrate, the phase trap is resistively heated to the desorption temperature ranging from 200 °C to 375°C. The phase trap is held at the desorption temperature while the sorption trap is heated. The sorption trap was rapidly heated to 370 °C for desorption. By keeping the phase trap temperature elevated, the retention of the compounds desorbed from the sorption trap is minimized to maintain a sufficiently narrow injection plug.

Results and Discussion

The flow of hydrogen from the pyrolysis chamber through the preconcentrator during the sampling mode was approximately 17 mL/min. The flow being introduced at the auxiliary carrier gas supply, to insure that all of the analytes from the pyrolysis chamber would flow through the preconcentrator, was approximately 3 mL/min. It was

determined that optimizing the preconcentrator during sampling to retain compounds with volatilities less than or equal to dodecane on the phase trap and compounds with volatilities greater than dodecane would be collected on the multi-bed sorption trap. This was accomplished by adjusting the temperature of the phase trap during sample collection. The limitation for the lower temperature was that it could not be lower than the initial oven temperature used in the gas chromatograph oven. This is necessary because any compounds retained on the phase trap portion of the preconcentrator must be subject to on-column focusing at the head of the analytical column at its initial temperature. For this instrumental set-up, the minimum temperature obtainable with the use of external cooling sources was 25 °C.

For determining the optimal collection temperature, the analytical column in the GC was replaced with a 20 cm length of deactivated, uncoated 0.25 mm i.d. fused-silica capillary column and the GC oven was maintained at 300 °C. The inlet was in "sample collection" mode for 120 seconds. After 120 seconds, the valves were changed to the "sample desorption" configuration and flow was allowed to equilibrate for 80 seconds. At an overall time of 200 seconds, the phase trap portion of the preconcentrator was desorbed and the temperature was maintained at the desorption temperature of 300 °C. At an overall time of 260 seconds, the multi-bed sorption trap was desorbed. Figure 4 shows a series of individual desorption cycles for straight chain alkanes from C_{10} through C_{14} that were run with the phase trap portion of the preconcentrator maintained at 25 °C during the sample collection phase. For each trace, 20 nL of the neat compound was injected onto a plug of quartz wool which was inside of a pyrolysis desorption tube. The

tube was placed inside of the pyrolysis chamber and which was then ramped to 500 °C and held for 30 sec to desorb the analytes.

Compounds that are completely retained on the phase trap portion of the preconcentrator will have peaks present between 200 sec and 260 sec. Compounds that are distributed over both the phase trap and the multi-bed trap will have a peak in the 200 to 260 sec range and a peak after 260 sec. Compounds that are retained solely of the multi-bed sorption trap will only have a peak after 260 sec, when the trap is desorbed. From the traces in Figure 4, in which the phase trap collection temperature was set at 25 °C, it can be seen that decane and undecane are collected solely on the multi-bed sorption trap and dodecane and tridecane are resident entirely on the phase trap. It should also be noted that the peak for undecane is very broad; indicating that it is becoming more difficult to desorb it as a narrow plug from the multi-bed sorption trap. If the collection temperature on the phase trap was elevated, it would be expected that dodecane would begin to be distributed onto the multi-bed sorption trap, and that it would be even more difficult to desorb as a narrow plug than the undecane. The distribution of the straight chain alkanes at 25°C fit the desired distribution pattern and further work on the inlet system was done using 25 °C as the temperature of the phase trap during sample collection.

Figure 5 shows a chromatogram of a sample containing the straight chain alkanes from hexane through tetracosane. The sample consisted of 40 nL of a mixture that was 50 % dichloromethane and 50 % of an equal parts (v/v) mixture of the straight chain alkanes from hexane through tetracosane. The sample was desorbed by ramping the pyrolysis chamber to 500 °C and holding it for 90 seconds. The inlet was in “sample collection”

mode for 120 seconds. After 120 seconds, the valves were changed to the "sample desorption" configuration and flow was allowed to equilibrate for 80 seconds. At an overall time of 200 seconds, the phase trap portion of the preconcentrator was desorbed and the temperature was maintained at the desorption temperature of 300 °C. At an overall time of 260 seconds, the multi-bed sorption trap was desorbed. The block, containing the tar trap and transfer lines, was held at 325 °C continuously. The GC oven program started with an initial temperature of 30 °C with a hold time of 330 seconds, followed by a ramp of 30 °C/min to a final temperature of 330 °C and a final hold of 280 seconds. A plot of peak widths at half height versus carbon number for the component peaks is shown in Figure 6. The peak widths for the analytes are in the desired range and only begin to significantly widen above *n*-docosane.

Conclusions

The pyrolysis-preconcentrator inlet described in this work was proposed for inclusion as part of an instrument package for the Mars Science Lander as proposed to the National Aeronautics and Space Administration (NASA). The Mars Analytical Chemistry Experiment (MACE) was the portion of the instrument package proposal this work was affiliated with. MACE was a collaboration primarily between the Jet Propulsion Laboratory (JPL), the University of Michigan (U of M) departments of Space Science and Chemistry, and consisted of a portable GCxGC-TOFMS with a pyrolysis-preconcentration inlet for the determination of the presence of biomarkers and organics in Martian soil. The pyrolysis-preconcentrator inlet was evaluated for a range of straight chain alkanes from hexane to tetracosane. It was to be evaluated with other classes of

compounds and over a more extended range of volatilities, but the pyrolysis-preconcentrator inlet was destroyed in a laboratory accident before those studies could be performed. Shortly after the incident, the overall combined proposal, that MACE was a part of, was rejected by NASA. A decision was made by Dr. Sacks to not reconstruct the inlet and continue the study due to financial considerations. As far as the study went, the pyrolysis-preconcentrator inlet was demonstrated to show a maximum useable range increased from approximately dodecane, using only the multi-bed sorption trap, to at least tetracosane, using the multi-bed sorption trap used in conjunction with the phase trap as part of the pyrolysis-preconcentrator inlet.

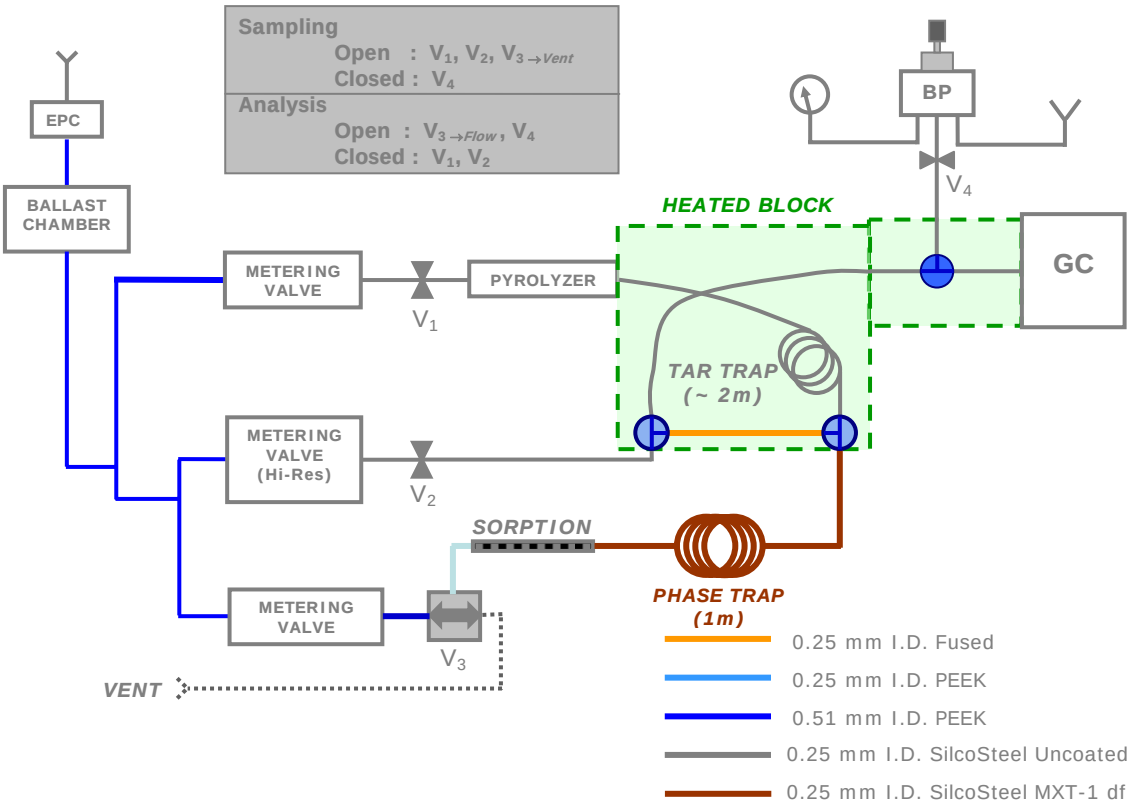

Figure 3.1 – A schematic of the pyrolysis-preconcentration interface developed and evaluated in this paper. The colored lines indicate the various types of tubing used in the interface.

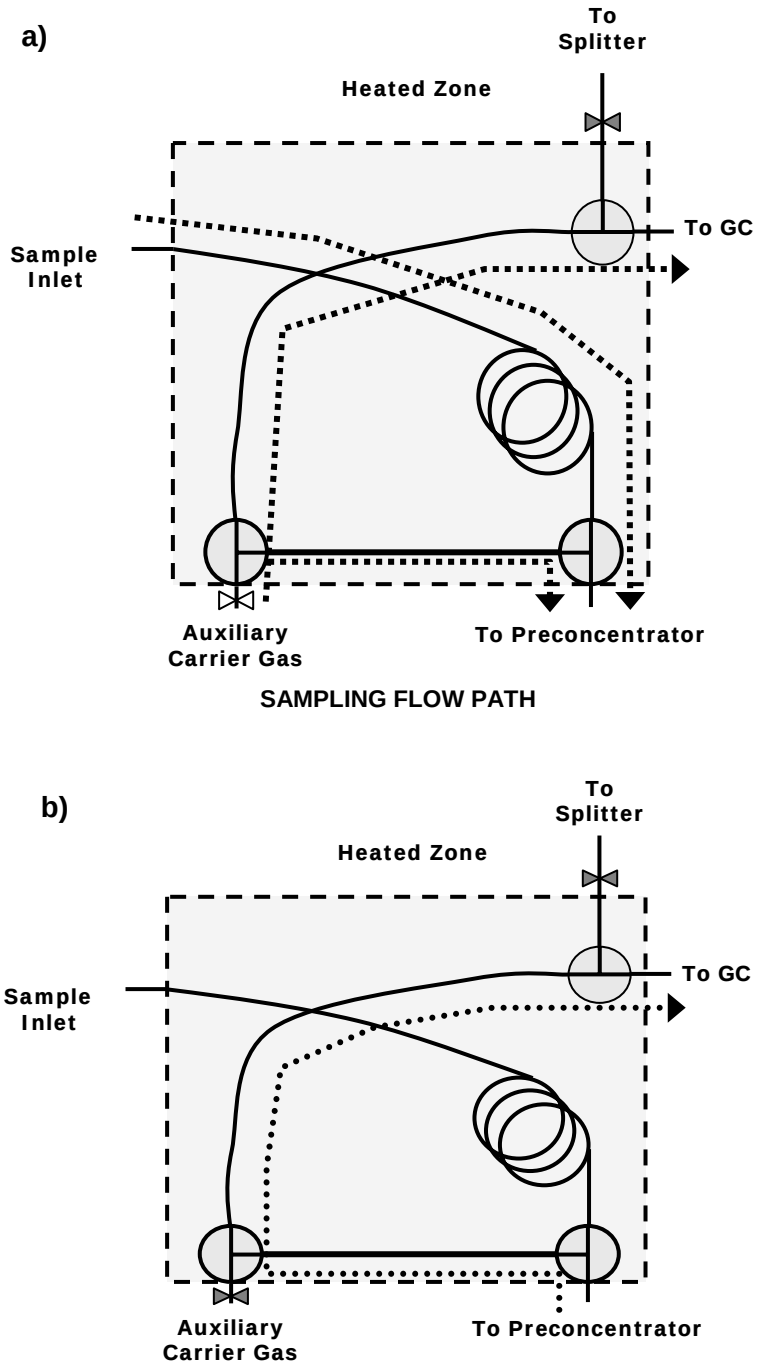

Figure 3.2 – A schematic of gas flow. The direction of carrier gas flow during sample collection is shown in (a). The direction of carrier gas flow during desorption is shown in (b).

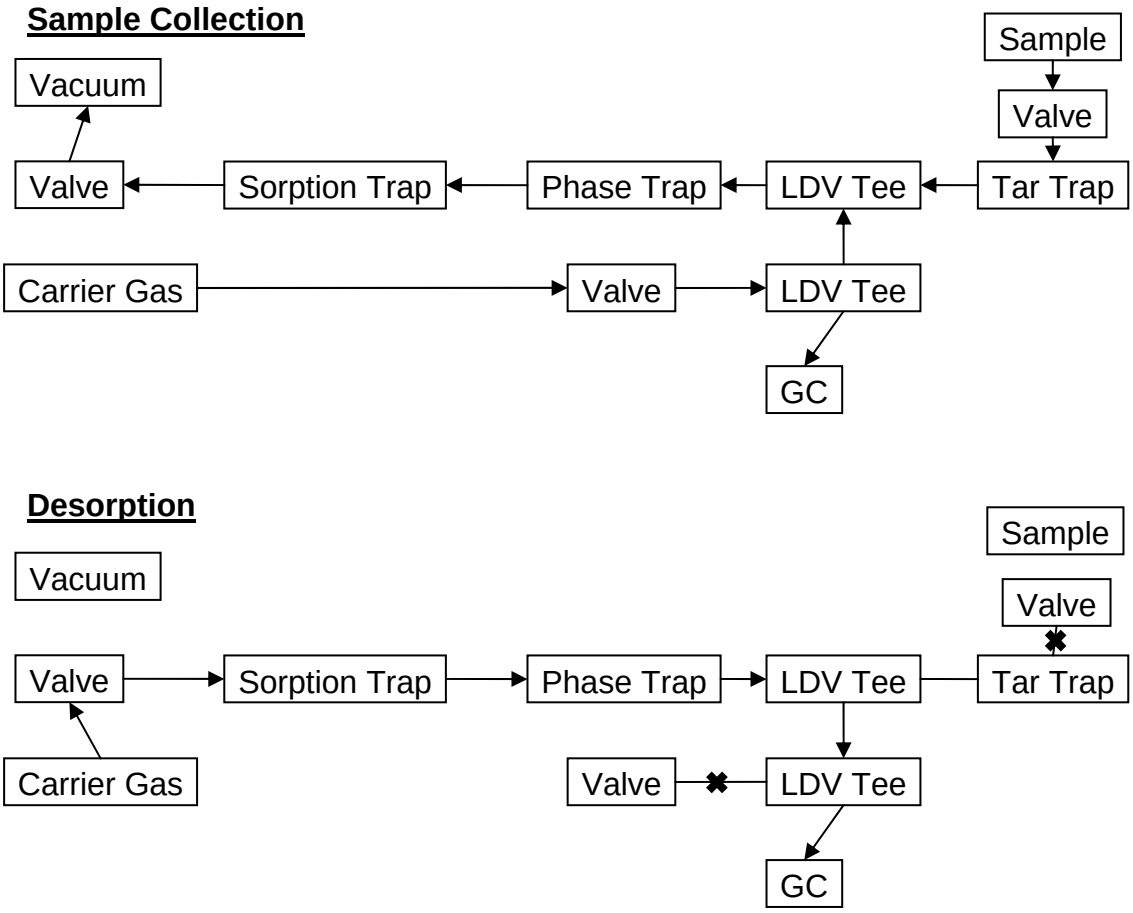

Figure 3.3 – Flowcharts showing the gas flow path during each mode (arrows) and closed valves that must be allowed to back-pressurize before desorption (**X).**

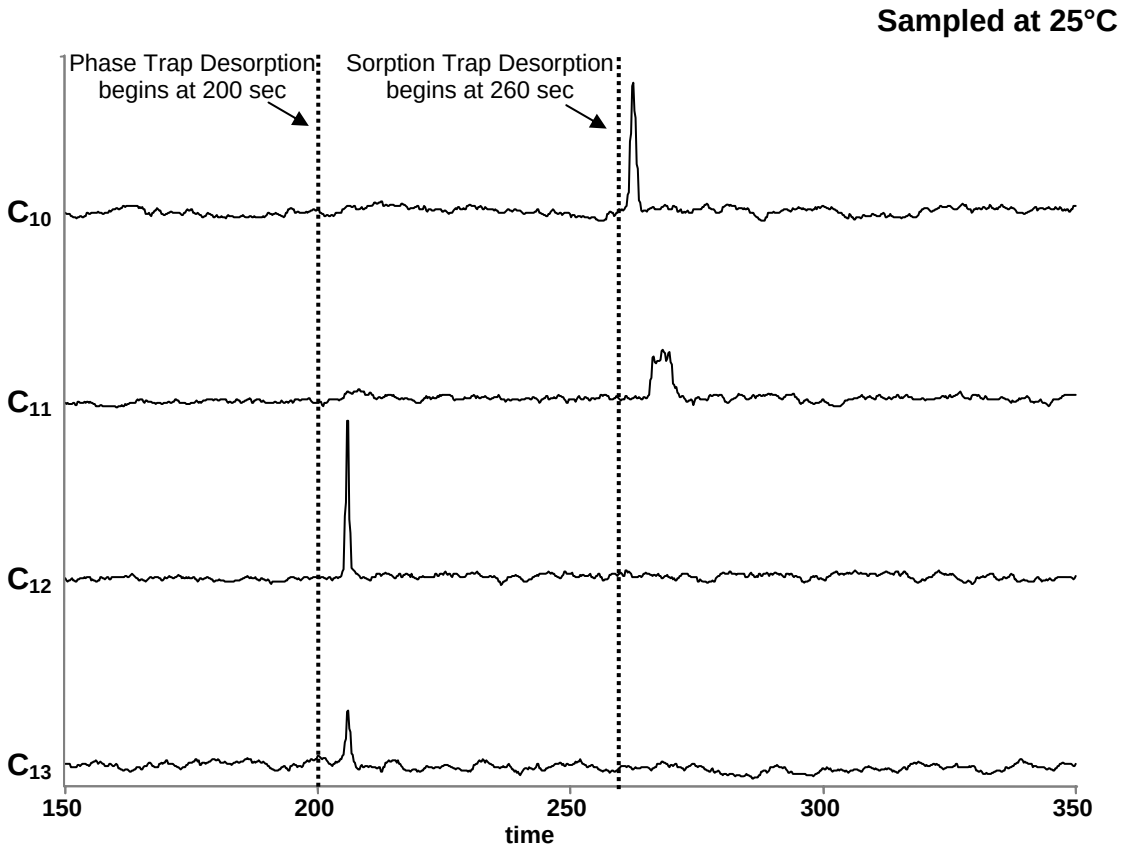

Figure 3.4 – Individual traces for the C_{10} through C_{13} straight chain alkanes with the phase trap held at 25 °C during sample collection. The phase trap was desorbed at the 200 sec mark and the multi-bed sorption trap was desorbed at the 260 sec mark.

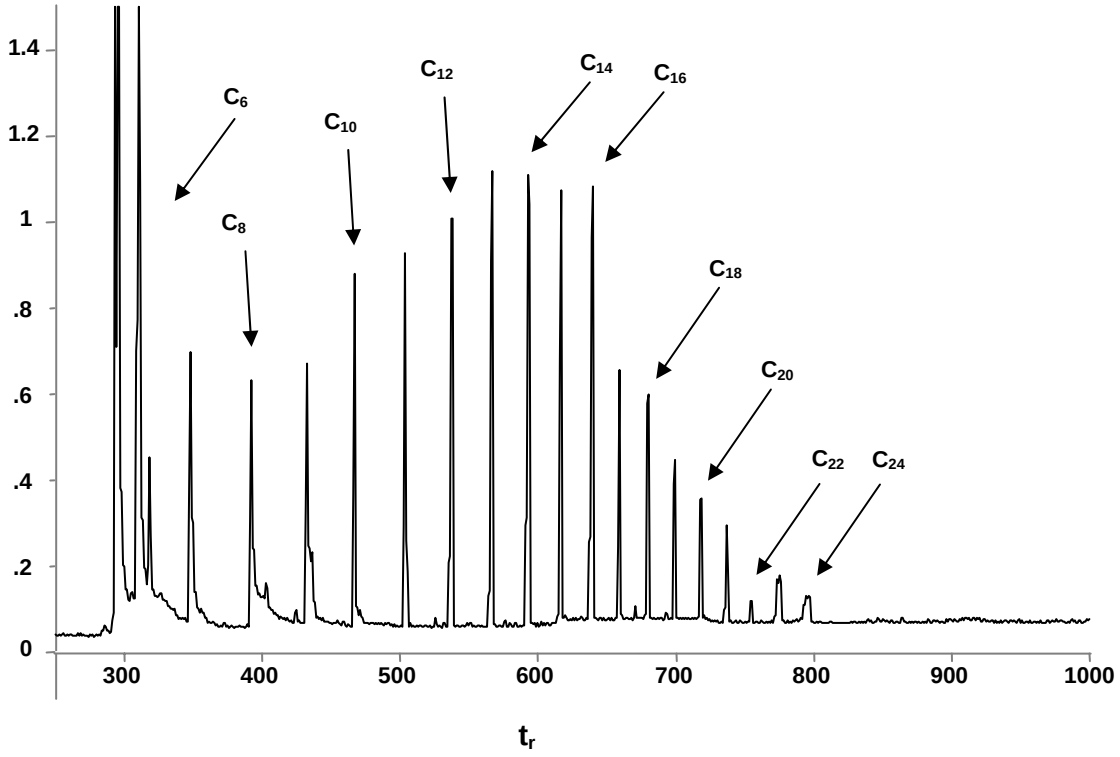

Figure 3.5 – A chromatogram of a sample containing the even numbered straight chain alkanes from hexane through tetracosane.

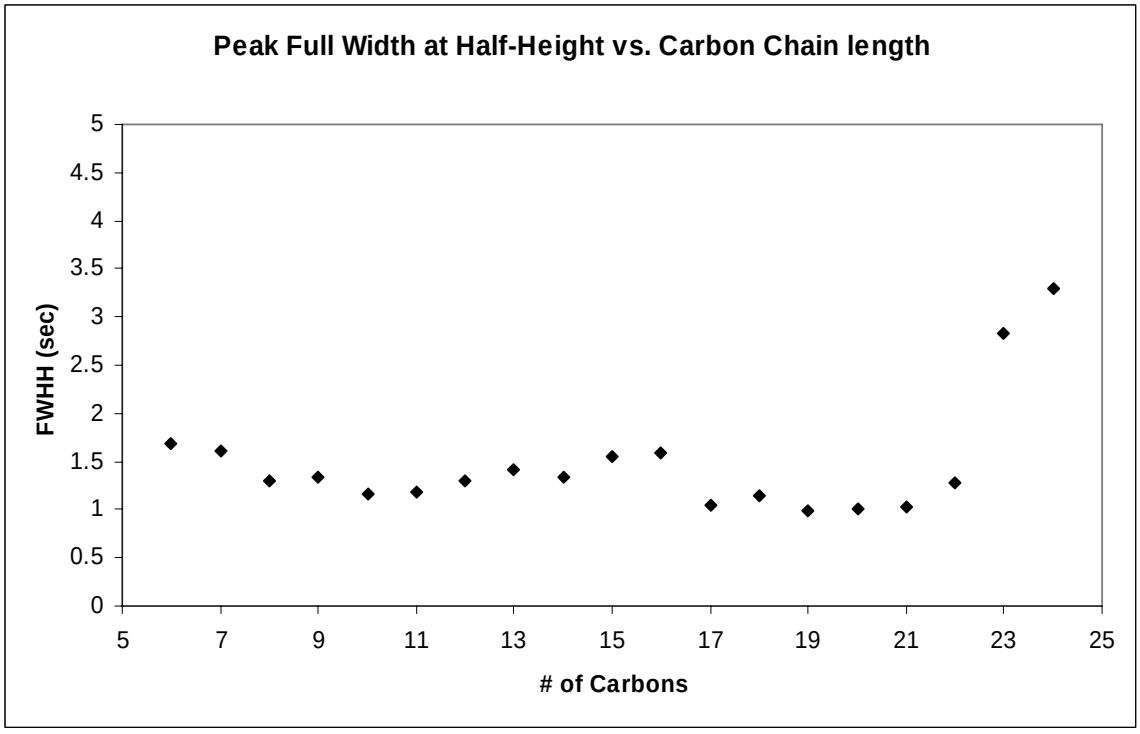

Figure 3.6 - A plot of peak widths at half height versus carbon number for the component peaks shown in Figure 5.

REFERENCES

[1] Dewulf, J.; Van Langenhove, H. *J Chromatogr., A* **1999**, *843*, 163
[2] Dewulf, J.; Van Langenhove, H. *Atmos. Environ.* **1997**, *31*, 3291.
[3] Peng, C.; Batterman, S. *J. Environ. Monit.* **2000**, *2*, 313
[4] Van Winkle, M.; Scheef, P. *Indoor Air* **2001**, *11*, 49
[5] Mitra, S.; Yun, C. *J. Chromatogr.* **1993,** *648*, 415
[6] Mitra, S.; Lai, A. *J. Chromatogr.Sci.* **1995,** *33*, 285
[7] Mitra, S.; Xu, Y.; Chen, W.; Lai, A. *J. Chromatogr. A* **1996,** *727*, 111
[8] Feng, C.; Mitra, S. *J. Chromatogr. A* **1998,** *805*, 169
[9] Lu, C.; Zellers, E.. *Anal. Chem.* **2001,** *73*, 3449
[10] Lu, C.; Zellers, E.. *Analyst* **2002,** *127*, 1061
[11] Mitra, S.; Xu, Y.; Chen, W.; McAllister, G. *J. Air Waste Manage. Assoc.* **1998,** *48*, 743
[12] Feng, C.; Mitra, S. *J. Microcolumn Sep.* **2000,** *12*, 267
[13] Batterman, S.; Zhang, G.; Baumann, M. *Atmos. Environ.* **1998**, *32*, 1647-1655
[14] Calogirou, A.; Larsen, B.; Brussol, C.; Duane, M.; Kotzias, D. *Anal. Chem.* **1996,** *68*, 1499-1506
[15] Atkinson, R.; Arey, J. *J. Acc. Chem. Res.* **1998**, *31*, 574-583
[16] Chuong, B.; Davis, M.; Edwards, M.; Stevens, P. *Int. J. Chem. Kinet.* **2002**, *34*, 300-308
[17] Van Es, A.; Janssen, H.; Cramers, C.; Rijks, J.. *J. High Resolut.Chromatogr.* **1988**, *11*, 852
[18] Balutsen, E.; David, F.; Janssen, H.; Cramers, C. *J. High Resolut.Chromatogr.* **1998**, *21*, 332
[19] Lu, C.; Whiting, J.; Sacks, R.; Zellers, E.. *Anal. Chem.* **2003,** *75*, 1400-1409
[20] Sanchez, J.; Sacks, R. *Anal. Chem.* **2003,** *75*, 978-985
[21] Sanchez, J.; Sacks, R. *Anal. Chem.* **2003,** *75*, 2231-2236
[22] Sanchez, J.; Sacks, R. *J. Sep. Sci.*. **2005,** *28*, 22-30
[23] Libardoni, M.; Stevens, P.; Waite, J.; Sacks, R. *J. Chromatogr. B* (Submitted)
[24] Whiting, J.; Sacks, R. *J. Sep. Sci.* **2006**, *29*, 218-227

CHAPTER 4

ANALYSIS OF HUMAN BREATH UTILIZING A MULTI-BED SORPTION TRAP AND COMPREHENSIVE TWO-DIMENSIONAL GAS CHROMATOGRAPHY

Introduction

The analysis of human breath samples has great potential as a minimally invasive medical diagnostic method as well as a means for monitoring human exposure to environmental toxins. Volatile organic compounds (VOCs) in human breath were identified as early as 1970.[1] Emission of VOCs from human breath includes hydrocarbons, alcohols, ketones and aldehydes at ppt to ppm levels. Equilibrium in the lungs between VOCs dissolved in blood and the lung gases provides the opportunity for the monitoring of these compounds in the gas phase, rather than in the liquid (blood or urine) phase. In the lungs, only a thin barrier separates the air in the alveoli from the blood in the capillaries.[2] This barrier is called the pulmonary alveolar membrane. The underlying mechanism for breath analysis is the relatively rapid equilibration between alveolar air and pulmonary blood. This is based on partitioning into the membrane and passive diffusion across it.[3,4] Therefore, analysis of VOCs in breath should be an excellent indicator of the levels of these components in blood.

Interest in analyzing human breath for VOCs is a result of the identification and correlation of certain components with a variety of diseases.[5,6] For example, volatile sulfur compounds are related to hepatic diseases and malodor.[7] The presence of straight-chain hydrocarbons is a result of lipid peroxidation of polyunsaturated fatty acids found in cellular membranes.[8] Increased levels of hydrocarbons have been associated with pulmonary, liver, autoimmune, bowel and neurological diseases.[3,9,10] Other VOCs have been identified as markers of more specific pathologies such as isoprene for hypercholesterolemia and acetone for diabetes.[11,12,13] In addition, researchers are investigating certain markers related to cancer, transplanted organ rejection and trace level contaminants leeched into the blood from dialysis tubing.[14,15,16,17,18,19]

Analysis of human breath samples by GC and GC–MS is complicated by the very low concentrations of many organic compounds and the large number of compounds that have been detected.[20] Several hundred organic compounds have been detected in breath samples, and in one case involving breath samples from 50 nominally healthy subjects, more than 3400 different VOCs were observed.[21] Healthy individuals differ widely in the composition of their breath with fewer than 30 shared compounds found in the breath of all humans. Major VOCs present in human breath include isoprene, acetone, ethanol, methanol and other alcohols. Minor components include pentane and higher aldehydes and ketones.

Because of the very low concentrations of many compounds in breath, some preconcentration is required prior to analysis. Sorption-based traps have been used for the preconcentration of organic compounds from large-volume vapor samples, but thermal

desorption often results in very wide injection plugs, and a cryogenic-focusing device may be needed between the sorption trap and the GC in order to obtain sufficiently narrow injection plugs.[22,23,24,25] Another drawback of sorption traps is the potential for thermal degradation of labile compounds during desorption. This has been shown to be a significant problem for some biogenic compounds including aldehydes and terpenes.[26,27]

Membrane extraction with a micro-scale trap interface has been used for the collection and injection of organic compounds from large-volume samples with single dimension GC analysis. The hydrophobic membrane excludes water vapor from the trap, but may also reduce recovery for some sample components. Similarly, a multi-bed sorption trap has been designed and evaluated in our laboratory.[28] This design has been used for the direct collection and injection of organic compounds from large-volume breath samples into a single-dimension GC.[29] Experimental results determined that water vapor is not strongly retained on the carbon-based sorbents. With hydrogen carrier gas, biogenic compounds such as α-pinene and β-pinene can be quantitatively desorbed from the trap at 300 °C with minimal decomposition.

The very large peak capacity and high sensitivity of comprehensive two-dimensional GC (GC × GC) make it an excellent candidate for the analysis of organic compounds in human breath.[30,31] Comprehensive two-dimensional separations are achieved by connecting in series two capillary columns using different stationary phases by means of a concentration-modulator interface. For thermal modulators, the device is cooled to collect sequential portions of the first column effluent and periodically heated to inject a series of narrow plugs for fast separation on the second column. High peak

capacity is achieved from chromatograms defined on a two-dimensional retention time plane rather than on a single retention-time axis. High sensitivity is achieved by the use of an efficient modulator, which injects very narrow vapor plugs into a micro-bore column for a high-speed, second-column separation. Another attractive feature of GC × GC is that more structured chromatograms are obtained, and the position of a peak in the retention plane provides information useful for the classification of compounds found in breath samples.

Since its initial development by John Phillips in the late 1980s, the thermal modulator has taken on different designs to provide the required heating and cooling.[32] Thermal modulators usually are mass conserving and can provide greater detection enhancement than devices using valves and sample loops. However, the latter devices require no cryogenic materials. Both thermal and pneumatic modulators have been described in several recent reviews.[33,34,35]

Recent work in our laboratory described the design and performance of a single-stage, resistively-heated and air-cooled thermal modulator that uses no consumables other than carrier gas and line power. It can provide modulated peak widths at half-height of under 20 ms.[36] The work presented in this report describes a GC × GC/sorption-trap instrument which utilizes a single-stage resistively-heated and air-cooled thermal modulator for the comprehensive analysis of human breath samples. Only electrical power and carrier gas are required for instrument operation. The GC × GC is combined with the multi-bed sorption trap for qualitative and quantitative analysis of organic compounds in the volatility range from about n-C_5 to n-C_{13}.

Experimental

Apparatus - A diagram showing major instrument components is presented in Fig. 1. The inset shows detail of the multi-bed trap. An HP 5890 GC is used as an experimental platform. The thermal modulator and the second (high-speed) column are located in the GC oven. The HP flame ionization detector (FID) is used with a fast (200 Hz) electrometer (Chromatofast Inc., Ann Arbor, MI). Independent temperature control of the two columns is achieved by locating the first column outside the GC oven and using at-column heating.[37] The 30-m long, 0.25-mm i.d. first column uses a 0.25-μm film of dimethyl polysiloxane (Rtx-1, Restek Corp., Bellefonte, PA). The column and co-linear heater wire and sensor wire are wrapped with fiber insulation. This ensemble is wound in a coil and the coil wrapped with metal foil. The column was prepared by RVM Scientific, Santa Barbara, CA. The temperature controller was also provided by RVM Scientific. The second column, which is located inside the 5890 oven, is 1.5-m long, 0.1-mm i.d. and uses a 0.1 μm film of polyethylene glycol (Rtx-Wax, Restek Corp.).

Modulator design - The single-stage thermal modulator uses an 8.0-cm long segment of 0.18-mm i.d. fused-silica-lined stainless steel tubing with a 0.18-μm thick film of dimethyl polysiloxane (Mxt-1, Restek Corp.). The center 5.5 cm of the modulator tube is heated by way of electrical contacts made directly to the modulator. The modulator is housed in a machined aluminum block containing a 1.6-cm o.d., 1.0-cm i.d., 5.0 cm long ceramic tube. Holes in the ceramic tube provide for the cooling air flow. The holes in the ends of the aluminum block are sealed with standard 11 mm injection-port septa. The modulator tube passes through the center of each septum, which provide a gas-tight seal.

The entire housing containing the modulator tube is wrapped with high temperature Kevlar tape and mounted to the inside wall of the GC × GC oven.

The modulator tube is resistively heated by the current from an adjustable-voltage dc power supply (Model DS-304M, Zurich MPJA, Lake Park, FL). A 0.5-s long heating pulse is applied to the modulator tube every 5.0 s. The pulse voltage and current are 4.44 V and 3.44 A (average), respectively. Heating pulse timing is controlled with a PC by means of a solid-state relay (RSDC-DC-120-000, Continental Industries Inc., Mesa, AZ).

Modulator cooling is provided by cold air from a conventional refrigeration unit (Model CC-100 Cryocool Immersion Cooler, Neslab Instruments, Portmouth, NH) by means of a heat exchanger built in house. A re-circulating pump is used to prevent ice accumulation in the heat exchanger. The cold-air flow rate was 35 L/min, and the air exiting the heat exchanger had a temperature of −45 °C. The device is very low maintenance and requires only line voltage for its operation.

Multi-bed trap design - The trap used for sample procencentration was constructed in house and has been described in detail. In brief, the trap consists of a 8.0-cm long, 1.35-mm i.d. Inconel 600 (Co–Ni alloy) metal tube (Accu-Tube Corp., Englewood, CO) packed with four discreet sorption beds indicated as Y, B, X and C in Fig. 1. Three of the beds use different grades of graphitized carbon (Carbopack Y, B and X, Supelco, Bellefonte, PA), and the forth bed (C) consists of carbon molecular sieves (Carboxen 1000, Supelco). Each bed contains approximately 2.2 mg of sorbent. The beds are separated by plugs of glass wool, and the bed ensemble is retained in the trap tube by

plugs of stainless steel mesh. Under sampling flow, the beds are ordered from weakest to strongest (largest surface area) from right to left in Fig. 1. In this way, only the most volatile and difficult to retain analytes will be exposed to the strongest sorbent bed. For desorption, the flow direction is reversed. The multi-bed trap was conditioned off-line at 250 °C for 2 h under a constant flow (75 mL/min) of dry nitrogen.

A vacuum pump (KNF, UN86 KNI, KNF-Neuberger, Trenton, NJ) is used to pull sample gas from right to left through the trap tube in Fig. 1. Sample flow rate is 50 cm^3/min. Valves V_1, a three-way valve (01380-05, Cole Parmer, Vernon Hills, IL) and V_2, a two-way valve (LFVA1230113H, Lee Co., Inestbrook, CT) are used for flow control. For sample collection, V_2 is open, and V_1 is open to the vacuum pump. After sample collection is complete, valve V_2 is closed, and valve V_1 is open to the hydrogen carrier gas. Carrier gas flows through the trap tube from left to right. During sample collection, the weakest adsorbent (bed Y) strips the least volatile components from the sample. The process continues, and only the most volatile and polar compounds are collected in the strongest adsorbent (bed C). After sample collection, the carrier gas flow through the trap is reversed relative to the direction from that of the gas flow during sampling. This prevents the least volatile compounds from ever reaching the strongest adsorbent from which they would be very difficult to thermally desorb. This results in quantitative desorption with no significant memory effects.

Thermal desorption is accomplished by resistively heating the metal trap tube to about 300 °C by means of current pulses from two ac autotransformers. Initial heating to about 300 °C is obtained from a 1.0-s long, 8.4 V pulse, and the trap temperature is

maintained at this value by a 15.0-s long, 2.8 V pulse. This produces a 1–2 s wide injection plug for the GC × GC. The heating pulses are controlled by means of solid-state relays (RSDC-DC-120-000, Continental Industries, Leesburg, VA) and LabTech Notebook software (LabTech, Andover, MA). This methodology allows the multi-bed trap to remain on-line and be reused. The multi-bed trap used for this study has more than 300 injections and is currently being used for further breath analysis investigations.

Materials and procedures - The standard HP 5890 electrometer lacks a sufficiently small time constant for monitoring the very narrow peaks from the second column, and a connection was made directly from the FID collector electrode to the high-speed electrometer. This necessitated operating the FID with an open-circuit ground. In order to reduce noise, the collector electrode assembly and the wire leading to the electrometer were wrapped with a grounded metal foil sheath. Despite this, the noise level was about 10 fold greater than with the standard HP electrometer. Data from the electrometer are sampled at 100–200 Hz by means of a 16-bit A/D board (PC1-DAS1602/16, Measurement Computing, Middleboro, MA) and a PC. Data are processed by Grams Spectral Notebook software (Thermo Galactic, Salem, NH). Peak volume integration, template overlay and display were performed with MatLab software (The Math Works, Natick, MA).

Test mixtures are prepared by injecting microliter quantities of either single components or neat mixtures of reagent-grade compounds into 12-L Tedlar gas sampling bags (SKC Inc., Eighty-Four, PA), diluting with compressed dry air and equilibrating for 30 min before sampling. Table 1 lists the test compounds with their respective chemical

formulas and boiling points. These compounds were chosen because they have been detected in human breath samples.[19,29]

Breath samples were collected in similar 1-L Tedlar gas-sampling bags. Typically, 250–800 cm^3 of a breath sample are passed through the multi-bed trap for each experiment. All of the human breath samples were collected in the morning prior to eating lunch and at least 30 min after consuming any food or beverages. Each breath sample was obtained following a deep breath, which was held for 10 s and then exhaling slowly for 10 s prior to filling the gas sampling bag.

Hydrogen carrier gas was used after purification with filters for hydrocarbons, oxygen and water vapor. The inlet pressure was set to give a flow rate of 2.2 cm^3/min at the FID. Both columns were operated with a temperature programming rate of 3.0 °C/min following a 3.0 min isothermal interval at 22 °C (room temperature) for the first column and 30 °C for the second column. The final temperatures were 175 °C for the first column and 185 °C for the second column.

Results and discussion

Instrument performance - Carrier gas flow velocities through the columns and the thermal modulator were computed from standard equations for gas flow through capillary tubes.[38] The average and exit velocities for the first column were 28.8 cm/s and 31.2 cm/s, respectively. The base width (4σ) of the bands eluting from the first column ranged from about 20 s for the weakly retained sample components to about 30 s for the most strongly retained components. Thus, for the 5.0 s modulation period, 4–6 second-

dimension chromatograms were obtained for each first-dimension peak. The average gas velocity in the thermal modulator tube was 200 cm/s, and the average velocity in the second column was 270 cm/s. The corresponding holdup times for each column are 0.04 s and 0.57 s, respectively.

The temperature of the modulator tube during trapping varied with both cooling gas flow rate and oven temperature. At the start of a run with an oven temperature of 30 °C, the modulator reached a minimum temperature of −26 °C using a cooling-gas flow rate of 35 L/min. For these conditions, the air leaving the heat exchanger was at −45 °C. For higher cooling-gas flow rates, heat exchange was less efficient, and the trapping temperature increased. At lower flow rates heat gain during transport from the heat exchanger to the modulator increased with a corresponding increase in trapping temperature. During analysis, the modulator temperature increased nearly linearly as the oven is heated, reaching a maximum temperature of 26 °C at the end of a run (oven temperature 175 °C). Even with a temperature increase in the modulator throughout the analysis due to the GC oven temperature ramp, the temperature differential between the first column and the modulator was still substantially large. This large delta T was sufficient for trapping high-boiling compounds that elute from the first column at elevated temperatures.

Chromatograms of test mixture - Fig. 2 shows the GC × GC chromatogram of the 40-component test mixture. The horizontal axis shows retention times on the first column, and the vertical axis shows retention times on the second column. The spots are the projections of the peaks onto the retention-time plane. The numbers correspond to the

compound numbers in Table 1. Peaks 4, 5, 9 and 16 are all from alcohols, and they show substantially more broadening than the other compounds. This is typical of alcohols on wax columns with conventional GC as well as with GC × GC. The insets in Fig. 2 show selected portions of the chromatogram on an expanded time scale for component pairs that are only partially separated in the chromatogram. Note that component pairs 22 and 23 (m-xylene and p-xylene) and 25 and 38 (o-xylene and 2-heptanone) are not separated on either column and appear as single peaks in the chromatogram. The peak capacity for the chromatogram is estimated at about 1500 peaks for a resolution of 1.5.

Quantitative analysis - The quantity of material injected into the GC can be varied by varying the concentrations in the gas-sampling bag and by varying the sampling duration. For quantitative analysis, the sums of the modulated peak areas from the linear chromatogram for a specified mixture component were computed from standards. Calibration data were collected for 13 of the compounds listed in Table 1. Calibration ranges (low ppb to low ppm) were chosen to cover approximately three orders of magnitude. Five replicate experiments were conducted for each concentration, and average peak area values were computed. Table 2 gives the mass range, linear-regression correlation coefficients, average percent relative standard deviations and detection limits [(mass/concentration) and (volume/volume)] for the 13 compounds studied. Detection limits are based on extrapolation of the plots to a signal-to-noise ratio of 3.0.

Correlation coefficients are all in the range of 0.993–0.999 indicating linear peak-area response to concentration over at least three decades of concentration. Detection limits are about an order of magnitude greater than values reported in other GC × GC

studies. This is the result of the need to operate the HP 5890 FID with a floating ground in order to retrofit the FID to a high-speed electrometer. However, detection limits typically are an order of magnitude lower than previously reported using the same multi-bed sorption trap and the same sample size but with a conventional (one-dimensional) separation and FID detection. The very substantial reduction in detection limits is the result of the very narrow injection plug widths from the electrically-heated modulator and the subsequent narrow peaks from the second column separation. Because of the very low concentrations of many human-breath components, the lower detection limits obtained by GC × GC are of great benefit.

Human breath analysis - Typically, about half of the components detected in human breath are respired at lower concentration than the ambient concentration in the inhaled air. The difference in the concentrations inhaled and exhaled reflects an increased body burden for these components and is of interest to the public health community. Components that are respired at greater concentration than in the air inhaled may be the result of metabolic processes as well as from recent diet, use of hygiene products, smoking and other non-metabolic sources. Accurate measurements from human breath samples require the use of parallel sampling of breath and environmental air so that the concentration differences (alveolar gradient) can be computed. The work reported here focused on the development of a reliable, quantitative screening method with lower detection limits and enhanced separation power relative to conventional GC separations, rather than to study specific applications. Thus, the alveolar gradient was not computed, and only the respired samples were collected.

Human breath samples were collected in Tedlar gas sampling bags from co-workers on this project. Considerable interest surrounds the adsorption properties of compounds on the bag walls. Studies by McGarvey and Shorten, concluded that methanol and other small molecular weight alcohols will adsorb to the bag walls and should be analyzed within 24 h of sampling to avoid discrepancies.[39] In a more recent study, Cariou et al., investigated the use of double-wall Tedlar bags to limit humidity evolution within dry air samples.[40] All breath samples collected for this study were allowed to equilibrate for 30 min and then immediately analyzed. A sampling time of 300 s at 50 cm^3/min was used unless otherwise specified. Fig. 3 shows three-dimensional views of GC × GC chromatograms for a breath sample from two individuals. The chromatograms are very different, which is consistent with previous work showing great variability in the composition of human breath.[2,3,11,16] Factors affecting these differences include medical conditions, environmental influences and overall lifestyle. Blanks run under identical conditions using purified air as a sample inside the gas sampling bags showed only a featureless base line. Blank runs were performed before and after each breath sample.

In chromatogram 3(a), 64 peaks are observed with a signal-to-noise ratio >3.0. Two very large peaks are observed with small retention times on both columns. These peaks are for n-pentane (1) and acetone (3). Most of the n-alkanes from C_5 to C_{12} are observed with relatively large peaks for C_{11} (35) and C_{12} (39). A total of 10 compounds from the 40-component test mixture in Table 1 were detected and are listed in Table 3. These peaks were identified by means of retention time matches on both columns with the 40-component test mixture chromatogram in Fig. 2 as well as a software template overlay. The template overlay allows for visual comparison between the standards and

the unknown breath samples. The numbers in Table 3, column 3(a) refer to concentrations in ppb for cases where calibration plots were obtained, and the concentration values were within the calibration range listed in Table 2. A (x) listed in Table 3 denotes an identified compound but no quantitative data. Note that some wraparound (a condition occurring when compounds on the second column do not elute prior to the next modulator cycle) is observed in chromatogram 3(a) between C_{10} (29) and C_{11} (35). This indicates the presence of very polar compounds that elute from the second column after the second modulator heating pulse occurs relative to the pulse from which the compounds were injected into the second column.

For chromatogram 3(b), 33 peaks are detected with a signal-to-noise ratio of 3.0 or greater. Acetone (3) and n-pentane (1), which are the largest peaks in chromatogram 3(a), are barely detectable in chromatogram 3(b). A number of higher molecular weight alkanes from n-C_9 to n-C_{12} have relatively large peaks. The largest peak in the chromatogram is in the retention region for the xylenes and ethylbenzene. Peak area reproducibilities (RSD values) for three 250-cm^3 aliquots drawn from the same gas sampling bag are less than 1%. Identified compounds are listed in Table 3 and quantitative data are listed in column 3(b).

Fig. 4 shows the chromatogram from an 800 cm^3 (16 min sampling time) breath sample from the same individual in Fig. 3(a). Note that this is near the upper limit of human lung capacity, and larger samples will require multiple breaths. Alternatively, a lower-noise electrometer could be used with smaller samples to achieve a low limit of detection for trace components. Chromatogram 4(a) shows the two-dimensional

projection (contour plot) with identified compounds. The vertical streak occurring for a first-column retention time of about 3 min is caused by severe breakthrough of acetone and n-pentane, which overloaded the columns and the modulator for this larger sample.

A total of 212 peaks are observed in the chromatogram at a signal-to-noise ratio of 3.0 or greater. All n-alkanes from C_5 to C_{12} are detected. A total of 25 compounds from the 40-component test mixture in Table 1 were detected and are listed in Table 3. Concentrations obtained by comparison with the calibration data are listed in the table for 10 of the compounds. The complexity of the chromatogram shows the usefulness of GC × GC and the available peak capacity it offers for this application.

The breath samples in Fig. 3 and Fig. 4 were collected about 5 min apart from the same individual in two different gas sampling bags. Note in Table 3 that the calculated concentrations for all seven components for which calibration data were available are in very good agreement indicating the overall reproducibility of the method and the efficacy of quantitative analysis of organic compounds in human breath samples at ppb levels.

Fig. 5 shows chromatograms from a smoker just before (a) and 5-min after smoking a cigarette (b). The sample size was 250 cm^3. Although an 800 cm^3 sample would have been ideal for this study, the subject was not able to completely fill a 1-L bag with one respired breath after a 10 s exhale. The latency from the previous cigarette was greater than 8 h. For chromatogram 5(a), 38 components were detected, and 11 compounds from the 40-component test mixture were identified by retention time comparison and template overlay. The number of detected peaks increases to 77 in chromatogram 5(b), and 23 components were identified from the 40-component test

mixture. For visual purposes, only quantified compounds are listed in Fig. 5. All identified compounds are listed in column 5(a) and 5(b) of Table 3. Note that nearly all of the peaks present in Fig. 5(a) show increased concentration in Fig. 5(b).

Of particular interest in Fig. 5 and Table 3 is the concentration of 2,5-dimethylfuran (15) before and after smoking. This carcinogenic compound is considered a bio-marker for tobacco smoke.[41] From the calibration plot for this compound, the concentration prior to smoking was determined to be 19.4 ppb. After smoking, the concentration of 2,5-dimethylfuran increased to 81.2 ppb. This compound was not detected in any of the samples obtained from the non-smoker or the blank runs.

In another study, breath samples were collected at different times after the subject chewed a piece of fruit-flavored gum for 5 min. Breath samples were collected at 5, 30 and 60 min after disposing of the gum. A sampling time of 300 s at 50 cm^3/min was used. Fig. 6 displays the three-dimensional views of the major components for sampling times of 5 min (a), 30 min (b) and 60 min (c). In all cases, the peak area scale has been compressed relative to previous figures so that all observed peaks are from the major breath components. The chromatograms are believed to contain peaks for mono-terpenes and other essential-oil components used for flavoring. It is clear from this figure that the elimination of these components from the body over time can be monitored.

Conclusions

This report has described a GC × GC system that uses a reusable multi-bed sorption trap and a single stage resistively-heated and air-cooled thermal modulator for

the screening and quantitative analysis of human breath. A linear dynamic range of three orders of magnitude and detection limits in the part-per-trillion concentration range have been demonstrated and should be very useful for breath analysis. In addition to the lower detection limits, the very large peak capacity, larger than can be achieved by a one-dimensional separation in an equivalent run time, provides significantly greater specificity than conventional one-dimensional GC. Although an FID detector was used in this study, the use of a mass spectrometer would provide valuable information regarding the chemical structure of the analytes. A mass spectrometer capable of acquiring data at a fast acquisition rate would be necessary for the narrow modulated peaks that reach the detector. In this respect, a time-of-flight mass spectrometer with a fast acquisition rate would be ideal for this work. Less expensive scanning mass spectrometers are not capable of acquiring data at a suitable rate.

An important advantage of the GC × GC system described here is greatly reduced resource requirements relative to systems requiring cryogenic materials and compressed gases for modulator heating and cooling. With the present system, only carrier gas, flame gas and electric power are required. Work is in progress to further reduce the size and weight of the instrument in order to achieve portability. Current research in our lab is focused on coupling a miniaturized time-of-flight mass spectrometer to the GC × GC platform. To this end, a bread–board system with independently heated transfer lines to obviate the need for the GC platform is being evaluated. The system replaces chilled air with a liquid coolant and a relatively small liquid chiller. Preliminary work suggests enhanced performance due to the more rapid modulator cooling achieved with liquid cooling.

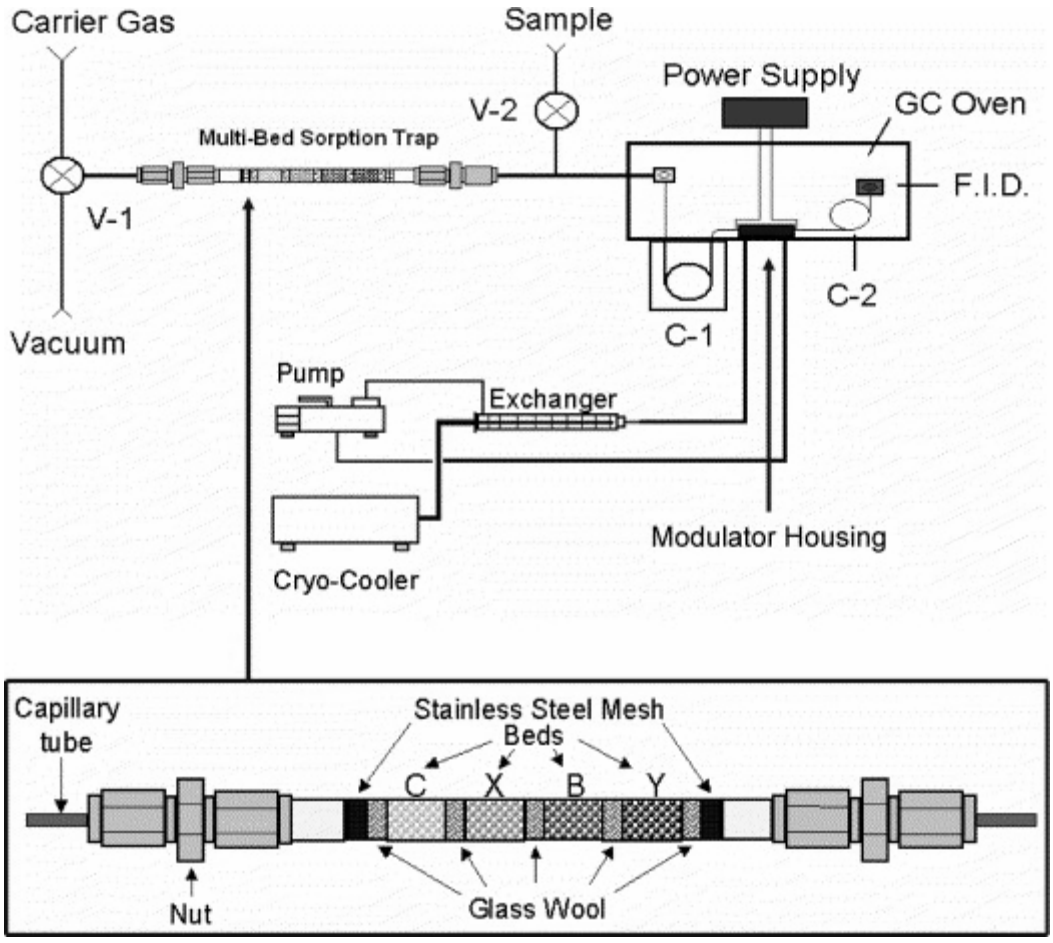

Figure 4.1 - Schematic of the GC × GC instrument used for human breath anaysis. A multi-bed sorption trap is used for sample collection and introduction into the GC × GC-FID.

No.	Name	B.P. (°C)
1	Pentane	35–36
2	Isoprene	34
3	Acetone	56
4	Ethanol	78
5	2-Propanol	82
6	Hexane	69
7	2-Butanone	80
8	Ethylacetate	77
9	1-Propanol	97
10	2-Butanol	98
11	Benzene	80
12	Isooctane	98–99
13	Heptane	98
14	2-Pentanone	100–101
15	2,5-Dimethylfuran	93
16	1-Butanol	118
17	Toluene	111
18	Octane	125–127
19	Hexanal	131
20	Butylacetate	126
21	Ethylbenzene	136
22	m-Xylene	139
23	p-Xylene	138
24	Nonane	151
25	o-Xylene	143–145
26	Cumene	152–154
27	α-Pinene	155
28	β-Pinene	167
29	Decane	174
30	1,2,4-Trimethylbenzene	168
31	Benzaldehyde	178–179
32	Limonene	176
33	1,2,3-Trimethylbenzene	175–176
34	1,2-Dichlorobenzene	180
35	Undecane	196
36	3-Pentanone	102
37	1-Pentanol	136–138
38	2-Heptanone	149–150
39	Dodecane	216
40	1,3-Dichlorobenzene	172–173

Table 4.1 – A 40-component mixture based on compounds found in human breath samples.

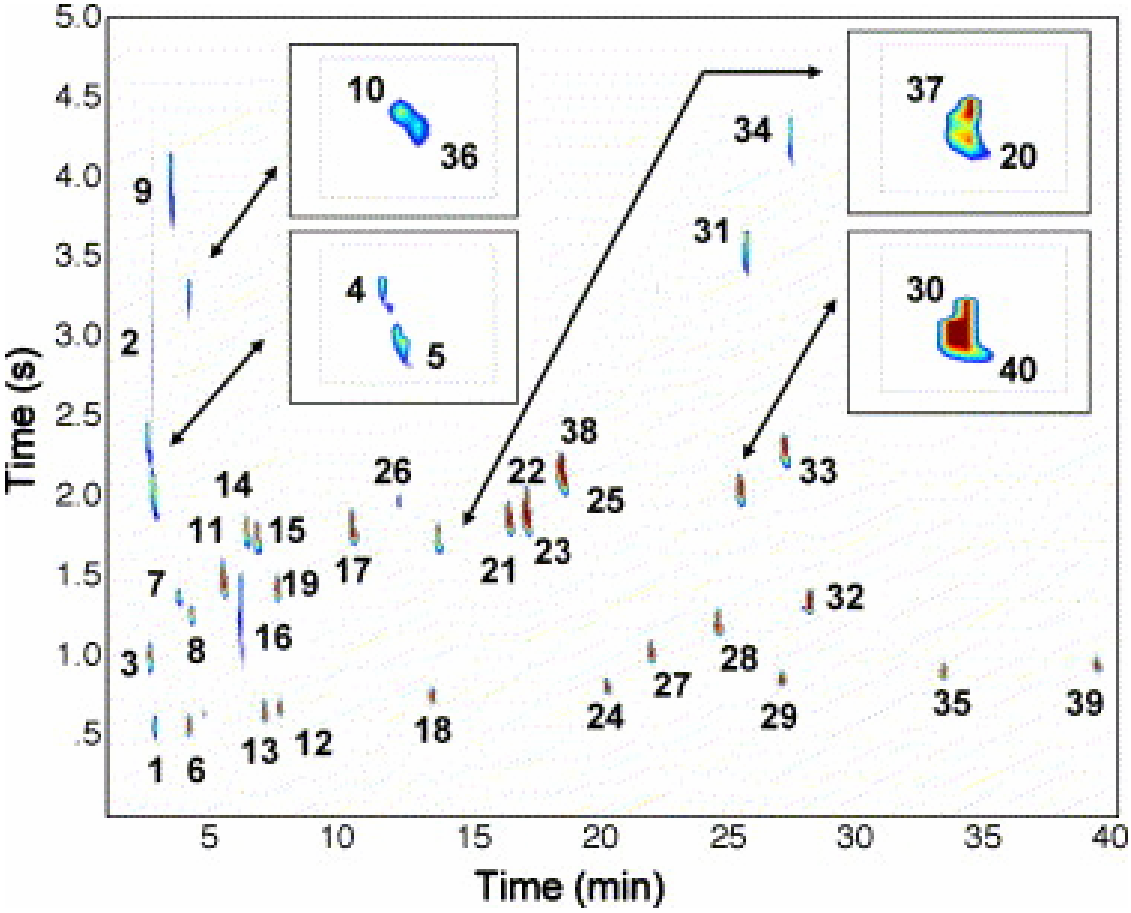

Figure 4.2 - Two-dimensional (contour) chromatogram of a 40-component test mixture containing compounds found in human breath. The insets show expanded views of portions of the chromatogram containing overlapping peaks. Peak numbers correspond to compound numbers in Table 1.

No.	Compound	Mass range (µg)	v/v (ppb)	R^2	RSD (%)	LOD (pg)	LOD (ppt)
8	Hexane	1–1283	7–7790	0.998	0.83	54	216
16	Heptane	1–1189	6–6953	0.991	0.81	50	198
21	Octane	1–1101	6–6269	0.996	0.79	57	228
27	Nonane	1–1023	5–5702	0.998	0.85	48	193
32	Decane	1–953	5–5222	0.998	0.75	46	185
39	Undecane	1–892	5–4822	0.997	0.81	40	161
43	Dodecane	1–841	4–4485	0.998	0.86	37	148
7	2-Propanol	2–678	13–3459	0.993	0.86	62	250
14	Benzene	2–672	11–3078	0.997	0.71	53	211
18	2,5-Dimethylfuran	2–648	9–2871	0.998	0.76	56	222
20	Toluene	2–661	9–3060	0.999	0.65	44	174
30	α-Pinene	1–412	6–1924	0.999	0.81	68	274
35	Limonene	1–400	6–1893	0.999	0.88	66	263

Table 4.2 - Statistical data from calibration plots of 13 compounds found in the test mixture.

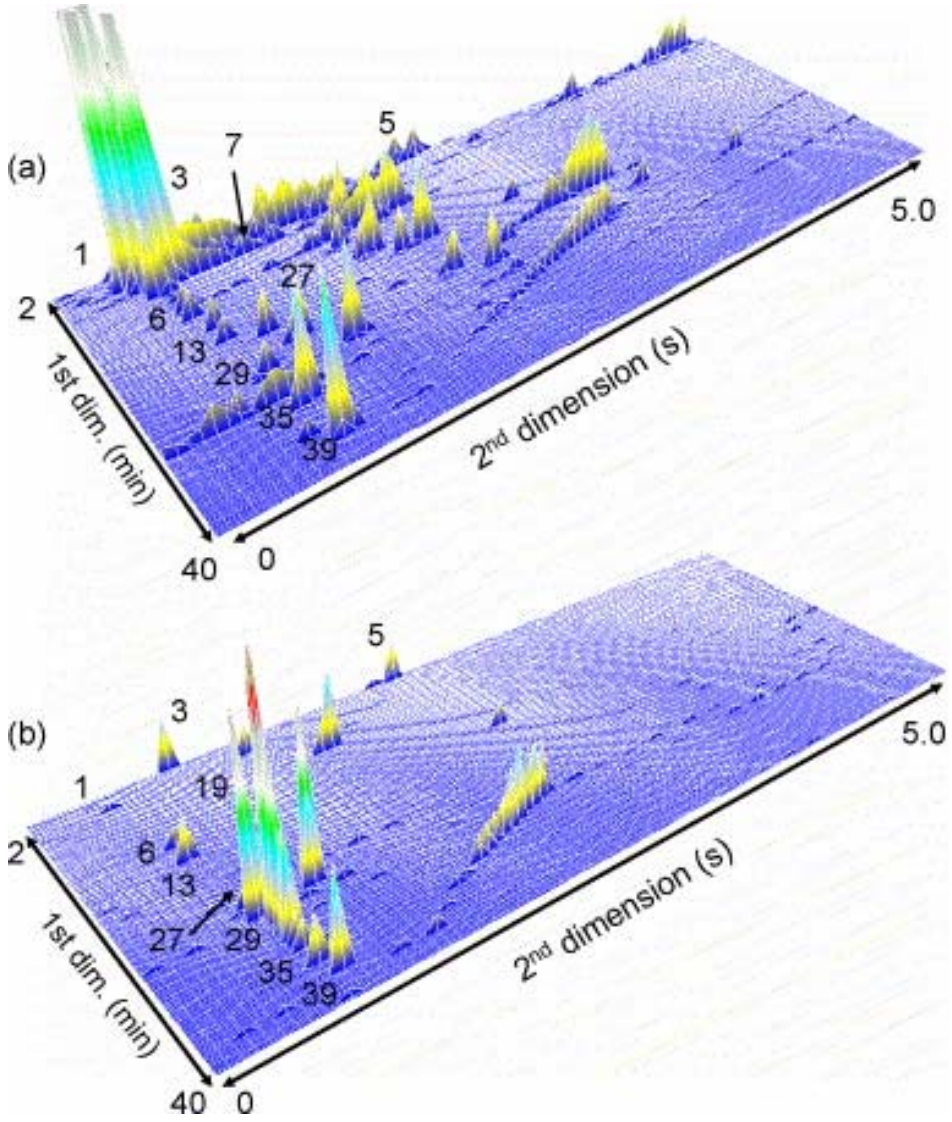

Figure 4.3 - Three-dimensional view of GC × GC chromatograms of human breath sample collected from two individuals. A sample collection time from the 1-L gas sampling bags of 300 s at a flow rate of 50 cm^3/min was used. Identified compounds are listed in columns 3(a) and 3(b), respectively, in Table 3.

Table 4.3 - Compounds identified in human breath samples

No.	Name	Figure				
		3(a)	3(b)	4	5(a)	5(b)
1	Pentane	x	x	x	x	x
3	Acetone	x	x	x	x	x
6	Hexane	95	22	94	22	71
8	Ethylacetate	n/d	n/d	x	x	x
4	Ethanol	n/d	n/d	x	x	x
7	2-Butanone	x	n/d	x	n/d	x
11	Benzene	n/d	n/d	n/d	n/d	47
5	2-Propanol	137	155	135	101	411
15	2,5-Dimethylfuran	n/d	n/d	n/d	19	81
9	1-Propanol	n/d	n/d	x	x	x
10	2-Butanol	n/d	n/d	x	n/d	n/d
13	Heptane	31	7	30	1	10
12	Isooctane	n/d	n/d	x	n/d	n/d
14	2-Pentanone	n/d	n/d	x	n/d	x
17	Toluene	n/d	n/d	n/d	n/d	54
18	Octane	n/d	n/d	1	n/d	n/d
19	Hexanal	n/d	x	x	n/d	x
21	Ethylbenzene	n/d	n/d	x	n/d	x
23	p-Xylene	n/d	n/d	x	n/d	x
22	m-Xylene	n/d	n/d	x	n/d	x
25	o-Xylene	n/d	n/d	x	n/d	n/d
38	2-Heptanone	n/d	n/d	x	n/d	n/d
24	Nonane	n/d	n/d	1	n/d	2
26	Cumene	n/d	n/d	x	n/d	n/d

27	α-Pinene	8	6	8	8	35
28	β-Pinene	n/d	n/d	x	n/d	n/d
30	1,2,4-	n/d	n/d	x	n/d	n/d
40	1,3-	n/d	n/d	x	n/d	n/d
29	Decane	1	3	2	n/d	8
32	Limonene	n/d	n/d	7	x	x
31	Benzaldehyde	n/d	n/d	x	n/d	n/d
34	1,2-	n/d	n/d	x	n/d	n/d
35	Undecane	4	21	5	1	2
39	Dodecane	11	7	12	0	1

(x) present but not quantified; (n/d) not detected.

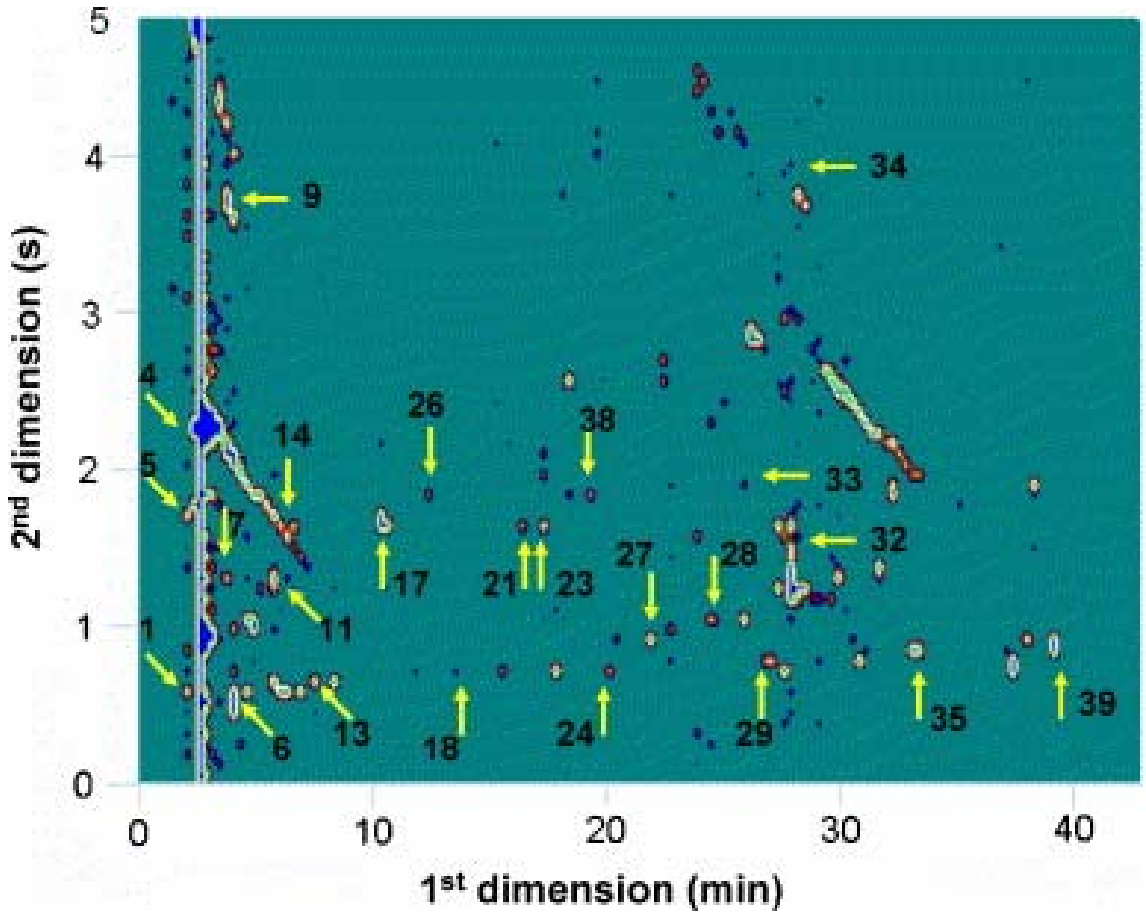

Figure 4.4 - Two-dimensional (contour) chromatogram of human breath sample collected from the same individual as in Fig. 3(a), but using a sample collection time from the gas sampling bag of 960 s at a flow rate of 50 cm^3/min. Identified and quantified compounds are listed in column 4(a) in Table 3.

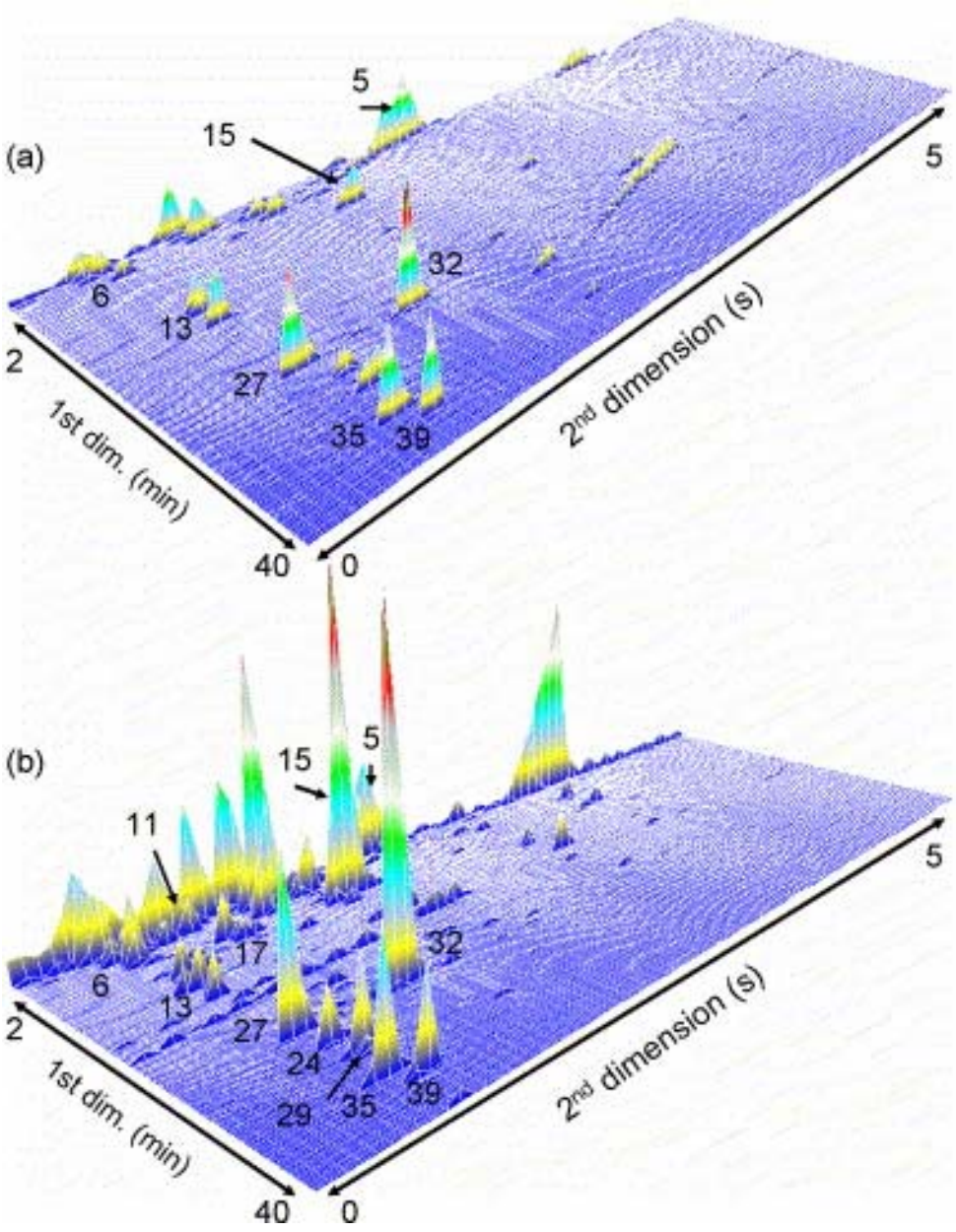

Figure 4.5 - Three-dimensional views of GC × GC chromatograms collected from human breath sample of an individual just prior to smoking a cigarette (a) and 5 min after smoking a cigarette (b). A sampling time of 300 s at a flow rate of 50 cm^3/min was used. Identified compounds and selected quantitative results are listed in Table 3, column 5. Peak (15) represents 2,5-dimethyl furan, a bio-marker for cigarette smoke. Prior to smoking, the concentration of 2,5-dimethyl furan was 19 ppb, 5 min after smoking a cigarette, the concentration of 2,5-dimethyl furan was 81 ppb.

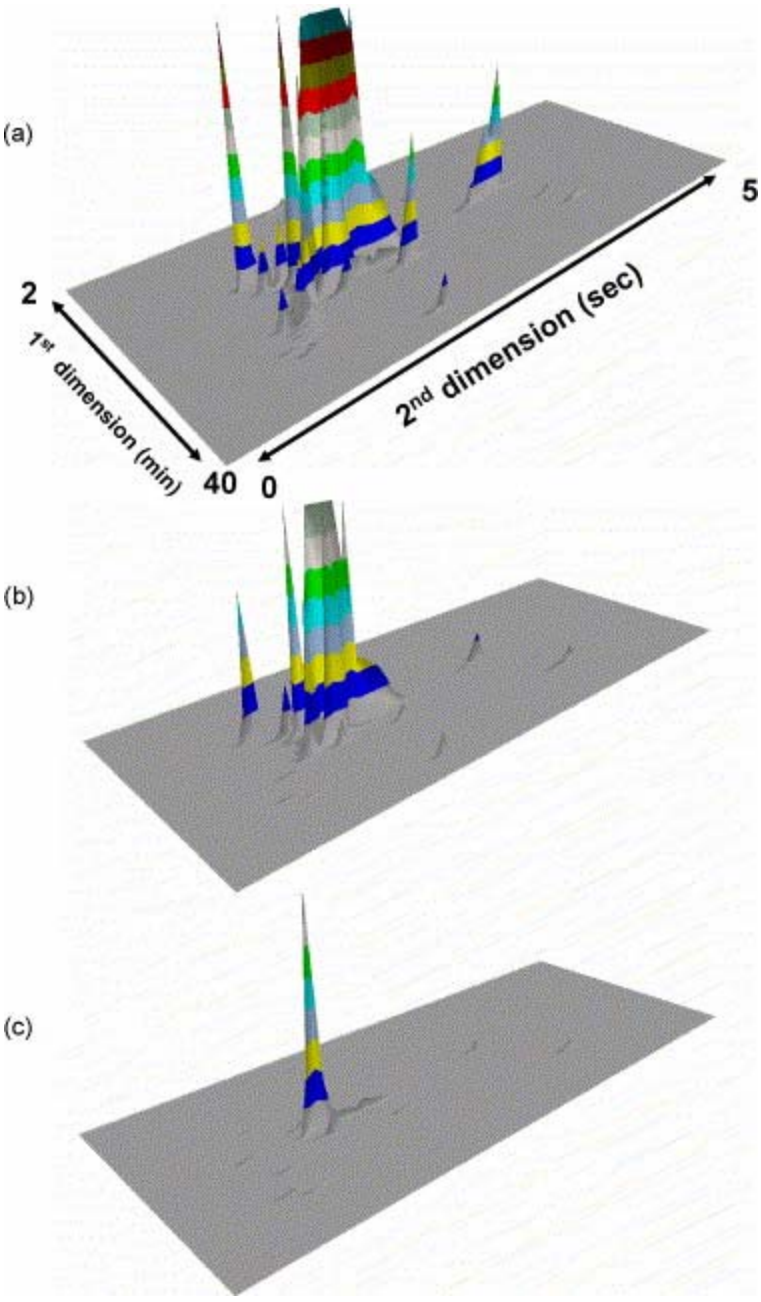

Figure 4.6 - Three-dimensional views of GC × GC chromatograms from human breath sample obtained from an individual 5 min (a), 30 min (b), and 60 min (c) after chewing a piece of fruit-flavored gum. Major breath components are displayed on the chromatograms and show a decrease over time.

REFERENCES

[1] S. Chen, L. Zieve and V. Mahadevan, *J. Lab. Clin. Med.* **75** (1970), p. 628.
[2] H. Lord, Y. Yufan, A. Segal and J. Pawliszyn, *Anal. Chem.* **74** (2002), p. 5650.
[3] M. Phillips, *Sci. Am.* **267** (1) (1992), p. 74.
[4] J.H. Raymer, K.W. Thomas, A.B. Pellizzari, D.A. Whitaker, S.D. Cooper, T. Limero and J.T. James, *Aviat. Space Environ. Med.* **65** (1994), p. 353.
[5] H. Kaji, M. Hisamura, N. Saito and M. Muraro, *J. Chromatogr.* **145** (1978), p. 464.
[6] V. Ruzsanyi, J.I. Baumbach, S. Sielemann, P. Litterest, M. Westhoff and L. Freitag, *J. Chromatogr. A* **1084** (2005), p. 145.
[7] M. Giardina and S.V. Olesik, *Anal. Chem.* **75** (2003), p. 1604.
[8] S.M. Gordon, J.P. Szidon, B.K. Krotoszynski, R.D. Gobbons and H.J. O'Neill, *Clin. Chem.* **31** (1985), p. 1278.
[9] J.K. Schubert, W.P.E. Muller, A. Benzing and K. Geiger, *Intensive Care Med.* **24** (1998), p. 415.
[10] J.K. Schubert, K.H. Spitter, G. Braun, K. Geiger and J. Guttmann, *J. Appl. Physiol.* **90** (2001), p. 486.
[11] R. Hyspler, S. Crhova, J. Gasparic, Z. Zadak, M. Cizkova and V. Balasova, *J. Chromatogr. B* **739** (2000), p. 183.
[12] C. Grote and J. Pawliszyn, *Anal. Chem.* **69** (1997), p. 587.
[13] A. Manolis, *Clin. Chem.* **29** (1983), p. 5.
[14] N. Rizvi and D.F. Hayes, *Lancet* **353** (1999), p. 1897.
[15] H.J. O' Neill, S.M. Gordon, M.H. O'Neill, R.D. Gibbons and J.P. Szidon, *Clin. Chem.* **34** (1988), p. 1613.
[16] C. Preti, J.N. Labows, J.G. Kostelc, S. Aldinger and R. Daniele, *J. Chromatogr.* **432** (1988), p. 1.
[17] M. Phillips, K. Gleeson, J.M.B. Hughes, J. Greenberg, R.N. Cataneo, L. Baker and W.P. McVay, *Lancet* **333** (1999), p. 1930.
[18] G. Stix, *Sci. Am.* (2003), p. 26.
[19] S. Davies, P. Spanel and D. Smith, *Nephrol. Dial Transplant.* **16** (2001), p. 836.
[20] J.D. Fenske and S.E. Paulson, *J. Air Waste Manage. Assoc.* **49** (1999), p. 594.
[21] M. Phillips, J. Herrera, S. Krishman, M. Zain, J. Greenebrg and R.N. Cataneo, *J. Chromatogr. B* **729** (1999), p. 75.
[22] J. Dewulf and H. Van Langenhove, *J. Chromatogr. A* **843** (1999), p. 163.
[23] C. Peng and S. Batterman, *J. Environ. Monit.* **2** (2000), p. 313.
[24] A. Van Es, H. Janssen, C. Cramers and J. Rijks, *J. High Resolut. Chromatogr.* **11** (1988), p. 852.
[25] E. Baltusen, F. David, H. Janssen and C. Cramers, *J. High Resolut. Chromatogr.* **21** (1998), p. 332.
[26] C. Coeur, V. Jacob, I. Denis and P. Foster, *J. Chromatogr. A* **786** (1997), p. 185.
[27] X.-L. Cao and C. Hewitt, *Chemosphere* **27** (1993), p. 695.
[28] J.M. Sanchez and R.D. Sacks, *Anal. Chem.* **75** (2003), p. 978.
[29] J.M. Sanchez and R.D. Sacks, *Anal. Chem.* **75** (2003), p. 2231.
[30] P.J. Marriott and R.M. Kinghorn, *Anal. Sci.* **14** (1998), p. 651.
[31] P.J. Marriott and R. Shellie, *Trends Anal. Chem.* **21** (2002), p. 573.
[32] Z. Lui and J.B. Phillips, *J. Chromatogr. Sci.* **29** (1991), p. 227.
[33] J.B. Phillips and J. Beens, *J. Chromatogr. A* **856** (1999), p. 331.
[34] P. Marriott and R. Shellie, *Trends Anal. Chem.* **21** (2002), p. 573.
[35] L.M. Blumberg, *J. Chromatogr. A* **985** (2003), p. 29.
[36] M. Libardoni, J.H. Waite and R. Sacks, *Anal. Chem.* **77** (2005), p. 2786.
[37] R. Mustacich, J. Everson and J. Richards, *Am. Labor.* (2003), p. 38.
[38] M. McGuigan and R. Sacks, *Anal. Chem.* **73** (2001), p. 3112.
[39] L.J. McGarvey and C.V.J. Shorten, *Am. Ind. Hyg. Assoc.* **61** (2000), p. 375.
[40] S. Cariou and J.M. Guillot, *Anal. Bioanal. Chem.* **384** (2006), p. 468.
[41] S.M. Gordon, L.A. Wallace, M.C. Brinkman, P.J. Callahan and D.V. Kenny, *Environ. Health Perspect.* **110** (7) (2002), p. 689.

CHAPTER 5

ANALYSIS OF HUMAN BREATH UTILIZING A POLYDIMETHYL SILOXANE FOAM TRAP, A CRYOGENICALLY COOLED - THERMAL DESORPTION INLET AND COMPREHENSIVE TWO-DIMENSIONAL GAS CHROMATOGRAPHY

Introduction

Examining human breath for characteristic odors has been a diagnostic tool for hundreds of years. An example is that people with *Diabetes Mellitus* who are suffering from a dangerous side effect called diabetic ketoacidosis can often be detected by the characteristic "sweet acetone" odor present in their breath.[1] Chen, et al. published work identifying specific volatile organic components in human breath in 1970.[2] Pauling, et al. published work relating to the quantitative analysis of human breath by gas-liquid chromatography in 1971.[3] Previous work in our group on human breath analysis has also been done.[4,5]

Aspects of GCxGC and preconcentration that are advantageous for the analysis of human breath have been previously discussed in Chapter 4. In this study, a different inlet system is evaluated. In place of the multi-bed sorption preconcentrator used in previous work, a section of polydimethylsiloxane (PDMS) foam is used as the sorbent. In the inlet using the multi-bed sorption trap, the acts of thermally desorbing analytes from the sorbent and injecting the analytes onto the analytical column are combined in a single step. In order to achieve a sufficiently narrow injection plug, the sorbent beds are heated

very rapidly. Prior work has shown problems with decomposition of certain classes of thermally labile compounds, such as mono-terpenes and aldehydes.[6,7] Mono-terpenes are known to decompose in the presence of atmospheric ozone[8,9,10,11,12] In the current study, an inlet system is used where the analytes are thermally desorbed from the adsorbent into a cryogenically cooled inlet liner. This allows for the use of non-ballistic heating profiles during thermal desorption of the analytes from the sorbent and use of an increased flow of carrier gas across the sorbent, thereby decreasing residence time of the analytes in the heated zone. The currently available PDMS foam sampling medium is not an ideal choice, but will give an opportunity to evaluate the dual inlet system.

Experimental

For this study, a Pegasus 4D GCxGC Time-of-Flight Mass Spectrometer (LECO Corp., St. Joseph, MI) was used. It was equipped with a thermal desorption unit (TDU)-cryogenic inlet system (CIS 4) (GERSTEL-US, Baltimore, MD). A schematic of the system is shown in Figure 1. The TDU is a thermal desorption inlet designed for desorbing a variety of sample introduction media. In the case of this study the glass TDU tubes have a 20 mm x 5 mm cylinder of polydimethylsiloxane (PDMS) foam housed inside of the 60 mm x 5 mm i.d. TDU tube. A representation of the PDMS foam inside of the TDU tube is shown in Figure 2. The TDU is mounted directly on top of the CIS 4 inlet. The lower end of the TDU tube slips over the upper end of the CIS 4 liner. In this way, there is no transfer line necessary between the TDU and the CIS 4. Figure 3 shows the TDU as it is mounted on top of the CIS 4. The CIS 4 inlet has the ability to use cryogens to lower the initial temperature of the CIS 4 liner in order to trap and focus

analytes transferred from the TDU and inject them as a narrow plug onto the analytical column. Liquid nitrogen (LN_2) was used as the cryogen in this study. Both the TDU and the CIS 4 have the ability to be temperature programmed. The TDU has a maximum temperature ramp rate of 720 °C/min, a minimum temperature of 10 °C and a maximum temperature of 350°C. The CIS 4 has a maximum temperature ramp rate of 12 °C/sec, a minimum temperature of -150 °C and a maximum temperature of 450 °C.

Breath samples were collected in 3 L Tedlar bags (mod. 232-03, SKC Inc., Eighty Four, PA). Each breath sample was obtained following a deep breath, which was held for 10 sec and then exhaling slowly for 10 sec prior to filling the sample bag. All prior samples were taken at least 3 hours after any food or beverage, other than water, had been consumed. The apparatus for transferring the samples from the sample bags to the PDMS foam is shown in Figure 4. Prior to sample collection, the PDMS foam tubes were conditioned at 270 °C under a 50 mL/min flow of dry N_2(g) for approximately 2 hours. The sample bag is attached to a very short, < 2 cm, length of ¼" Teflon tubing with a Teflon adaptor at its other end. Another identical Teflon adapter is placed at the end of a ¼" i.d copper tube attached to a gas flow meter (mod. FMA-5605, Omega Engineering, Stamford, CT). In between the gas flow meter and the vacuum pump (mod. UN86-KNI, KNF-Neuberger, Trenton, NJ), a metering valve (mod. NuPro SS-4BMG, Swagelok Co., Solon, OH) is placed to set the sampling flow. The TDU tube containing the PDMS foam is placed in between the pair of Teflon adapters, provided by Ed Pfannkoch of GERSTEL-US, so that the flow direction during sample collection is the opposite of that during sample desorption. Sampling flow for this study was set at 50 mL/min. The sampled volume was set by controlling the sampling time. For this study,

samples were either collected for 20 minutes, giving a total sample volume of 1 L or 40 minutes, giving a total sample volume of 2 L.

For the GCxGC portion of this study, a Modular Accelerated Column Heater (MACH)-Low Thermal Mass (LTM) column was utilized for the first dimension column(GERSTEL-US, Baltimore, MD). The column housed in the MACH-LTM was a 10 m x 0.18 mm i.d. x 0.2 μm df Rtx-5 capillary column (Restek Corp., Bellefonte, PA). The second dimension column was housed in the GC oven and was a 1.0 m x 0.10 mm i.d. x 0.1 μm df DB-17 capillary column (Agilent Technologies., Wilmington, DE). The modulator of the Pegasus 4D is a quad-jet, dual stage thermal modulator.

The experimental conditions for the TDU/CIS4 inlet are as follows. The TDU was operated in splitless mode with an initial temperature of 30 °C. It was then ramped at 700 °C/min to 310 °C and held there for 120 seconds. The initial temperature for the CIS 4 was -120 °C. After the TDU had completed its program, it was ramped at 12 °C/sec to 310 °C and held for 120 seconds. The start of the CIS 4 temperature program coincides with the beginning of the GC program.

The experimental conditions for the GC are as follows. The initial temperature for the first dimension column, the MACH-LTM, was 40 °C. It was ramped at 5 °C/min to 240 °C and held for 2 min. The second dimension column was operated at a +15 °C offset from the first dimension column. The modulation period was set for 5 seconds. Helium was used as a carrier gas and was set at a constant flow of 1.5 mL/min via pressure ramping. The GC-MS transfer line was set at 280 °C and the acquisition rate was set at 200 spectra/sec over a *m/z* range of 40 to 350.

Results and Discussion

In the first comparison of this study, 1 L breath samples from the same subject were collected prior to the consumption of 10 oz. of orange juice and 15 minutes after the consumption of the orange juice. Figure 5 shows the contour plot chromatogram of the breath sample that was collected prior to consumption of the orange juice. The 3D surface plot of the same chromatogram is shown in the inset. Figure 6 shows the contour plot chromatogram of the breath sample that was collected 15 minutes after the consumption of the orange juice. The 3D surface plot of the same chromatogram is shown in the inset. A visual comparison of the two chromatograms shows a dramatic increase in the intensity of some peaks and a reduction in intensity of others. Of particular interest are the significant increases in intensity of peaks located in the same region as the mono-terpenes. This is region is indicated by the orange dashed box in Figure 6. The peaks in this region showing the largest increase in intensity included α-pinene, myrcene, limonene and 4-carene.

Acetone showed a decrease in area and intensity after the consumption of the orange juice. During method development there was a lack of reproducibility for small, polar components from 1 L samples taken from the same 3 L sample bag. It is believed that since the sample collection bed consisted only of a section of PDMS foam, that small polar compounds would be difficult to reproduce from run to run due to trapping efficiency. This effect was not observed in previous work utilizing the multi-bed sorption trap. It is intended to address this in future work by replacing the PDMS foam sorption bed with a custom-prepared multi-bed sorbents housed in TDU tube. This would allow

the combination of the trapping efficiency of the multi-bed sorption trap with the desorption control and injection flexibility of the TDU/CIS 4 inlet system.

In the second comparison of this study, 2 L breath samples from the same subject were collected prior to the consumption of 16 oz. of a sugar-free energy drink and 15 minutes after the consumption of the sugar-free energy drink. Figure 7 shows the contour plot chromatogram of the breath sample that was collected prior to consumption of the energy drink. The 3D surface plot of the same chromatogram is shown in the inset. Figure 8 shows the contour plot chromatogram of the breath sample that was collected 15 minutes after the consumption of the energy drink. The 3D surface plot of the same chromatogram is shown in the inset. Table 1 shows areas for six compounds present in both pre and post samples and the percentage change in area from the pre sample to the post sample. The pre-consumption of energy drink sample had 203 peaks with a s/n ratio of ≥ 100. The post-consumption of energy drink sample had 339 peaks with a s/n ratio of ≥ 100, which equates to a 67% increase in the number of peaks meeting the signal s/n ratio criteria following the consumption of the energy drink.

Conclusions

The TDU/CIS 4 inlet system used in this study is well suited for the analysis of components in human breath using GCxGC-TOFMS. The PDMS foam tubes used for sampling in this study have limitations with regard to their trapping efficiency of very volatile, small, polar components, such as acetone. The next step would be to combine the trapping efficiency of the multi-bed sorption trap with the desorption control and injection flexibility of the TDU/CIS 4 inlet system. This system would not be ideal for a

field portable system and the previously described multi-bed sorption trap system, with its lack of need for cryogens. If field portability and reduction of consumables is not an issue, then the TDU/CIS 4 inlet system described in this study, with the PDMS foam sorbent replaced by a multi-beds of carbon-based sorbents would demonstrate more flexibility in its ability to optimize desorption and injection parameters for target analytes. The primary advantage of the TDU/CIS 4 inlet system is that it allows for the decoupling of the desorption conditions from the injection conditions. The coupling of this with the effectiveness of the multi-bed sorption trap to collect analyte over a wide range of functional groups and volatilities presents a very capable and flexible system.

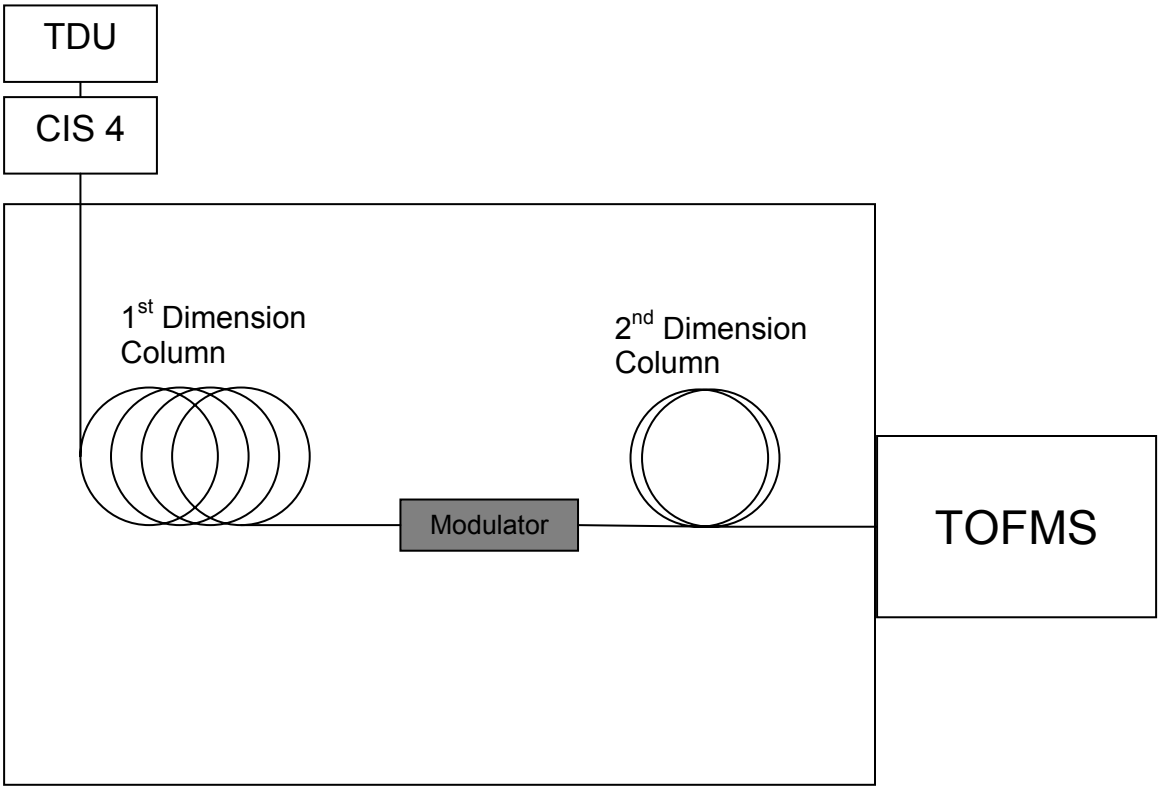

Figure 5.1 – A schematic of the TDU/CIS 4 GCxGC-TOFMS system.

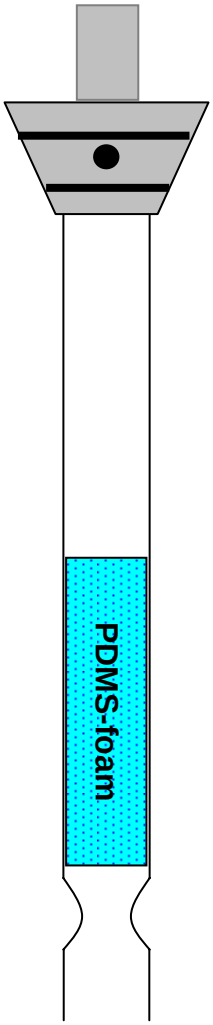

Figure 5.2 – A representation of the PDMS foam inside of the TDU tube.

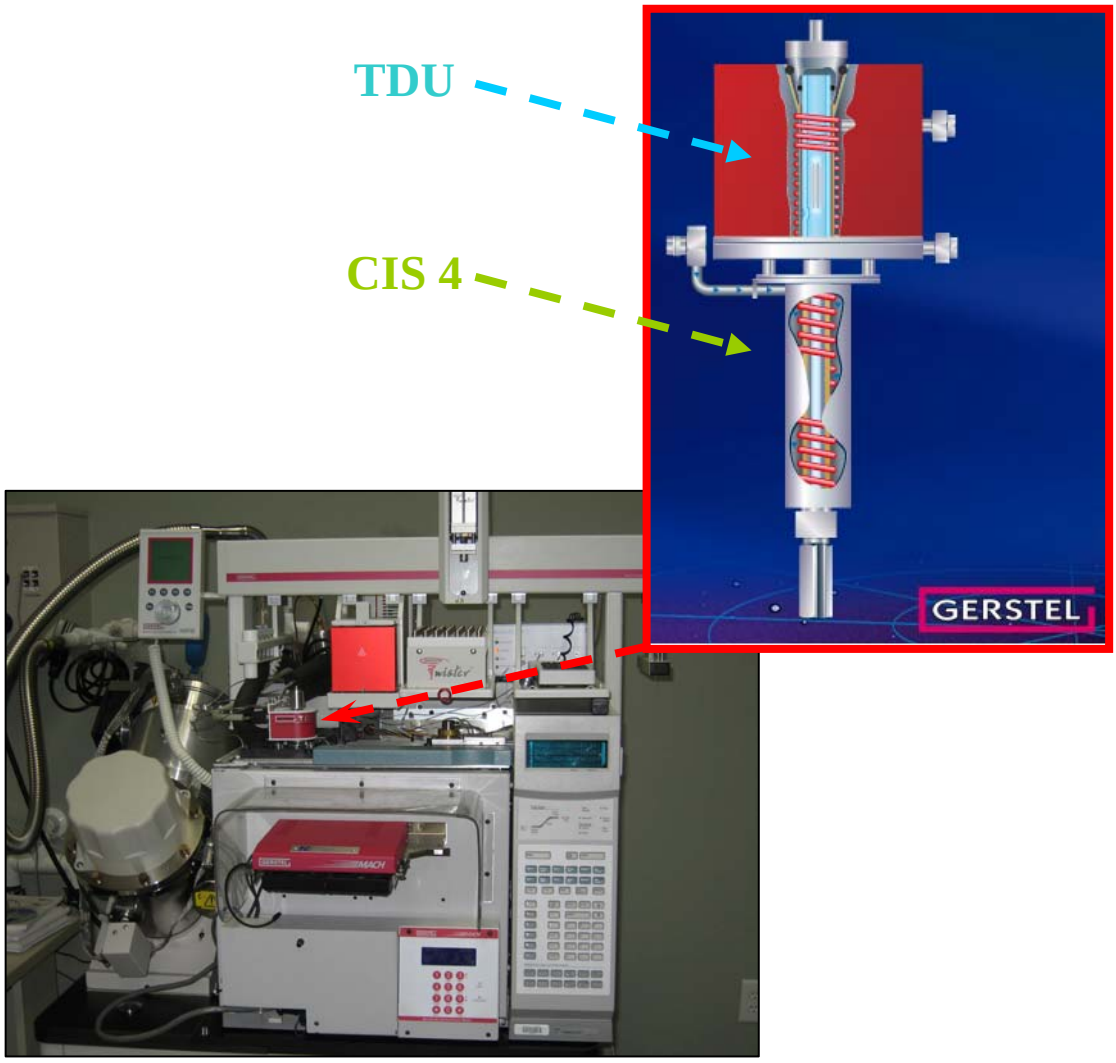

Figure 5.3 – A figure showing the TDU/CIS 4 inlet system as mounted on the GCxGC-TOFMS.

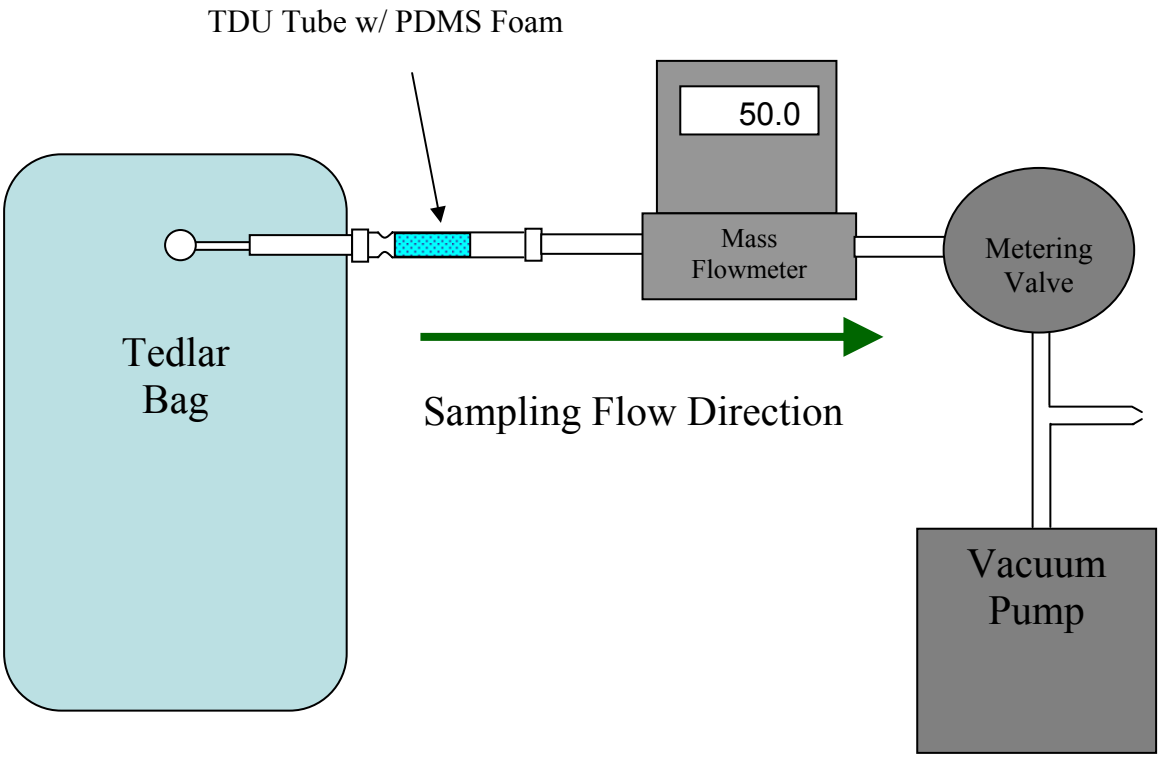

Figure 5.4 – A schematic of the sampling apparatus used to transfer the breath sample from the sampling bag to the PDMS foam.

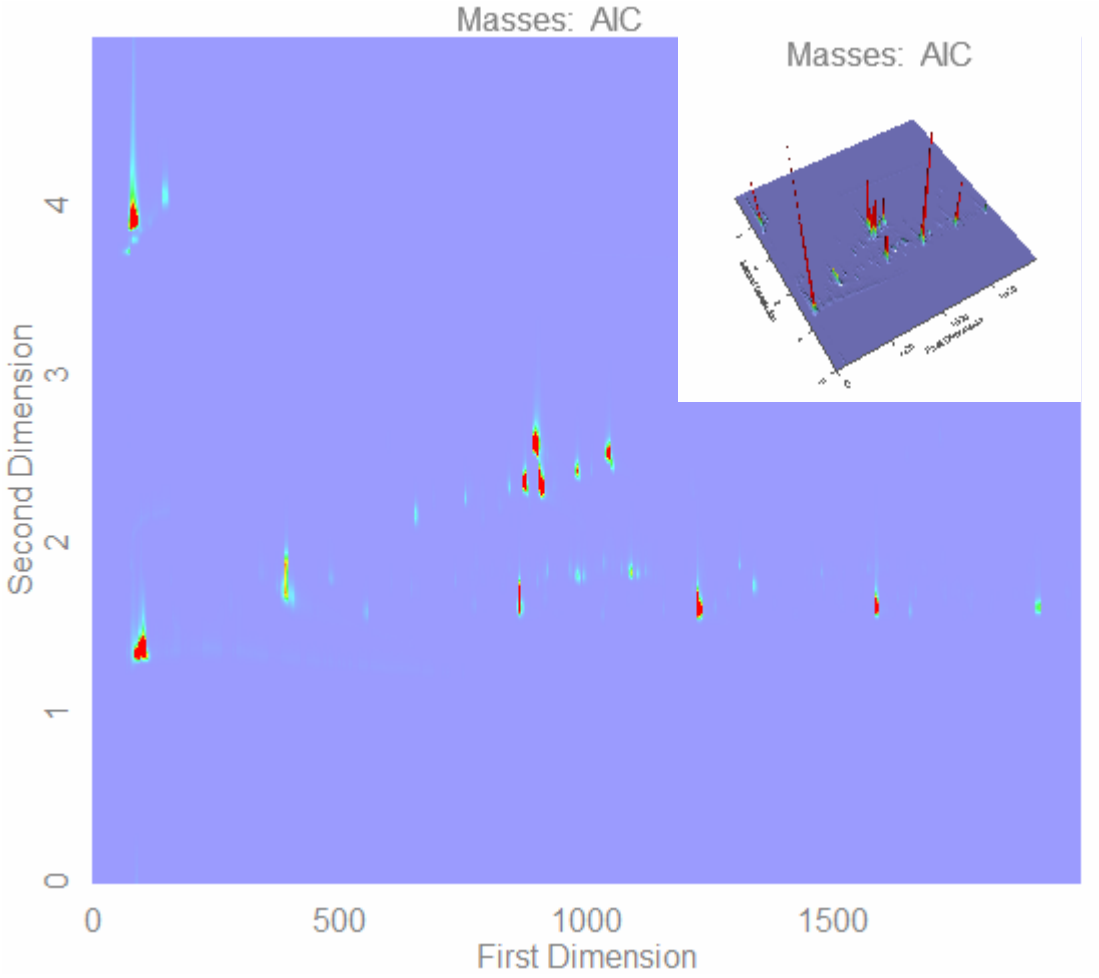

Figure 5.5 – A GCxGC chromatogram of a 1 L sample of human breath taken prior to the consumption of orange juice. The 3D surface plot is shown in the inset.

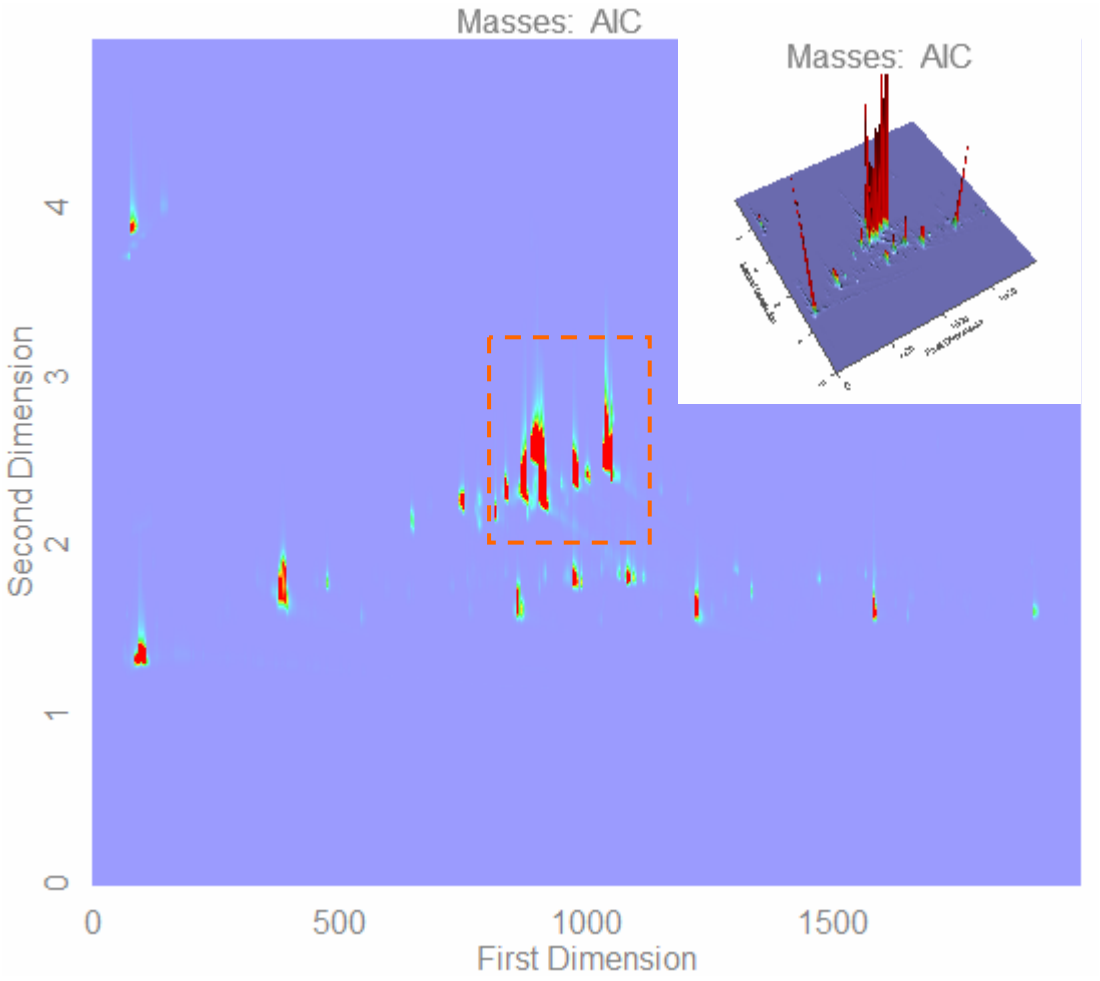

Figure 5.6 – A GCxGC chromatogram of a 1L sample of human breath taken 15 minutes after the consumption of 10 oz. of orange juice. The 3D surface plot is shown in the inset.

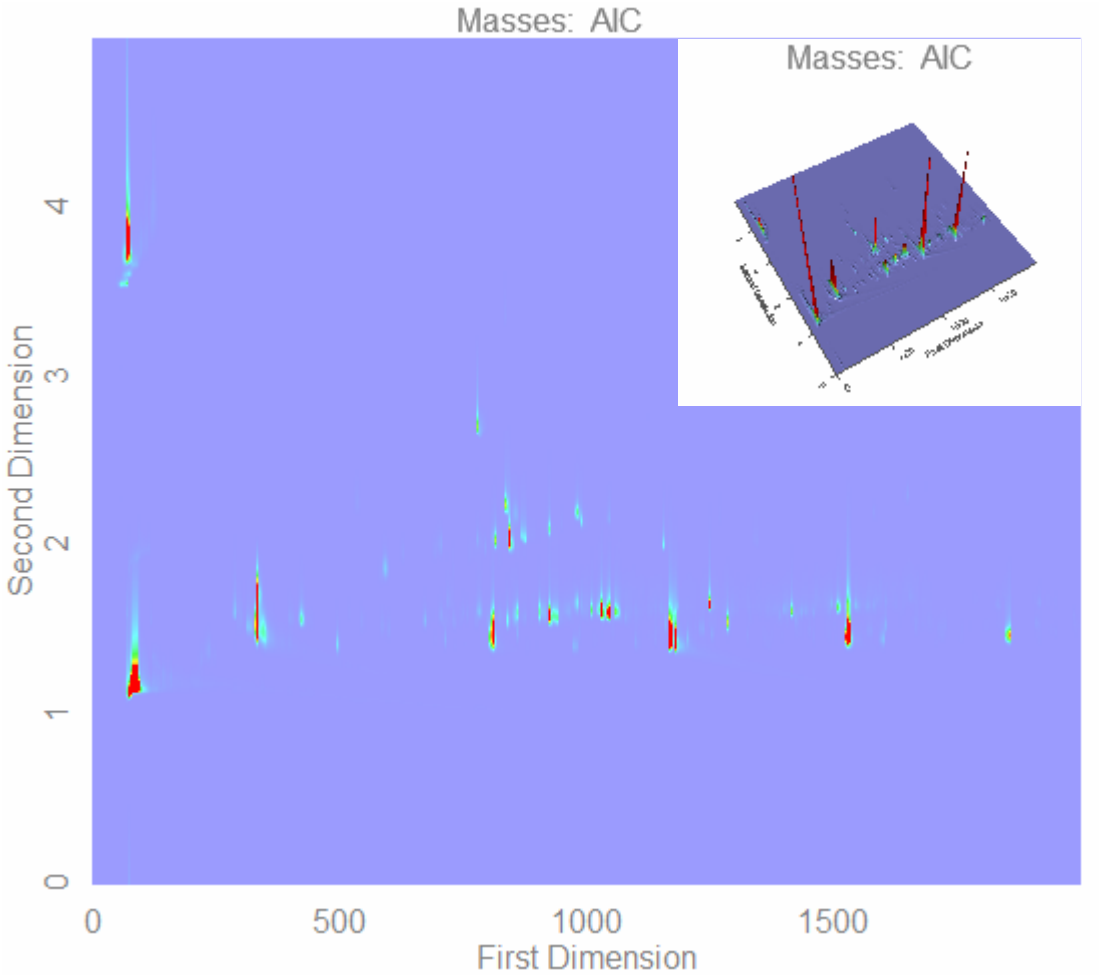

Figure 5.7 – A GCxGC chromatogram of a 2 L sample of human breath taken prior to the consumption of a sugar-free energy drink. The 3D surface plot is shown in the inset.

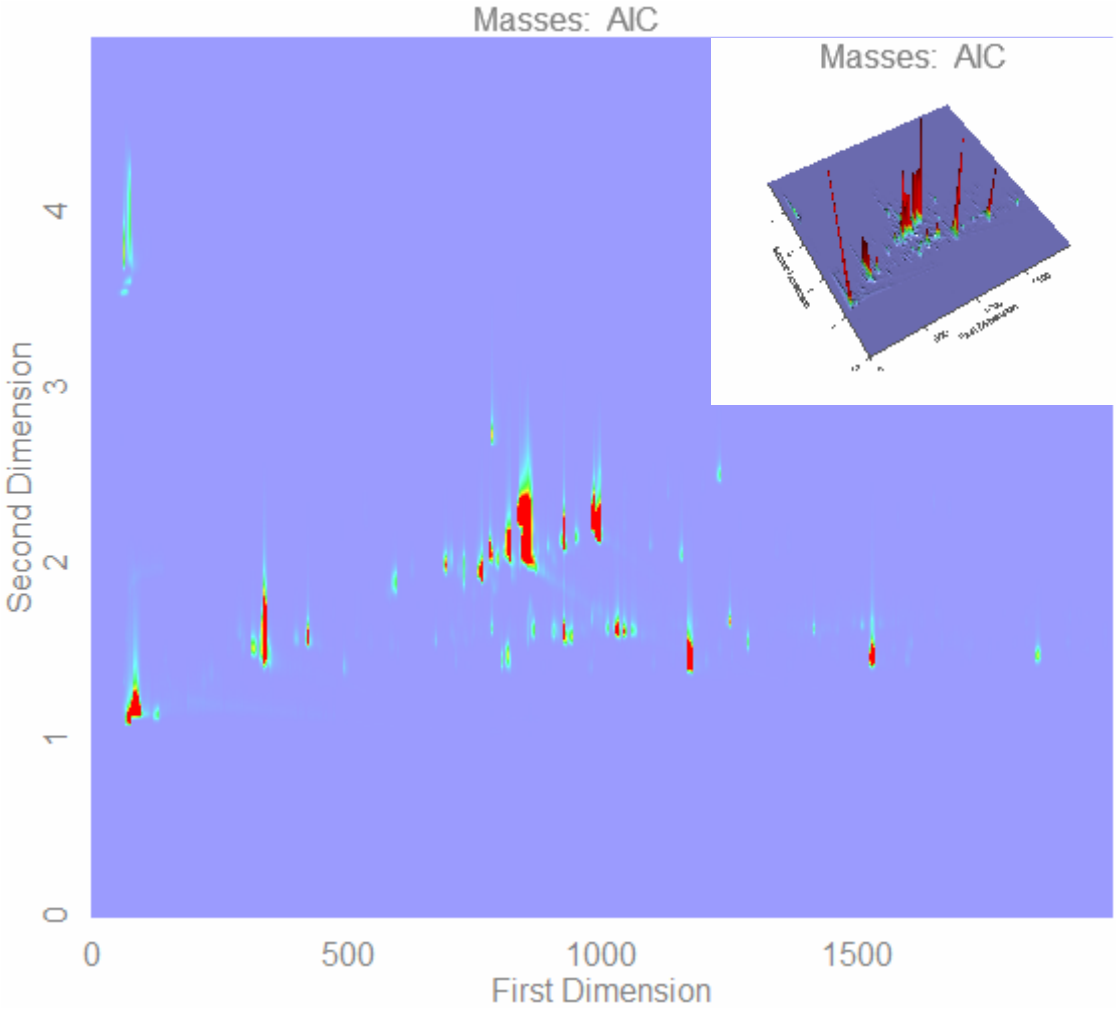

Figure 5.8 – A GCxGC chromatogram of a 2 L sample of human breath taken after the consumption of 16 oz. of a sugar-free energy drink. The 3D surface plot is shown in the inset.

	Area		
Compound	**Pre-Energy Drink**	**Post-Energy Drink**	**% Change**
Limonene	4465	84924	1802.0%
Nonanal	24820	14041	-43.4%
α-Myrcene	13114	2778841	21089.9%
α-Pinene	43291	922422	2030.7%
Hexane	87494	86032	-1.7%
Eucalyptol	92072	103658	12.6%

Table 5.1 – A table showing the change in area and percentage change for six selected components from prior to the consumption of the sugar-free energy drink to after the consumption of the energy drink.

REFERENCES

[1] Strang, J. *American Journal of Nursing*, **1934**, *34*, 205.
[2] S. Chen, L. Zieve and V. Mahadevan, *J. Lab. Clin. Med.* **75** (1970), p. 628.
[3] Pauling, L.; Robinson, A.; Teranishi, R.; Cary, P. *Proc. Nat. Acad. Sci.*, **1971**, *68*, 2374.
[4] J.M. Sanchez and R.D. Sacks, *Anal. Chem.* **78** (2006), 3046.
[5] Libardoni, M.; Stevens, P.; Waite, J.; Sacks, R. *J. Chromatogr. B*, **2006**, *842*, 13.
[6] J.M. Sanchez and R.D. Sacks, *Anal. Chem.* **75** (2003), 978.
[7] J.M. Sanchez and R.D. Sacks, *Anal. Chem.* **75** (2003), 2231.
[8] Coeur, C.; Jacob, V.; Denis, I.; Foster, P. *J. Chromatogr. A*, **1997**, *786*, 185.
[9] Calogirou, A.; Larsen, B.; Brussol, C.; Duane, M.; Kotzias, D. *Anal. Chem*, **1996**, *68*, 1499.
[10] Schrader, W.; Geiger, J.; Klockow, D.; Korte, E. *Environ. Sci. Technol.*, **2001**, *35*, 2717.
[11] Hollender, J.; Sandner, F.; Möller, M.; Dott, W. *J. Chromatogr. A*, **2002**, *962*, 175.
[12] Fick, J.; Pommer, L.; Andersson, B.; Nilsson, C. *Environ. Sci. Technol.*, **2001**, *35*, 1458.

CHAPTER 6

CONCLUSIONS

The research presented in this dissertation has demonstrated the usefulness of a multi-bed sorption trap using discrete beds of carbon-based sorbents and its use in inlet systems for gas chromatography and comprehensive two-dimensional gas chromatography. The experimental studies presented in this work address different uses of the multi-bed sorption trap for various analyses.

The multi-bed sorption trap was first evaluated as a preconcentrating inlet for the analysis of volatile organic compounds. The system utilized in that study used ambient air as the carrier gas with a photo ionization detector. This system was intended as a proof of concept for a field portable system whose only consumable would be electricity. Ambient air was used as a carrier gas by placing a vacuum pump at the outlet of the column. A photo ionization detector was used in place of a flame ionization detector because of its compatibility with the lower pressure at the column outlet. The use of air as a carrier gas provided for less efficiency in the separation, but this was considered as an acceptable trade-off for the elimination of a carrier gas supply. A significant limitation for the combination of the in-line multi-bed sorption trap and air as carrier gas is greater decomposition of some sensitive compounds including some environmentally significant terpenes as well as aldehydes and ketones.

The multi-bed sorption trap was then combined with a length of thick-film metal capillary column in order to expand the usable range of the preconcentrator. This work was part of a proposed pyrolysis-preconcentrator-GCxGC-TOFMS instrument that was to be part of the instrument package on the Mars Science Lander to look for biomarkers and organics in Martian soil. The pyrolysis-preconcentrator inlet was evaluated for a range of straight chain alkanes from hexane to tetracosane. One advantage of the system as described was that it allowed for the decoupling of the pyrolysis/sample collection conditions from the conditions necessary to obtain a sufficiently narrow injection plug for analysis on a GC. This decoupling of these processes allowed conditions for each step to be independently optimized. The system was proven to increase the upper limit from C_{13} to at least C_{24}. Theoretically, there is no reason the upper limit should not extend to at least C_{40}.

The multi-bed sorption trap was also pair with a comprehensive two-dimensional gas ghromatograph to examine human breath. The multi-bed sorption trap had already been proven useful to examine human breath by single dimension gas chromatography. This study took advantage of the applicability of GCxGC to the analysis of complex samples. GCxGC provides for better chromatographic resolution and increased peak capacity, by performing separations on two columns with different separation mechanisms. This study also used a novel resistively-heated, air-cooled thermal modulator in the GCxGC.

The final study in this work used a separate thermal desorption inlet (TDU) and cryogenically-cooled inlet (CIS 4) connected in series to analyze changes in human breath. The TDU/CIS 4 inlet allowed for the decoupling of the desorption and injection

parameters as had already been achieved with the pyrolysis-preconcentrator inlet. Instead of collecting on a thick film phase trap, the TDU/CIS 4 inlet takes advantage of a cryogenically-cooled inlet liner that can be rapidly heated to achieve a narrow injection plug. The decoupling of the processes with this inlet allows for slower temperature programming for the desorption of analytes from the sorbent while allowing increase gas flow, thereby decreasing residence time of the analytes in the heated zone while not exposing them to excessive temperatures which could increase observed decomposition. In this study a PDMS foam, which is not an ideal sorbent, was used. The goal was to examine the TDU/CIS 4 inlet. The next logical progression for this work is to obtain TDU tubes with the PDMS foam replaced by a custom packed multi-bed sorbent.